Cultured microalgae from shallow water and intertidal soft sediments in the Red Sea, Saudi Arabia

Anders Wold

Master of Science

Thesis

Department of Biosciences

Section for Aquatic Biology and Toxicology (AQUA)

UNIVERSITY OF OSLO

18.06.2015

Year: 2015

Title: Cultured microalgae from shallow water and intertidal soft sediments in the Red Sea, Saudi Arabia

Author: Anders Wold

http://www.duo.uio.no

Printed: Reprosentralen, University of Oslo

Abstract

The tropical Red Sea coast of Saudi Arabia is dominated by intertidal soft sediments, seagrass meadows and mangrove beaches. These habitats have been under high pressure for decades partly due to anthropogenic activity. The water of the Red Sea is characterised by its high temperature and salinity throughout the year.

The microalgae is a group of organisms characterised by their small size, unicellular or colonial organisation and ability or secondarily lost ability to photosynthesise including closely related non-photosynthetic species. The photoautotrophic microalgae are responsible for approximately 45% of the World's primary production and thus play a major role in many ecosystems. It is estimated that more than 40,000 algal species (including macroalgae) have been described, but recent advances in high throughput sequencing suggest there is a vast unknown diversity yet to be discovered. Little is known about the microalgal species diversity associated with the tropical habitats of the west coast of Saudi Arabia.

Eleven strains were isolated in the shallow waters and beaches of Saudi Arabia. They were studied morphologically with light microscopy, scanning electron microscopy and transmission electron microscopy and molecularly with phylogenetic trees inferred from 18S and partial 28S (D1/D2) rDNA. Sixteen unique sequences and two previously recorded sequences were acquired and will be uploaded to NCBI GenBank.

Four strains have been identified to species: *Cafeteria roenbergensis* Fenchel & Patterson, *Lotharella reticulosa* Ota, *Cylindrotheca* cf. *closterium* (Ehrenberg) Reimann & Lewin and *Oxyrrhis marina* Dujardin. The latter two have previously been recorded in the Red Sea. The first two have been recorded in similar habitats. Four strains have been identified to genus: genera *Amphidinium* Claparède & Lachmann, *Chlamydomonas* Ehrenberg, *Nitzschia* Hassall and *Tetraselmis* Stein, all of which are previously recorded in the Red Sea and similar habitats.

Three potentially novel species with affinity for known species were partially described. They belong to genera *Proteomonas* Hill & Wetherbee, *Pavlova* Butcher and *Rhizochromulina* Hibberd & Chrétiennot-Dinet respectively.

Acknowledgement

The work with this thesis was carried out mainly at the Section for Aquatic Biology and Toxicology (AQUA). Some of the laboratory work and the analyses were also carried out the Section for Genetics and Evolutionary Biology (EVOGENE), and the Centre for Ecological and Evolutionary Synthesis (CEES) and the Electron Microscopy Unit for Biosciences facilities at the University of Oslo (UiO) from September 2013 to June 2015 and at the Red Sea Research Center (RSRC) at the King Abdullah University of Science and Technology (KAUST) in Saudi Arabia in November 2012 and January 2014.

First I would like to thank my main supervisor Bente Edvardsen for sharing your expertise on phylogeny, writing, providing relevant literature, proofreading of my thesis and your knowledge on ecology and the microalgae.

Also, a big thanks to my co-supervisor Wenche Eikrem for helping me with preparation for EM, providing relevant literature, proofreading of my thesis and sharing some of your enormous knowledge of microalgal morphology with me.

I would also like to thank my other two co-supervisors Stein Fredriksen and Stein Kaartvedt for providing relevant literature and proofreading.

An extra big thanks goes to Sissel I. Brubak for all the help and assistance with cultivation and the molecular work.

To the guys at the Electron Microscopy Unit: thanks for teaching me how to operate the different electron microscopes and preparation techniques.

Furthermore, I owe a big thanks to Elianne S. Egge and Anders K. Krabberød for all the help with molecular work, analysis and very interesting discussions on microalgal topics.

Finally I would like to thank Kristine Dobbe and Annie Evankow for proofreading, Randi F. Ose for helping me with the cloning, the guys at KAUST for giving me a pleasant stay in Saudi Arabia, to Siri R. Moy and the rest of the guys at my study room and all the people at UiO for making all these years unforgettable.

Table of Contents

1 Introduction

1.1 Red Sea

The Red Sea is characterised by its unusually high salinity with an average of 40 PSU throughout the year (Bower et al. 2000). It has a high rate of evaporation, an insignificant rate of precipitation and freshwater run-off from rivers and poor circulation due to a narrow connection to the adjacent Indian Ocean (Maillard & Soliman 1986). The average water surface temperature is approximately 21°C to 28°C in the north and 26°C to 32°C in the south (Nandkeolyar et al. 2013).

The Red Sea coast of Saudi Arabia is dominated by intertidal soft sediments, seagrass meadows, mangrove beaches and coastal water of salinity up to 65 PSU (Price et al. 1987; Khalil 2004).

1.2 Mangrove, seagrass and intertidal soft sediment ecology

1.2.1 Mangrove ecology

Mangroves are woody trees mostly found on sheltered sandy coasts in the tropics (Price et al. 1987). They are dependent on high temperatures trough the year (LuZhen et al. 2010). Their high amount of root biomass and ability to excrete excessive salt through the bark and shed leaves are adaptations to living in highly saline environments (Waisel et al. 1986; Snowdon et al. 2000). Mangroves are a taxonomically diverse group comprised of more than 50 species across 15 families (Ricklefs & Latham 1993). Of the four mangrove species found in the Red Sea and Saudi Arabian coast, *Avicennia marina* (Forsk.) Vierh (grey mangrove) is dominant (Price et al. 1987).

A vast number of marine and terrestrial taxa is associated with mangroves and surrounding sediments (Farnsworth & Ellison 1996; Das et al. 2006; Sahoo & Dhal 2009), including commercially important shellfish, prawn, fish and microalgae (Rodelli et al. 1984; Sasekumar et al. 1992). The trees also prevent coastal erosion by stabilising the sediment (Marshall 1994). Estimates have shown that 35% of the World's mangroves have disappeared at an annual rate of 2.1% since the early 1980s (Valiela et al. 2001). The loss is partly explained by anthropogenic activity such as harvesting of the mangroves or associated fauna and human population growth (Nurkin 1994; Jin-Eong 1995). It is therefore important to study and learn more about mangrove habitats.

1.2.2 Seagrass ecology

Seagrasses are angiosperms found in marine systems. They generally grow in muddy and sandy shallow coastal waters, covering approximately 0.1-0.2% of the global ocean (Duarte 2002). The rough morphological organisation of a seagrass plant from top to bottom is leaves, stem, rhizomes (modified horizontal subterranean stems, connecting individual plants) and roots. The seagrasses form an ecological group. The group is polyphyletic and comprises 58 species divided across 12 genera and four families. Of the 13 species in the Red Sea, *Halophila stipulacea* (Forsskål) Ascherson is the dominant species, and genera *Halophila* Du Petit-Thouars and *Enhalus* Richard are the dominant genera (Short et al. 2007).

Seagrass meadows function as habitats for a large range of marine animals (Orth et al. 1984) and microalgae (Armitage et al. 2005), and serve as a direct food source for sea urchins (Valentine & Heck Jr. 1999) and dugongs (Preen 1995). They also form a habitat for both macro- and microalgae growing on the plants as epiphytes, and in the sediment beneath the plants. Both the epiphytic microalgal assemblages and the benthic communities in the sediment are often dominated by pennate diatoms (Moncreiff & Sullivan 2001). Also, seagrass roots and rhizomes stabilise sediments by inhibiting erosion, and the seagrass leaves filter suspended sediment and nutrient particles from the water column above (Björk et al. 2008).

Seagrasses are experiencing a decline worldwide, partly due to anthropogenic activity (Orth et al. 2006). A major threat is run-off of nutrients and sediments affecting the water quality and reducing the light penetration. Other stress factors are associated with aquaculture, pollution, boating, construction, dredging and destructive fishing. It has been shown that 110 km^2 of seagrass areas have disappeared every year since 1980, and that 29% of the known seagrass areas have disappeared since 1879 (Waycott et al. 2009). Hence, it is important to study and learn more about seagrass habitats.

1.2.3 Intertidal soft sediment ecology

Intertidal soft sediments are coastal habitats characterised by the small particle diameter of the sediment. Based on the diameter, the particles are grouped into three categories: mud (<0.0039-0.0625 mm), sand (0.0625-2 mm) and gravel (2-256<mm) (McLachlan & Brown 2006). The particles of the Saudi Arabian coast become progressively finer from the north to the south, and are mostly in the transition between sand and mud in the central part (Price et al. 1987). The particle size influences the porosity, permeability and capillarity of the sediment, of which the latter two are important for the species composition in the sediment (Fenchel 1969). Finer particles are more

readily drifting away due to turbulence and is hence found in the sediment of more sheltered habitats. Shallow coastal bays are highly productive and they make up approximately 13% of the World's coastline (Hardison et al. 2013). A large range of species are found in these habitats, including flatworms, rotifers, annelids, molluscs and microalgae (McLachlan & Brown 2006). These habitats are under pressure from human activity through pollution (e.g. sewage, crude oil etc.) and habitat destruction (e.g. harbours, sand mining etc.) (McLachlan & Brown 2006). It is therefore important to study this type of habitat.

1.3 Microalgae

Microalgae is a group of organisms characterised by their small size, unicellular or colonial organisation and ability or secondarily lost ability to photosynthesise including closely related non-photosynthetic species. Representatives of this functional group are found in the eukaryotic supergroups and phyla Archaeplastida (divisions Chloro-, Glauco- and Rhodophyta), Excavata (division Euglenophyta), Hacrobia (divisions Haptophyta and Cryptophyta) and the SAR-complex comprised of Stramenopila (division Ochrophyta), Alveolata (division Dinophyta) and Rhizaria (division Chlorarachniophyta) (Burki 2014), and in addition the prokaryotic division Cyanophyta (Graham et al. 2009). Microalgae have been given much attention due to their vast morphological and functional diversity and ecological impact.

The eukaryotic microalgae range from tiny non-motile cells of 0.8 µm (*Ostreococcus tauri* Courties & Chrétiennot-Dinet) to large cell colonies visible to the naked eye (genus *Phaeocystis* Lagerheim). Nutrition strategies include photoautotrophy, heterotrophy (phagotrophy of molecules/organisms, parasitism, etc.) or a combination of the two (mixotrophy). Their distribution includes terrestrial habitats as symbionts in lichens or as free-living cells on trees (Neustupa & Škaloud 2008) or rocks (Broady 1981) and as flagellated and non-motile unicellular or colonial forms organised in chains or collective mucilage in all aquatic habitats.

The photoautotrophic microalgae are responsible for approximately 45% of the World's primary production (Field et al. 1998) and thus play a major role in many ecosystems. It is therefore essential to describe and understand their diversity and distribution. Pelagic systems have been subject to several extensive studies. Benthic and shallow water systems, though, are less well understood.

It is estimated that more than 40,000 algal species (including macroalgae) have already been described (Guiry 2012). Still, recent advances in high throughput sequencing suggest there is a vast unknown diversity yet to be discovered (Caron et al. 2012; Pawlowski et al. 2012). It is therefore

important to study the morphology and phylogeny to learn more about these species.

1.4 Benthic microalgae

The ecology of benthic microalgae has been subject to several studies, especially their role in the foodweb as primary producers (MacIntyre et al. 1996; Aberle-Malzahn 2004; Hardison et al. 2013). The species composition, though, is less well understood. Some extensive studies have been conducted, mainly focusing on heterotrophic microalgae and protozoa (Fenchel 1967; Larsen & Patterson 1990); Ekebom et al. 1996; Al-Qassab et al. 2002; Lee & Patterson 2002). Autotrophs have been given some attention (Garai 2005), especially diatoms (Jaschinski et al. 2009; Al-yamani & Saburova 2011), dinophytes (Murray & Patterson 2002; Hoppenrath et al. 2014) and cyanophytes (Kaas 1987; Fumanti et al. 1996). Extensive flagellate (Al-yamani & Saburova 2010) and diatom (Al-yamani & Saburova 2011) diversity studies have been carried out in the Persian Gulf. The habitats of the Persian Gulf are similar to those of the Red Sea with regards to temperature, salinity and sediment properties (e.g. particle size) (Emery 1956).

The benthic microalgae of the Red Sea are less well known. Microalgal taxa commonly occurring in the benthos include the diatom genera *Licmophora* Agardh and *Navicula* Bory de Saint-Vincent (Fumanti et al. 1996; Al-yamani & Saburova 2011), dinophyte genera *Amphidinium* Claparède & Lachmann and *Prorocentrum* Ehrenberg (Taylor et al. 2007; Al-yamani & Saburova 2010) and the euglenophyte genera *Eutreptia* Perty and *Petalomonas* Stein (Larsen & Patterson 1990; Al-yamani & Saburova 2010) to mention a few.

1.5 Morphological and molecular phylogenetics

Historically, phylogenetic trees have predominantly been inferred from morphological and chemical (e.g. pigments) characters (Turrill 1942). Taxonomists have identified similarities and dissimilarities on the same morphological character in different species. With this data they have been able to deduce the most likely or parsimonious evolutionary relationships. This technique presents a variety of challenges. One problem is the time and expertise needed in order to correctly identify different characters, especially in smaller organisms. Morphological character delimitation is not always objective because of interpretations of the observations. Also, identifying plastic, homoplastic and analogous traits may be difficult. When present, these phenomena obstruct the evolutionary relationships between the species, and need to be recognised. A third problem worth mentioning is the sheer amount of characters used, as a high number of characters theoretically yields more robust

phylogenies. The more morphological characters, the more time consuming the identification process will be.

Which morphological traits should be considered viable criteria for delimitation between different taxa has been an ongoing discussion. The major algal lineages (divisions) are relatively clearly distinguished from each other, e.g. based on the ultrastructure of the chloroplast (Whatley 1993). This includes chloroplast membranes, thylakoid patterns, pigments, etc. Also, some morphological characters are exclusively or almost exclusively found in specific divisions, such as the vestibules of the cryptophytes, flagellar organisation of dinophytes (transverse and longitudinal flagella in furrows) and the haptonema of the haptophytes (Graham et al. 2009). Species delimitation within a genus, on the other hand, is not always as obvious or clear. *Emiliania huxleyi* (Lohmann) Hay & Mohler is easily identified in the scanning electron microscope based on the distinct coccoliths covering the cells (Throndsen et al. 2007). Groups like genus *Tetraselmis*, on the other hand, still lack clear morphological criteria for delimitation between similar species (Guiry & Guiry 2015).

Molecular phylogenetics is a powerful tool used to infer evolutionary relationships between species and higher taxonomic levels. This tool includes phylogenetic trees constructed and based on DNA, RNA and protein sequences, but henceforth, the latter will be excluded from the terminology. When Frederick Sanger and colleagues introduced the "dideoxy" chain-termination sequencing method called "Sanger sequencing" (Sanger et al. 1977), they presented a fast and cheap way to acquire sequences of nucleotides. This gave rise to numerous phylogenies based on molecular data. Even though several sequencing techniques were developed during the 1970s, Sanger sequencing would become the "gold standard" for years to come. During the 2000s, different next-generation sequencing technologies have been developed (454 Pyrosequencing, Illumina sequencing, SOLiD sequencing etc.). Common for these techniques is the ability to yield a vast amount of bases per unit time and money spent. Sanger sequencing has remained relevant, though, due to the relatively long sequences produced per run and the ease of use in smaller projects.

After the introduction of molecular phylogenetics, some of the problems from its morphological counterpart disappeared and others emerged. The delimitation of molecular characters (nucleotides in sequences) is done more or less objectively by an algorithm through base calling. This is the case for high quality bases only. When manual editing is needed, interpretation will be a factor. Also, the conservative nature of many marker regions makes continuous sequences with "analogous traits" rare. In the more variable parts of these regions, though, they do occur. This is commonly known as genetic saturation: a base at a given position changes so rapidly that it for instance has changed from A to T, and then back to an A at a later point. This gives the false

impression that the two species should be grouped closer together despite the fact that there has been two point mutations at the position in question. Bases of this kind, however, can be identified and removed. Finally, possibly the biggest advantage of molecular phylogenetics is the many readily available characters in the sequences. The economical expenses will increase with higher numbers of bases, but the time spent will not increase as significantly. However, large amounts of bases and taxa demands more sophisticated analysis and filtering of the dataset. The strengths of this technology is most apparent when coupled with the traditional method.

1.6 Objectives

The objectives of this study was to explore and reveal the diversity of microalgae associated with a tropical seagrass meadow located in a bay and two sand beaches with mangroves in the Red Sea. This was done by establishing mono-/clonal-cultures which were examined and described using light microscopy, electron microscopy (scanning and transmission) and DNA barcoding by Sanger sequencing of two different marker regions of the ribosomal DNA: the small subunit (18S) and the large subunit (28S) and phylogenetic placement. Also, novel species were partially described morphologically and placed systematically using molecular phylogenetic tools.

In order to reach the objectives, the following questions were asked:

1. Which microalgal taxa can we record from the sediment, the plankton above the sediment in a seagrass meadow and on beaches?

2. Can we find taxa not previously recorded in the Red Sea, or not recorded in similar tropical habitats?

3. Can we find novel species not previously described? If so, what are their morphology and phylogenetic position?

2 Materials and methods

2.1 Field work

2.1.1 Location description

The study was carried out in two locations in the Central Red Sea. The first location is a shallow protected bay east of King Abdullah Economic City, Saudi Arabia (c. 22°23'00.0"N 39°08'00.0"E). The bay is a semi-enclosed seagrass lagoon surrounded by mangrove forest, and the water exchange rate is low. The temperature and salinity in 2014 varied from 23°C (Dec., Feb.) to 32°C (Sept.) and 40 PSU (Jan.) to 42 PSU (Sept.) in the inner bay. In the outer bay it varied from 26°C (Jan., Feb.) to 32°C (July, Sept.) and 39 PSU (Jan.) to 40 PSU (Apr.-Nov.) in the outer bay (Banguera-Hinestroza et al. In prep.).

The second location is a semi-protected sand beach with mangroves at the King Abdullah University of Science and Technology (KAUST) (c. 22°19'02"N 39°05'27"E). There are no available temperature and salinity data from this location.

2.1.2 Sampling

The sampling of microalgae was done in the bay and adjacent sand beach during midday on the 12th and 13th of November 2012 and 7th of January 2014 and at the sand beach at KAUST during midday on the 17th of November 2012. Sediment samples at depths of 0-2 metres below sea level and sand samples were collected by hand and stored in plastic bags. Planktonic samples were collected with water bottles (Niskin) at 5 metres and with horizontal net hauls from a boat further out in the bay.

The sampling of 2012 was done by Bente Edvardsen and Wenche Eikrem (AQUA, UiO). The sampling of 2014 was done by the author.

2.1.3 Raw cultures

Raw cultures were established by transferring sediment and sand to Petri dishes. The material was covered with a layer of lens paper with glass cover slips on top, which the cells attached to after moving through the lens paper when exposed to natural light in a climate chamber. After 1-3 days the cover slips were rinsed with prefiltered (Whatman, GF/C-filter, 1.2 µm mesh size) water collected from the Red Sea. The water samples and net haul samples were transferred directly to

flasks.

All the flasks of raw cultures were filled with approximately 36 mL of Red Sea seawater and about 4 mL of 40 PSU IMR ½ medium (Eppley et al. 1967). The latter was prepared in and transported from the medium laboratory at the University in Oslo to KAUST, and 1-5 mL of sample material was added, making a mixed medium volume 40-45 mL and 40 PSU IMR 1/20.

The raw cultures from 2012 were established by Bente Edvardsen and Wenche Eikrem (AQUA, UiO). The raw cultures from 2014 were established by the author.

2.2 Cultures

2.2.1 Culture medium

All cultures were grown in 40 PSU modified IMR (IMR ½) culture medium (later changed to 34 PSU). For diatom strains, silicon dioxide was added to the culture medium along with hydrogen chloride to balance for the increase in pH. A single grain of autoclaved (GETINGE, Halmstad, Sweden) rice was added to the flasks containing heterotrophic/mixotrophic strains to serve as a carbon source for the bacteria. See Appendix I for lab protocol on preparation of IMR ½. The recipe used in this study deviates from the original in that the seawater was not diluted with distilled water and all nutrients were added in half strength (thus IMR ½) and 10 nM of selenite was added (Edvardsen & Paasche 1992).

The cultures were grown at 19°C, a photon flux rate of approximately 30-40 µmol photons m^{-2} s^{-1} and a 12:12 h light-dark cycle and later at a photon flux rate of about 30-40 µmol photons m^{-2} s^{-1} and a 24:0 h light-dark cycle.

2.2.2 Dilution series

Planktonic species were isolated by dilution series. The dilutions were performed using Corning Costar 24 wells 3.4 mL cell culture plates with flat bottoms. 1.8 mL of 40 PSU IMR ½ were transferred to all the 24 wells. 0.2 mL of raw culture were then added to the four wells (A-D) in column one. After thoroughly mixing the content in the A1-well, 0.2 mL was transferred from the A1-well to the A2-well. This procedure was repeated for column one through six for the four rows of wells, making a total of four dilution series with $1:1x10^1$, $1:1x10^2$, $1:1x10^3$, $1:1x10^4$, $1:1x10^5$ and $1:1x10^6$ levels of dilution for each raw culture. The plates were examined with light microscopy after 1-4 weeks. The wells appearing to contain cells of a single algal species had some of its content moved to a 40 mL Nunclon flask. The plates with wells containing two or more different

species had some of its content become the starting point for another set of dilution series.

The dilution series were grown at 23°C, a photon flux rate of approximately 40-60 µmol photons m^{-2} s^{-1} and a 16:8 h light-dark cycle.

2.2.3 Agar dishes

Benthic species were isolated using agar dishes. A flask of 200 mL Milli-Q water and 8 mL of agar powder and a flask of 800 mL 40 PSU IMR ½ and 12 grams of sea salt were autoclaved separately and later mixed. The mix was then poured into several Petri dishes and then stored for cooling. A drop of raw culture was transferred to the agar dish and smeared out with a glass rod. Between the isolations, the rod was rinsed in >90% ethanol and Milli-Q water to remove the ethanol. After 3-4 weeks of incubation, several brown or green spots had appeared on the surface of the agar. The spots were picked up and transferred to a microscope slide. The sample was then examined under a light microscope. If the sample appeared to only contain cells of a single algal species, the rest of the coloured agar from the same spot was transferred to a 40 mL flask with 40 PSU IMR ½ medium with (for brown spots) or without (for green spots) silica added for better diatom growth.

The agar dishes were grown at 23°C, a photon flux rate of approximately 40-60 µmol photons m^{-2} s^{-1} and a 16:8 h light-dark cycle.

2.2.4 Culture examination

After isolation, the cultures were left to grow dense before examination. The flasks appearing to contain cells of a single algal species were given strain codes. Isolation as described earlier was reapplied to the flasks containing cells of multiple species.

Successfully isolated strains were then identified to the lowest systematic rank possible. This information was used to determine which marker regions and primers to use for the molecular work, to determine if any special treatment was needed during DNA isolation, or if any special treatment of the culture medium or the culture flasks was needed.

2.2.5 Other isolation techniques

Some species were isolated with other techniques than dilution series and agar dishes. For flasks containing cells of a single non-diatom autotrophic species together with diatom cells, germanium dioxide (GeO_2) was added to the flask for a final concentration of 5-10 mg/L. This was done to prevent diatom growth (Lewin 1996). After several days, when the cultures were dense, and if only the non-diatom species were present, they would be transferred to new flasks with regular IMR ½.

For flasks containing cells of a single heterotrophic species together with autotrophic cells, the flasks were wrapped in aluminium foil to stop the light influx to prevent growth of the autotrophes. After a few days, cultures containing the heterotrophic species only were transferred to new flasks.

2.3 Molecular work

2.3.1 DNA isolation

DNA isolation was performed on 10-20 days old cultures. 2-15 mL of culture was transferred to 2 mL Eppendorf tubes or 15 mL tubes (Corning CentriStar). Lower volumes were used for denser cultures. The 2 mL tubes were centrifuged at 8 000 rpm for 10 minutes (Eppendorf Centrifuge 5415R), and the 15 mL tubes at 4 000 rpm for 8 minutes (Eppendorf Centrifuge 5810R). The supernatant was removed, and the algal pellets were transferred to 1.5 mL Eppendorf tubes. To get the cells of the UIO346 and UIO350 strains to burst, the pellets of these cultures were frozen at -20°C and thawed at room temperature once or several times. Some pellets of UIO350 were also transferred to 2 mL cryo vials with Milli-Q water and glass beads to a total volume of 1.6 mL. The vials were then run in a Precellys 24 beadbeater (Bertin Technologies, Montigny-le-Bretonneux, France).

The DNA isolation of the algal pellets was done using the NucleoSpin Plant II DNA extraction kit from Macherey-Nagel (Düren, Germany) following the manufacturer's instructions. The RNase A incubation time of 10 minutes was increased to up to 60 minutes for either one of the two cell lysis steps (2a and 2b) for some of the sturdier cells.

2.3.2 DNA amplification

PCR (Polymerase chain reaction) was used to amplify the 18S (SSU: small subunit) and partial 28S (D1/D2 of LSU: large subunit) marker regions of the ribosomal DNA (rDNA). Each 0.2 mL Eppendorf tube contained 9 µL Milli-Q water, 12.5 µL GoTaq Green Master Mix (Promega, Madison, WI, USA), 12.5 µL of the forward and reverse primer and 1 µL of the DNA isolate for a total of 25 µL. The different primers used are shown in table 1, the different PCR primer combinations are shown in table 2, the different PCR programs (Eppendorf Mastercycler EP Gradient S) are shown in table 3, and the different strains isolated in this study are shown in table 4 and 5. For the UIO378 strain the PCR products were cleaned using the Wizard SV gel and PCR Clean-Up system (Promega, Madison, WI, USA) and cloned with the TOPO-TA kit (Invitrogen,

Carlsbad, CA, USA) following the manufacturer's instructions. The PCR, cleaning and sequencing of UIO378 was done by Anders K. Krabberød (EVOGENE, UiO).

Table 1. Oligonucleotide primers used for PCR and sequencing.

Primer code	PCR	Seq.	Sd.	Nucleotide sequence 5' to 3'	Position based on the *Saccharomyces cerevisiae* numbering system*
1F[a]	18S	18S	F	AAC CTG GTT GAT CCT GCC AGT	1-21 in 18S
528F[b]		18S	F	CGG TAA TTC CAG CTC C	575-590 in 18S
1055F[b]		18S	F	GGT GGT GCA TGG CCG	1263-1277 in 18S
300R[b]		18S	R	TCA GGC TCC CTC TCC GG	397-381 in 18S
1055R[b]		18S	R	CGG CCA TGC ACC ACC	1277-1263 in 18S
1528R[a]	18S	18S	R	TGA TCC TTC TGC AGG TTC ACC TAC	1795-1772 in 18S
CrN1F[c]	18S		F	CTG CCA GTA GTC ATA TGC TTG TCT C	14-38 in 18S
NuF[d]	18S		F	GTC ATA TGC TTG TCT CAA AGA C	23-44 in 18S
NuWR[e]	18S		R	ACG ACT TTT ACT TCC TCT AAA TC	1759-1737 in 18S
DIRF[f]	28S	28S	F	ACC CGC TGA ATT TAA GCA TA	184-203 in 28S
D2CR[f]	28S	28S	R	CCT TGG TCC GTG TTT CAA GA	816-797 in 28S

[a] From Medlin et al. (1988).

[b] From Elwood et al. (1985).

[c] From Hoef-Emden et al. (2002).

[d] From Ishida et al. (1999).

[e] Modified from NuR from Ishida et al. (1999).

[f] From Scholin et al. (1994).

Sd, synthesis direction; F, forward; R, reverse.

***** The interval of bases at which the primers would bind in the rDNA of *S. cerevisiae*.

Table 2. Primer combinations used in PCR.

Primer combination	rDNA region	Primer combination no.
1F and 1528R	Complete 18S	1
DIRF and D2CR	Partial 28S (D1/D2)	2
CrN1F and 1528R	Complete cryptophyte nuclear 18S	3
NuF and NuWR	Complete chlorarachniophyte nuclear 18S	4

Table 3. PCR programs.

PCR program no.	rDNA region	Temperature (°C)	Duration	Cycles
1	18S	95	2 minutes	
		95	45 seconds	
		50	30 seconds	30
		72	2 minutes	
		72	10 minutes	
		8	Hold	
2	28S	95	2 minutes	
		95	45 seconds	
		55	30 seconds	30
		72	1 minute	
		72	10 minutes	
		8	Hold	

Table 4: Strains with information on sampling data and locality.

UIO code	Original code	Date	Locality	Habitat	Material
345	75f	13.11.2012	Innermost part of the bay	Plankton	Net haul, 15 µm
346	13	12.11.2012	Innermost part of the bay	Sand beach	Sediment
349	75e	13.11.2012	Innermost part of the bay	Plankton	Net haul, 15 µm
350	75c	13.11.2012	Innermost part of the bay	Plankton	Net haul, 15 µm
352	59	12.11.2012	Station 2 in the bay	Plankton	Water
353	15	12.11.2012	Innermost part of the bay	Large seagrass	Sediment
375	16	12.11.2012	Innermost part of the bay	Open	Sediment
376	K-01a	07.01.2014	Innermost part of the bay	Sand beach	Sand
378	68	17.11.2012	KAUST beach	Sand beach	Sand
381	K-01b	07.01.2014	Innermost part of the bay	Sand beach	Sand
383	45	17.11.2012	KAUST beach	Sand beach	Sand

Table 5. Strains with information about PCR reactions.

UIO code	Original code	rDNA region	PCR primer combination no. (18S / 28S)	PCR program no. (18S / 28S)
345	75f	18S/28S	1 / 2	1 / 2
346	13	18S/28S	1 / 2	1 / 2
349	75e	18S/28S	1 / 2	1 / 2
350	75c	18S/28S	1 / 2	1 / 2
352	59	18S	5 / -	1 / -
353	15	18S/28S	1 / 2	1 / 2
375	16	18S/28S	1 / 2	1 / 2
376	K-01a	18S	4 / -	1 / -
378	68	18S/28S	1 / 2	1 / -
381	K-01b	-	- / -	- / -
383	45	18S/28S	1 / 2	1 / 2

2.3.3 Gel electrophoresis

Gel electrophoresis was used to determine whether or not the correct marker regions had been successfully amplified. A 1% agarose gel was prepared by adding 0.5 g agarose powder (Merck Millipore, Billerica, MA, USA) to 50 mL of 1x TAE buffer (Tris-acetate-EDTA). The mix was heated in a microwave at 750W for 1 minute to dissolve the powder in the solution. Then it was cooled to approximately 50°C. Before pouring the solution in the gel mold, 5 µL of DNA stain (GelRed™ Nucleic Acid Stain, Biotium, Hayward, CA, USA) was added, and a 12 well comb was mounted. After 30-40 minutes the comb was removed from the solid gel, and the mold with the firm gel was placed in the gel electrophoresis chamber filled with 1x TAE buffer. The first well was loaded with 5 µL ladder (GeneRuler Express DNA Ladder, Thermo Scientific, Waltham, MA, USA), and the other wells were loaded with 5µL of PCR product. The electrophoresis ran for 40 minutes at 80V and 220 mA. Photographs of the gel were taken in a UV cabinet.

2.3.4 Analysis of DNA concentration and DNA purity

The DNA isolates of the PCR products that did not give bands in the gel electrophoresis step were analysed for DNA concentration and DNA purity. This was done by spectrophotometry using a microplate reader (Synergy Mx Monochromator-Based Multi-Mode Microplate Reader, BioTek, Winooski, VT, USA) with a Take3 Micro-Volume Plate in combination with the Gen5 Data

Analysis Software, measuring the optical density (OD). Four replicates of 2 µL drops nuclease free water were used as blanks to reset the instrument, and two replicates of 2 µL of each DNA isolate were measured for dsDNA (double-stranded DNA) concentration in µg/µL, and absorbance at 260 and 280 nm to find the purity of the samples (260/280 ratio).

2.3.5 PCR product purification and sequencing

The PCR products which provided clear bands of the correct lengths in the gel electrophoresis step were purified prior to sequencing. Eppendorf tubes were filled with 30 µL Milli-Q water, 20 µL of PCR product and 2 µL ExoSAP-IT (USB Products Affymetrix, Inc., Santa Clara, CA, USA). The tubes were incubated at 37°C for 30 minutes to remove the residual primers and nucleotides, followed by an incubation at 80°C for 15 minutes to deactivate the ExoSAP-IT. For the products being sequenced in the ABI-lab at University of Oslo (ABI 3730 DNA Analyzer, Life Technologies, Waltham, MA, USA), 8 µL of each sample and 2 µL of the appropriate sequencing primers (Table 1) were transferred to Eppendorf tubes prior to delivery. For the products being sequenced in the GATC Biotech sequencing lab in Constance, Germany (ABI 3730xl), 5 µL of each sample and 5 µL of the appropriate sequencing primer were transferred to Eppendorf tubes prior to shipping.

For the 18S and 28S rDNA PCR products, the 528F and DIRF primers respectively were used for the first sequencing reactions. For reactions yielding nucleotide sequences of acceptable quality, the PCR-products were sequenced with the rest of the sequencing primers (Table 1). For low quality sequences, the culture from which the cells were harvested for DNA isolation was re-checked for contaminating algal cells. If previously undetected contaminants were observed, the isolation steps were repeated.

2.4 Microscopy

2.4.1 Light microscopy

The cells were examined alive or fixed with formalin under a Microphot FX and an inverted Nikon Eclipse TS100 (Nikon, Tokyo, Japan) microscope. Phase contrast (40X magnification) and differential interference contrast (60X magnification) was used. Digital photographs were taken with Nikon D5000 and Nikon D5200 digital cameras. The micrographs were sharpened and brightened in Paint.NET 4.0.5 (Brewster 2014).

2.4.2 Scanning electron microscopy (SEM)

SEM mounts were prepared with the following protocol: cover slips were covered with poly-l-lysine (0.2 mg/mL), dried over night and rinsed in Milli-Q water. Then, a drop of culture fixed with 2% glutaraldehyde (final concentration) was placed on the cover slips. After approximately one hour, the cover slips were rinsed in IMR ½ medium and three times in 0.1 M sodium cacodylate buffer with pH 7.8 (Agar Scientific Ltd., Essex, England). Post-fixation was done for one hour in 1% osmium tetroxide (OsO_4) in 0.1 M cacodylate. Then, the cover slips were rinsed 6x 10 minutes in 0.1 M cacodylate. Dehydration was done in ethanol series. Each step lasted 10 minutes. The different concentrations were 30%, 50%, 70%, 90%, 96% and finally 4 steps at 100%. Finally, the cover slips were critical-point dried in a BAL-TEC 030 CPD (Technion, Haifa, Israel) then glued to stubs and coated with approximately 5 nm of platinum in a sputter coater (Cressington 308R Desktop Advanced Coating System; Ted Pella Inc., Redding, CA, USA).

The mounts were examined and photographed in a JEOL JSM 6400 scanning electron microscope (JEOL Ltd., Tokyo, Japan) at the Electron Microscopy Unit for Biosciences, Department of Biosciences, University of Oslo. The micrographs were sharpened and brightened in Paint.NET.

2.4.3 Transmission electron microscopy (TEM)

Ultra-thin sections were prepared from cultures fixed with 2% glutaraldehyde (final concentration). 5-10 mL of fixed culture was spun down at 4 000 rpm for 20 minutes (Eppendorf Centrifuge 5810R). The supernatant was removed from tubes containing firm pellets and rinsed in medium (40 PSU IMR ½) 2 times for 10 minutes followed by 3 rinses 0.1 M cacodylate with pH 7.8 for 10 minutes. Post-fixation was done in 1% OsO_4, 1.5% ferricyanide and 0.1 M cacodylate for 1 hour. Rinsing was done using the following protocol: 3x 10 minutes in 0.1 M cacodylate; 5 minutes in 0.1 M cacodylate; 3 minutes 0.1 M cacodylate. Dehydration was done following the protocol for SEM preparation. Epoxy infiltration was started by storing the material over night in 50% ethanol and 50% epoxy without accelerator. The tubes were then spun down at 4 000 rpm for 20 minutes. The pellets were kept in epoxy with added accelerator for 1 hour. Polymerisation of the epoxy was done by storing the tubes at 60°C over night. Finally, ultra-thin sections were cut using an ultramicrotome (Reichert, Vienna, Austria). The sections were transferred to formvar coated copper grids.

Sections were examined and photographed in a Philips CM150 (Philips, Eindhoven, The Netherlands) transmission electron microscope at the Electron Microscopy Unit for Biosciences, Department of Biosciences, University of Oslo. The micrographs were sharpened and brightened in

Paint.NET.

2.4.4 Measurements

The dimensions of cells, flagella and other conspicuous cell features were measured in Paint.NET by drawing lines on top of the micrographs and measuring the lines. The line lengths were then compared to micrographs of a micrometer of corresponding magnification.

2.5 Sequence processing, alignments and phylogeny

2.5.1 Sequence processing

Sequences obtained from the DNA sequencing services were processed in Geneious 7.1.7 (Biomatters Ltd., Auckland, New Zealand). The 5' and 3' ends with low quality bases were trimmed automatically using the Trim End function with an error probability limit of 0.01-0.05. After trimming, consensus sequences were obtained with De Novo Assembly with the Highest Sensitivity configuration. Consensus sequences with low quality bases at either end were trimmed again, this time with an error probability limit of 0.05 only.

Ambiguous bases (N: any nucleotide; R: adenine or guanine; etc.) in the consensus sequences were checked manually by comparing them to raw sequences and chromatograms. In instances where a bad read in one chromatogram was conflicting with well defined reads in the other strands, the base suggested by the clear chromatogram(s) would be introduced manually in the consensus sequence. For bases lacking clear reads in any of the chromatograms, and bases having clear conflicting reads in two or more chromatograms, the ambiguous base would remain unedited.

After editing the consensus sequences manually, an NCBI search with BLAST (Basic Local Alignment Search Tool) was used to find the most similar reference sequences available (using a metadatabase (nr) including the GenBank database among others as database and Megablast (highly similar sequences) as search algorithm). The 10 most similar unique reference sequences and the consensus sequences were aligned using the MAFFT v7.017 alignment tool (Katoh et al. 2002). All manually edited bases were compared to bases at the same position in the other aligned sequences. At said positions, if the consensus sequence was the only sequence holding a certain base, the chromatograms would be re-examined to make sure the manual editing was correct.

2.5.2 Alignments

Reference sequences and the sequences from the present study were aligned using MAFFT Alignment v7.017 and checked manually. The following parameters were used: algorithm: auto; scoring matrix: 200PAM/k=2; gap open penalty: 1.53; offset value: 0.123. All available reference sequences for taxonomically accepted species closely related to the sequence from the present study were included.

Hyper-variable and ambiguously aligned regions were removed with Gblocks v0.91b (Castresana 2000). The following parameters were used: minimum block length: 5; minimum number of sequences for a flank position: 50% + 1; allowed gap position for 50% of the sequences.

2.5.3 Phylogenetic trees

The phylogenetic trees were constructing using PhyML (Guindon & Gascuel 2003) and the MrBayes (Huelsenbeck & Ronquist 2001) in the software Geneious. The following PhyML parameters were used for all phylogenetic analyses: substitution model: GTR; replicates: 200 or 1000; proportion of invariable sites: 0; number of substitution rate categories: 4; topology search: NNI/SPR; optimised for topology/length/rate. The following MrBayes parameters were used: substitution model: GTR; rate variaton: gamma; gamma categories: 4; chain length: 1,100,000; heated chains: 4; heated chain temp: 0.2; subsampling frequency: 200; burn-in length: 100,000; random seed: default setting; molecular clock with uniform branch lengths; gamma: 1, 1; shape parameter: exponential: 10.

3 Results and species discussion

3.1 Species taxonomy

The algal strains isolated from the Red Sea in the present study are presented below with taxonomic placement. The taxonomy is based on Riisberg et al. (2009) for class Bacillariophyceae (division Ochrophyta), Medlin & Mann (2007) for genus *Cylindrotheca* Rabenhorst, Hibberd & Norris (1984) for class Chlorarachniophyceae (division Chlorarachniophyta), WoRMS (2015) for genus *Oxyrrhis* Dujardin (class Dinophyceae) and Guiry & Guiry (2015) for the remaining taxa. An overview of the strains with information on sequenced marker regions is given in Table 6.

Division Bigyra Cavalier-Smith 1998
Class Bicosecophyceae Loeblich & Loeblich 1979
Order Bicosoecales Grassé 1926
Genus *Cafeteria* Fenchel & Patterson 1988
Cafeteria roenbergensis Fenchel & Patterson 1988
Division Chlorarachniophyta Hibberd & Norris 1984
Class Chlorarachniophyceae Hibberd & Norris 1984
Order Chlorarachniales Ishida & Hara 1996
Genus *Lotharella* Ishida & Hara 1996
Lotharella reticulosa Ota 2012
Division Chlorophyta Pascher 1914
Class Chlorodendrophyceae Massjuk 2006
Order Chlorodendrales Melkonian 1990
Genus *Tetraselmis* Stein 1878
Tetraselmis sp.
Class Chlorophyceae Willie 1884
Order Chlamydomonadales Fritsch 1927
Genus *Chlamydomonas* Ehrenberg 1833
Chlamydomonas sp.
Division Cryptophyta Cavalier-Smith 1986
Class Cryptophyceae Fritsch 1927
Order Pyrenomonadales Novarino & Lucas 1993
Genus *Proteomonas* Hill & Wetherbee 1986
Proteomonas aff. *sulcata* Hill & Wetherbee 1986
Division Dinophyta Round 1973
Class Dinophyceae Fritsch 1927
Order Gymnodiniales Apstein 1909
Genus *Amphidinium* Claperède & Lachmann 1859
Amphidinium sp.
Order Oxyrrhinales Sournia 1984
Genus *Oxyrrhis* Dujardin 1841
Oxyrrhis marina Dujardin 1841
Division Haptophyta Cavalier-Smith 1986
Class Pavlovophyceae (Cavalier-Smith) Green & Medlin 2000
Order Pavlovales Green 1976
Genus *Pavlova* Butcher 1952
Pavlova aff. *gyrans* Butcher 1952
Division Ochrophyta Cavalier-Smith 1996
Class Bacillariophyceae Haeckel 1878
Order Bacillariales Hendey 1937
Genus *Cylindrotheca* Rabenhorst 1859
Cylindrotheca cf. *closterium* (Ehrenberg) Reimann & Lewin 1964
Genus *Nitzschia* Hassall 1845
Nitzschia sp.
Class Dictyochophyceae Silva 1980
Order Rhizochromulinales O'Kelly & Wujek 1995
Genus *Rhizochromulina* Hibberd & Chrétiennot-Dinet 1979
Rhizochromulina aff. *marina* Hibberd & Chrétiennot-Dinet 1979

Table 6. Strains with DNA sequence information.

UIO code	Original code	Species	rDNA region
345	75f	*Cafeteria roenbergensis*	18S/28S
352	59	*Lotharella reticulosa*	18S (nuclear)
346	13	*Tetraselmis* sp.	18S/28S
350	75c	*Chlamydomonas* sp.	18S/28S
376	K-01a	*Proteomonas* aff. *sulcata*	18S (nuclear)
349	75e	*Amphidinium* sp.	18S/28S
381	K-01b	*Oxyrrhis marina*	-
375	16	*Pavlova* aff. *gyrans*	18S/28S
378	68	*Rhizochromulina* aff. *marina*	18S/28S
353	15	*Cylindrotheca* cf. *closterium*	18S/28S
383	45	*Nitzschia* sp.	18S/28S

3.2 Species identification

Below are the descriptions and discussions of the algal strains from the present study. The descriptions include morphological observations (cell size, flagella number etc.) with complementary micrographs, comments on the culture (colour, growth, etc.), systematic positions based on molecular phylogenies and locality and habitat for each strain. Accession numbers were included in the phylogenetic trees for reference sequences of unidentified species and sequences with the same name appearing in different clades. See Appendix II for a complete list of reference sequences and accession numbers used in the present study. The discussions include morphological and molecular comparisons with the original species diagnoses and other previous work, some comments on habitats and recommendations for future studies. Finally, a more detailed list of recorded distribution for each species or genus is presented.

Division Bigyra Cavalier-Smith
Class Bicosecophyceae Loeblich & Loeblich
Order Bicosoecales Grassé
Genus *Cafeteria* Fenchel & Patterson

Cafeteria roenbergensis Fenchel & Patterson

Observations

The cells of the *Cafeteria roenbergensis* strain (UIO345) were colourless, asymmetrical, anterio-posteriorly compressed, kidney- or D-shaped (Fig. 1a, b), posteriorly elongate with an anterio-ventral depression (Fig. 1c) or globular (not shown). The cells were 2.8 µm long and 2.7 µm wide (Fig. 1b) to 3.0 µm long and 1.9 µm wide (Fig. 1a). The anterior flagellum was 3.6 µm (Fig. 1b) to 4.4 µm (Fig. 1a) and the posterior flagellum 4.1 µm (Fig. 1a). Both flagella were inserted subapically in the anterio-ventral depression (Fig. 1c). Most observed cells were attached to the bottom or to the rice grain of the culture flask.

In the phylogeny (Fig. 2) the sequence from the present study clustered with a reference sequence named *Cafeteria roenbergensis*. *Cafeteria minima* (=*Cafeteria minuta* (Ruinen) Larsen & Patterson) formed the sister group. The sequence in question is 99.9% (1713/1715 bp) identical to the most similar reference sequence (*C. roen*bergensis, AF174364) in the phylogeny (Fig. 2) and 100% (1690/1690) identical to the most similar available reference sequences (*Cafeteria* sp., AF174365).

Locality: Seagrass bay, Saudi Arabia.
Habitat: Plankton, marine.

Discussion

The phylogeny from the present study is generally consistent with earlier phylogenies inferred from 18S rDNA (Cavalier-Smith & Chao 2006). Genus *Cafeteria* shows high affinity for genus *Bicosoeca* Clark. The cell size and shape, behaviour and flagella length were generally consistent with with the original description (Fenchel & Patterson 1988), except for the flagella which were slightly shorter in UIO345. This inconsistency may be due to difficulty in measuring the curved flagella of such a small size. The *C. roenbergensis* is distinguished from *C. minuta*, the only other taxonomically species in this genus (Guiry & Guiry 2015), in that the anterior flagellum is three-four times longer (10-12 µm) in the latter species (Larsen & Patterson 1990).

Cafeteria roenbergensis is relatively common in both marine benthic habitats and open water (Larsen & Patterson 1990; Ekebom et al. 1996).

For future studies I recommend acquiring clearer light micrographs to determine whether the flagella of UIO345 are substantially shorter than other in *C. roenbergensis* strains or not.

Previous recordings of Cafeteria roenbergensis

Atlantic Ocean, Canary Islands, Tenerife (Vørs 1993b).

Atlantic Ocean, Greenland (Vørs 1993a).

Atlantic Ocean, the Limfjord, Denmark (Fenchel & Patterson 1988).

Baltic Sea (Hällfors 2004).

Caribbean Sea, Belize (Vørs 1993b).

Mediterranean Sea, Marseille, France (O'Kelly & Patterson 1996).

Pacific Sea, Bowling Green Bay, Queensland, Australia (Larsen & Patterson 1990).

Weddell Sea, Antarctica (Vørs 1993a).

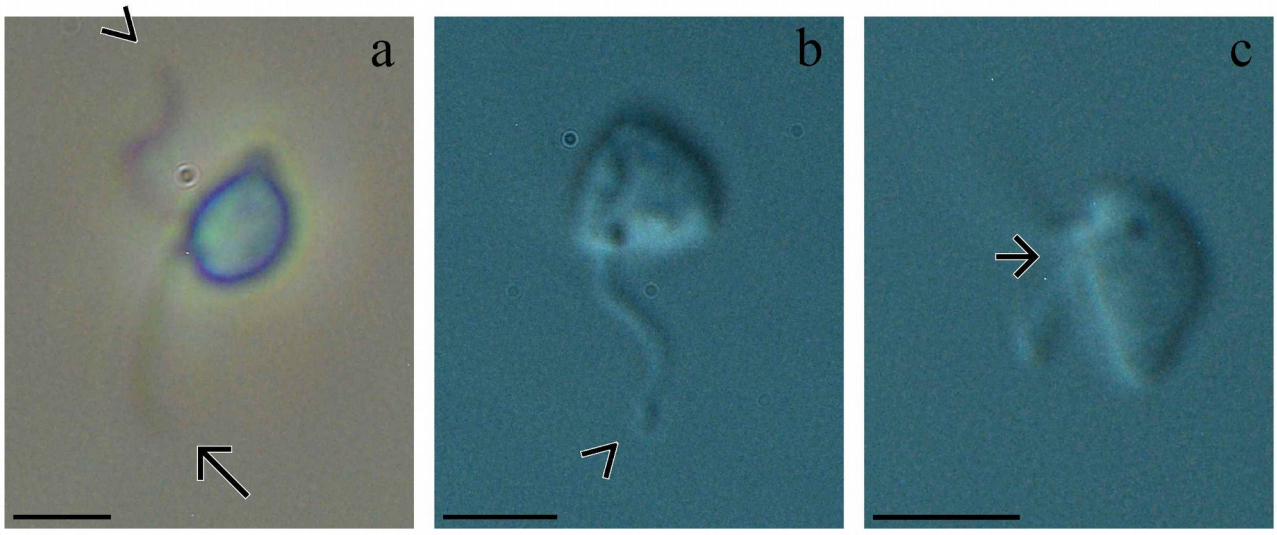

Figure 1. Phase contrast (a) and diffraction interference contrast (b-c) light micrographs of live *Cafeteria roenbergensis* cells (UIO345) (lateral view) showing cell shape, flagella and flagellar insertions. a: posterior flagellum (arrow), anterior flagellum (arrowhead); b: anterior flagellum (arrowhead); c: flagellar insertions (arrow); scale bars: a-c = 2 µm.

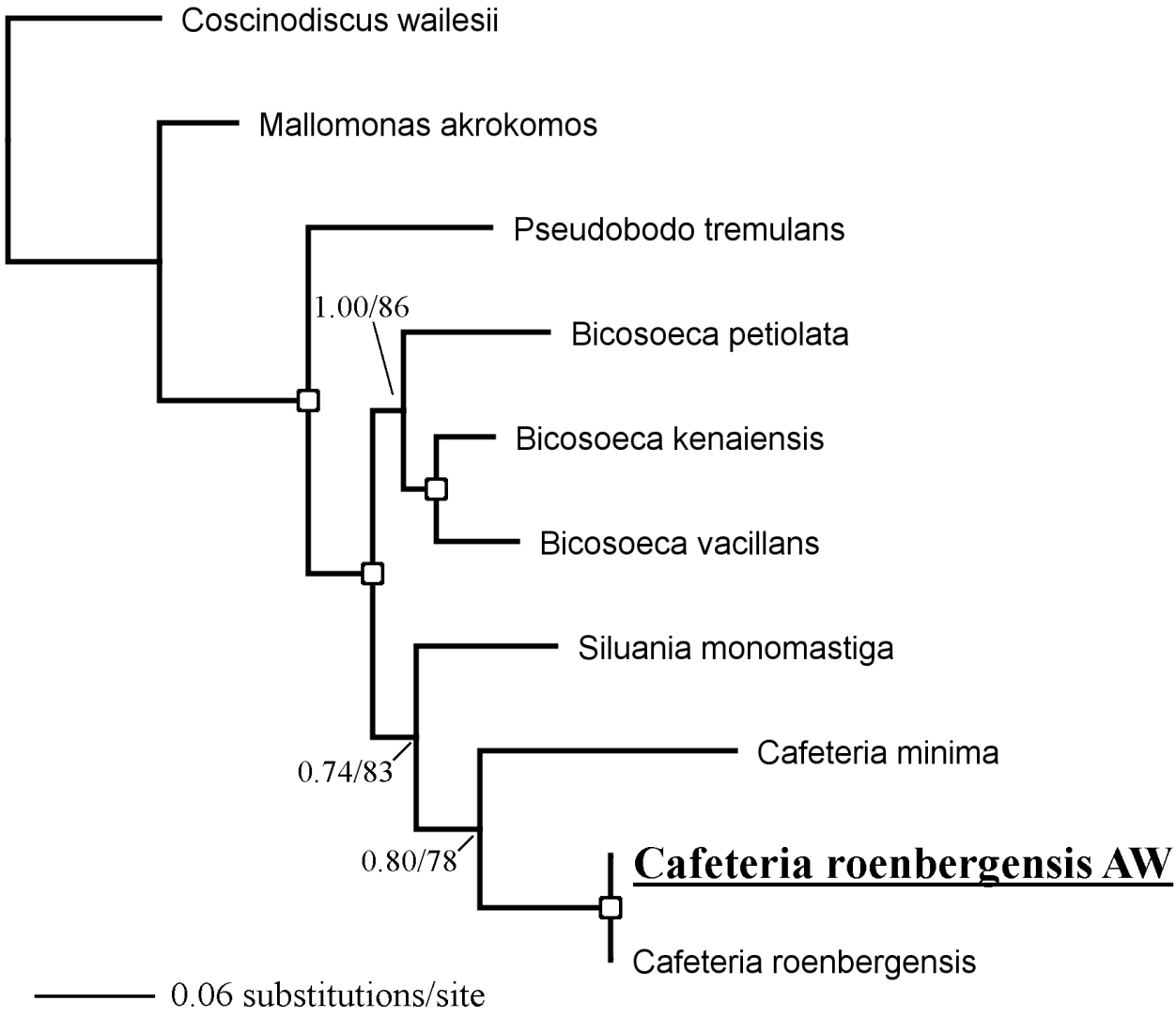

Figure 2. Maximum likelihood phylogeny of Bicosoecales (Bigyra) inferred from partial 18S rDNA sequences (1680 bp). The diatom *Coscinodiscus wailesii* Gran & Angst (HQ912668) was used as outgroup. Values indicate Bayesian posterior probabilities (pp) and PhyML (200 replicates) bootstrap support values (ML) (pp/ML). White squares indicate 1.00 pp and >90% ML. Support values <0.80 (pp) and <50% (ML) were excluded. The sequence from the present study is indicated with underline.

Division Chlorarachniophyta Hibberd & Norris
Class Chlorarachniophyceae Hibberd & Norris
Order Chlorarachniales Ishida & Hara
Genus *Lotharella* Ishida & Hara

Lotharella reticulosa Ota

Observations

The non-motile cells of the *Lotharella reticulosa* strain (UIO352) were spherical and 11.8 µm (Fig. 3a) to 27.1 µm (lower cell, Fig. 3i) in diameter. The cells displayed several green chloroplasts. The chloroplasts were distinct and located in the periphery of the coccoid cells (Fig. 3c) and overlapping in the cells in globular cells (Fig. 3d-e). The cells referred to as "globular cells" (Ota & Vaulot 2012) possessed granular cytoplasm and were usually significantly larger than the smaller coccoid cells. Most cells also displayed a large vacuole measuring up to 50% of the cell diameter (Fig. 3b) and an orange-brown particle measuring 25-30% of the cell diameter (Fig. 3a-b, e). No pyrenoid was observed. Some cells possessed conspicuous cell walls (Fig. 3g-h). Younger cultures were highly reticulated and displayed amoeboid cells with conspicuous filipodia (Fig. 3g-h). Swimming zoospores were rarely observed. It was elongate and 13.1 µm long and 2.9 µm to 4.2 µm wide and appeared to possess 3-4 chloroplasts (Fig. 3f). No flagellum was observed but assumed to be inserted apically. Observations suggested that the UIO352 strain grew very slowly at both 19 and 23°C. Young cultures were green in colour. The colour faded to grey as the cultures aged. Dense cultures gave off a very distinct odour.

In the phylogeny (Fig. 4) the sequence from the present study clustered with a reference sequence named *Lotharella reticulosa*. *Lotharella globosa* Ishida & Yaraand, *Lotharella oceanica* Ota and an unidentified chlorarachniophyte formed the sister group. The sequence in question is 99.5% (1674/1683 bp) identical to the most similar reference sequence (*L. reticulosa*, EF622539).

Locality: Seagrass bay, Saudi Arabia.
Habitat: Plankton, marine.

Discussion

The phylogeny from the present study is generally consistent with earlier phylogenies inferred from nucleomorph ITS rDNA (Gile et al. 2010), nuclear 18S rDNA (Ota & Vaulot 2012) and concatenated nuclear 18S and nuclear 28S rDNA (Ota et al. 2009). In all the analyses, genus *Lotharella* formed the sister group to genera *Bigelowiella* Moestrup, *Chlorarachnion* Geitler, *Norrisiella* Ota, Ueda & Ishida and *Partenskyella* Ota, Vaulot, Gall, Yabuki & Ishida. The topology

in the latter group has shown some incongruence between earlier studies including the present study. The topology within genus *Lotharella* in the present study is consistent with Ota & Vaulot (2012). The four different life stages of *L. reticulosa* described from the RCC375 strain from the original diagnosis (Ota & Vaulot 2012) were observed in the UIO352 strain. The morphological observations were generally consistent with respect to cell size and shape, the highly reticulated filipodia and chloroplast shape and location. No pyrenoid was observed in UIO352 but it is believed to be present as it is very small and may therefore be hard to observe in the light microscope. The only known chlorarachniophyte to lack pyrenoids is *Partenskyella glossopodia* Ota, Vaulot, Gall, Yabuki & Ishida which is very different from *L. reticulosa* morphologically and genetically (Ota et al. 2009).

As far as I know, the present study is the first to show a clear micrograph of the swimming zoospore of *L. reticulosa*. Attempts to show the flagellum were unsuccessful.

Lotharella reticulosa has only recorded once: in a relatively shallow habitat (5 m) in the Mediterranean Sea (Ota & Vaulot 2012), so no conclusions can be drawn regarding where it commonly occurs. Other chlorarachniophytes are known to mostly occur in the benthos, though, and specifically in temperate and tropical coastal regions (Ota et al. 2009).

For future studies I recommend acquiring the nucleomorph ITS rDNA sequence from UIO352 to use it for a concatenated nuclear 18S and nucleomorph ITS rDNA phylogeny. Also, TEM and light micrographs of the zoospore with a visible flagellum is needed as a supplement to the original diagnosis by Ota & Vaulot (2012).

Previous recordings of Lotharella reticulosa

Mediterranean Sea, Italy (Ota & Vaulot 2012).

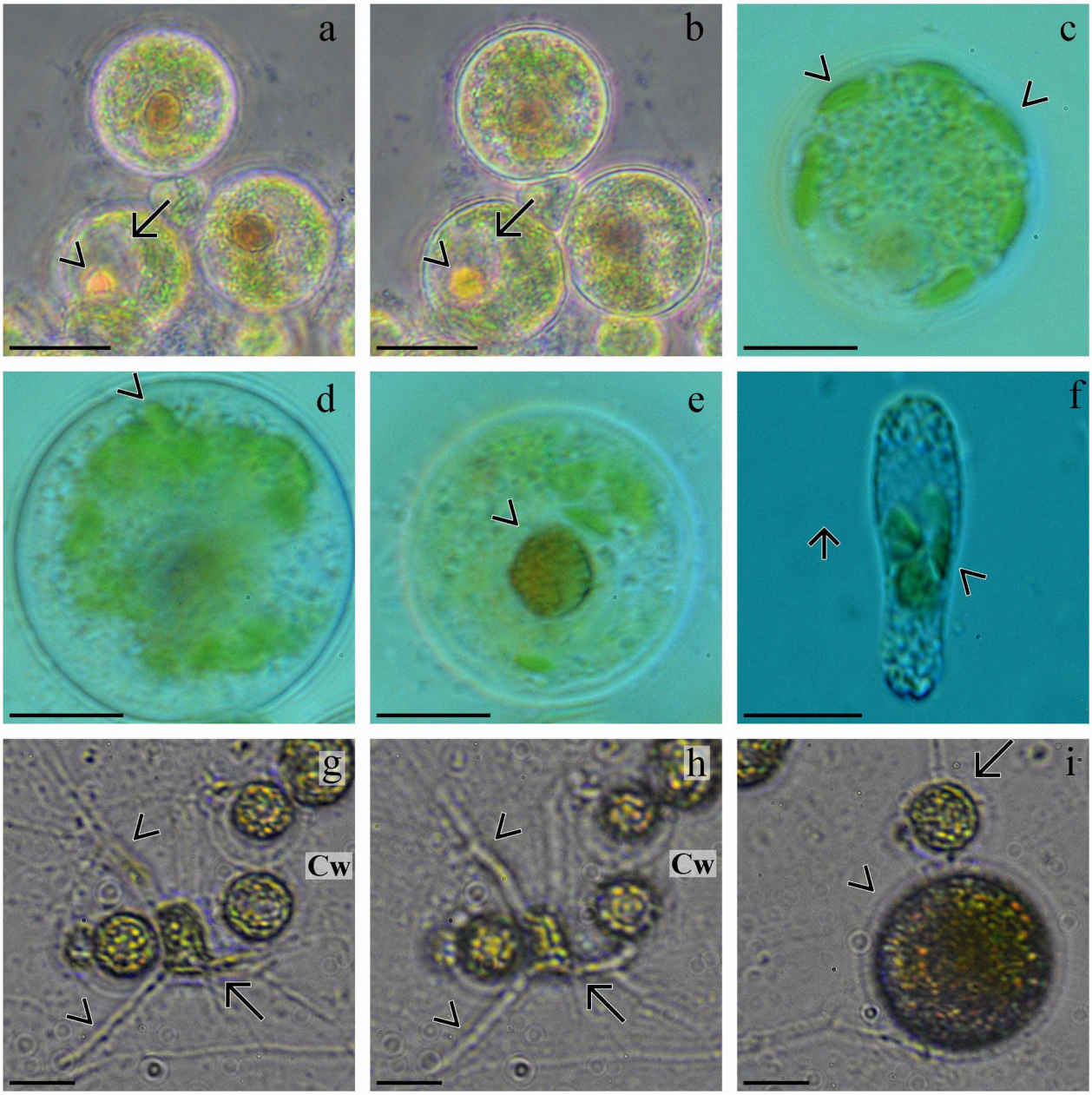

Figure 3. Phase contrast (a-b, g-i) and diffraction interference contrast (c-f) light micrographs of live amoeboid, coccoid, globular and flagellated *Lotharella reticulosa* cells (UIO352) showing cell shape, cell walls, chloroplasts, filipodia, vacuoles and orange-brown particles. a-b: three globular cells at two different focal points, vacuole (arrow), orange-brown particle (arrowhead); c: coccoid cell, chloroplast (arrowhead); d: globular cell, chloroplast (arrowhead); e: globular cell, orange-brown particle (arrowhead); f: flagellate, direction of swimming (arrow), chloroplast (arrowhead); g-h: cells at two different focal points, amoeboid cell (arrow), cell wall (Cw), filipodia (arrowhead); i: coccoid cells, coccoid cell (arrow), globular cell (arrowhead); scale bars: a-b = 10 µm, c-f = 5 µm, g-i: 10 µm.

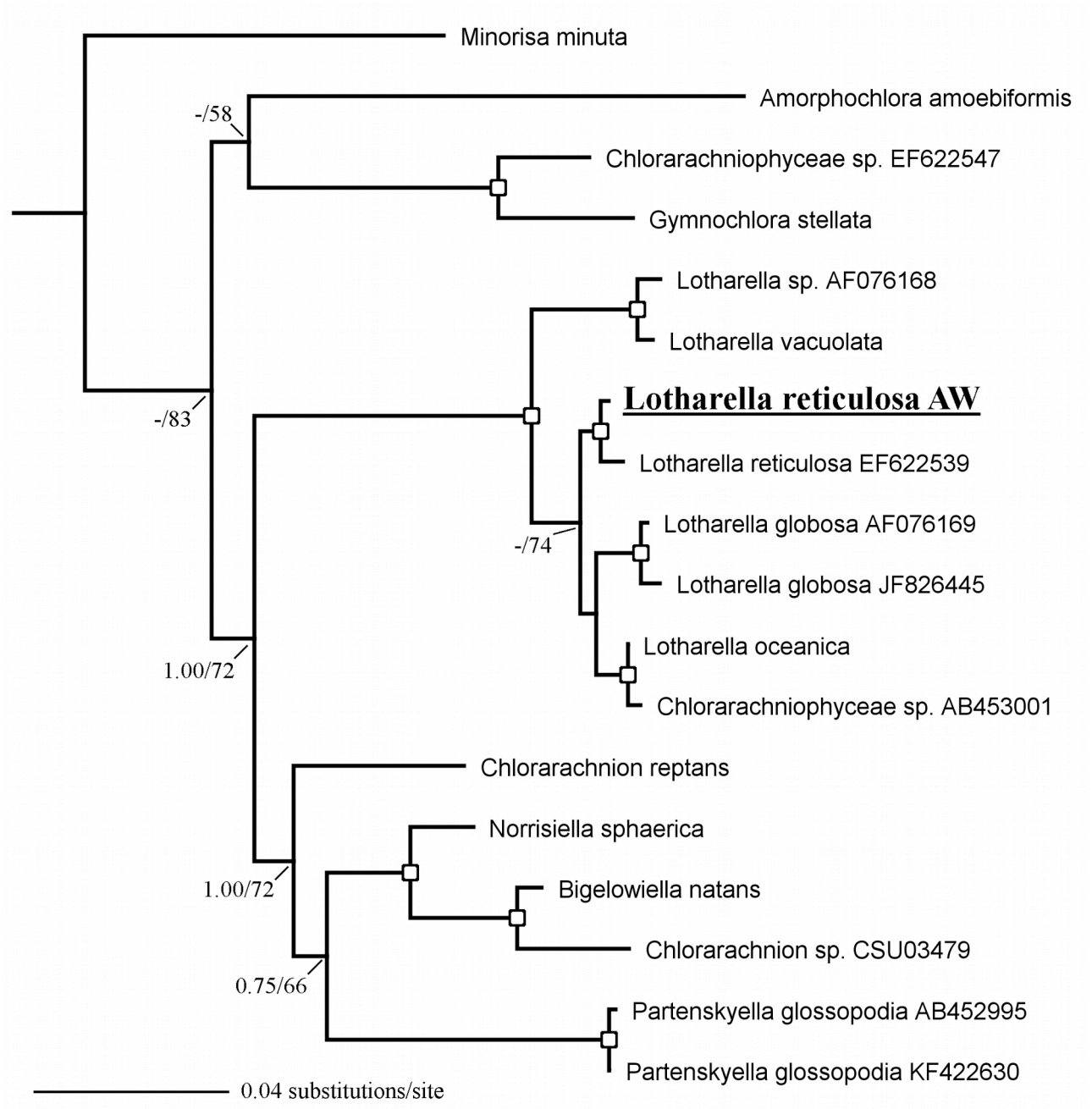

Figure 4. Maximum likelihood phylogeny of Chlorarachniophyceae (Chlorarachniophyta) inferred from partial nuclear 18S rDNA sequences (1718 bp). The Cercozoa species *Spongomonas minima* Dangeard (AF411280) was used as outgroup and pruned from the tree. Values indicate Bayesian posterior probabilities (pp) and PhyML (200 replicates) bootstrap support values (ML) (pp/ML). White squares indicate 1.00 pp and >90% ML. Support values <0.80 (pp) and <50% (ML) were excluded. Nodes marked with a hyphen (-) indicate topological incongruence between the Maximum likelihood and the Bayesian analyses. The sequence from the present study is indicated with underline.

Division Chlorophyta Pascher
Class Chlorodendrophyceae Massjuk
Order Chlorodendrales Melkonian
Genus *Tetraselmis* Stein

Tetraselmis sp.

Observations

The cells of the *Tetraselmis* sp. strain (UIO346) were ellipsoid with an apical depression (Fig. 5a) and sometimes a constricted cell equator in lateral view (Fig. 5b, c). The size ranged from 6 µm long and 4.1 µm wide (Fig. 5a) to 8.7 µm long and 5.1 µm wide (Fig. 5.e). The cells held a single green cup-shaped chloroplast (Fig. 5d, f) with a single pyrenoid of 1.8 µm x 2.0 µm (Fig. 5f) to 2.3 µm x 1.9 µm (Fig. 5f) and a conspicuous red-orange stigma (Fig. 5a-c) of 1.7 µm (Fig. 5e) and 2.2 µm (Fig. 5h). The chloroplasts were anteriorly lobed (Fig. 5d-f). No posterior lobes were observed. The four flagella were inserted in the apical depression (vaguely shown in Fig. 5a, b) and were approximately 6.8 µm (Fig. 5h). Observations suggested that most cells of the UIO346 strain were enclosed in a theca (Fig. 5a-g). These cells were always immotile whether the flagella were present or not. Fig. 5g shows two cells in the mother theca after cell division. These cells were oriented anterior next to anterior and posterior next to posterior. No stalks were observed. Observations also suggested that UIO346 grew well at both 19 and 23°C and was green in colour which faded to grey as the culture aged.

In the 18S rDNA phylogeny (Fig. 6) the sequence from the present study clustered with reference sequences named *Tetraselmis* sp., *T. striata*, *T. carteriiformis* (not taxonomically accepted) and *T. convolutae* (Parke & Manton) Norris, Hori & Chihara. *Tetraselmis suecica* (Kylin) Butcher, *T. tetrahele* (West) Butcher, *T. chuii* Butcher, *T. subcordiformis* (Willie) Butcher and *Tetraselmis* sp. formed the sister group. The sequence in question is 99.6% (1142/1147 bp) identical to the most similar reference sequence (*T. apiculata* (Butcher) Butcher, KJ756817).

In the 28S rDNA phylogeny (Fig. 7) the sequence from the present study clustered with a reference sequence named *T. striata*. The rest of the *Tetraselmis* reference sequences formed the sister group. The sequence in question is 96.6% (518/536 bp) identical to the most similar reference sequence (*T. striata*, HE610129).

Locality: Beach adjacent to the seagrass bay, Saudi Arabia.
Habitat: Sand beach, marine.

Discussion

The UIO346 strain shows high affinity for *T. striata* in the 28S rDNA phylogeny (Fig. 7) and some affinity to *T. striata* in the 18S rDNA phylogeny (Fig. 6). There are many described species within genus *Tetraselmis* (34), and most morphological criteria for species delimitation are poorly described leaving the taxonomy of the genus in a state of confusion (Guiry & Guiry 2015).

The cell size, pyrenoid shape, stigma size and location and chloroplast shape of UIO346 is consistent with the description of *T. striata* in the revision of genus *Tetraselmis* (subgenus *Parviselmis*) by Hori et al. (1986). On the other hand, the pyrenoid of *T. striata* was reported to be considerably smaller (0.8 µm-1.5 µm x 1.0 µm) than in UIO346 (2.3 µm x 1.9 µm (Fig. 5f)). An important character used for species delimitation within genus *Tetraselmis* as proposed by Hori et al. (1986) is the cytoplasmic canaliculi invading the pyrenoid matrix (pyrenoid and surrounding starch grains). Ultra-thin TEM sections of UIO346 is needed to study this character.

The cells size, stigma size and chloroplast shape of UIO346 is consistent with the description of *T. convolutae* in the revision of genus *Tetraselmis* (subgenus *Tetraselmis*) by Hori et al. (1982). On the other hand, the stigma of *T. convolutae* is located laterally rather than dorsally/ventrally as in UIO346 (Fig. 5h). Also, *T. convolutae* is reported to occasionally form short stalks. This has not been observed for UIO346.

The cell size, chloroplast shape and pyrenoid size, shape and location of UIO346 is consistent with the description of *T. rubens* Butcher (not taxonomically accepted) from Throndsen et al. (2007). On the other hand, the stigma is located ventrally in *T. rubens* rather than dorsally/ventrally as in UIO346 (Fig. 5h).

Genus *Tetraselmis* is commonly found both in marine benthic habitats and open water (Arora et al. 2013).

For future studies I recommend acquiring ultra-thin TEM sections and a complete 18S rDNA sequence for UIO346. At this point, UIO346 can only be described to the genus level based on the morphology and phylogenies from the present study.

A small selection of previous recordings of genus Tetraselmis

Atlantic Ocean, Conway, Wales (Hori et al. 1986).

Baltic Sea (Hällfors 2004).

Indian Ocean, Goa, India (Arora et al. 2013).

Mediterranean Sea, Spain (RCC500) (RCC 2015).

Pacific Ocean, North America and Japan (Hori et al. 1982).

Red Sea, Gulf of Eliat, Israel (RCC4479) (RCC 2015).

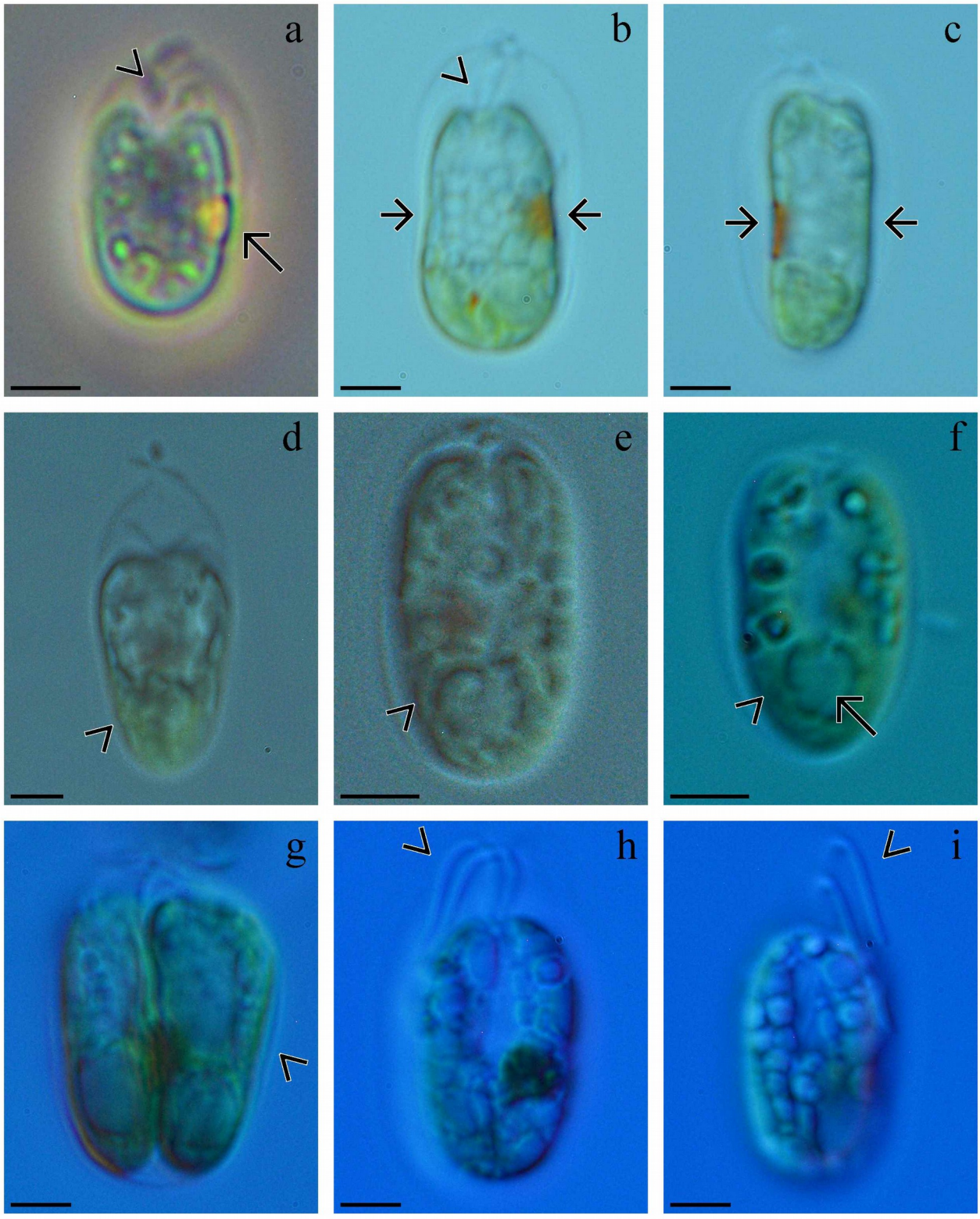

Figure 5. Phase contrast (a) and diffraction interference contrast (b-f) light micrographs of live *Tetraselmis* sp. cells (UIO346) showing cell shape, thecae, chloroplasts, stigmata, flagella and pyrenoids. a: lateral view, stigma (arrow), apical depression (arrowhead); b-c: lateral view, constriction (arrows), flagella (arrowhead); d-e: ventral/dorsal view, chloroplast (arrowhead); f: pyrenoid (arrow), chloroplast (arrowhead); g: two cells undergoing cell division inside the mother theca, theca (arrowhead); h-i: ventral/dorsal view of cell without theca at two different focal points, 4 flagella (arrowhead); scale bars: a-i = 2 μm.

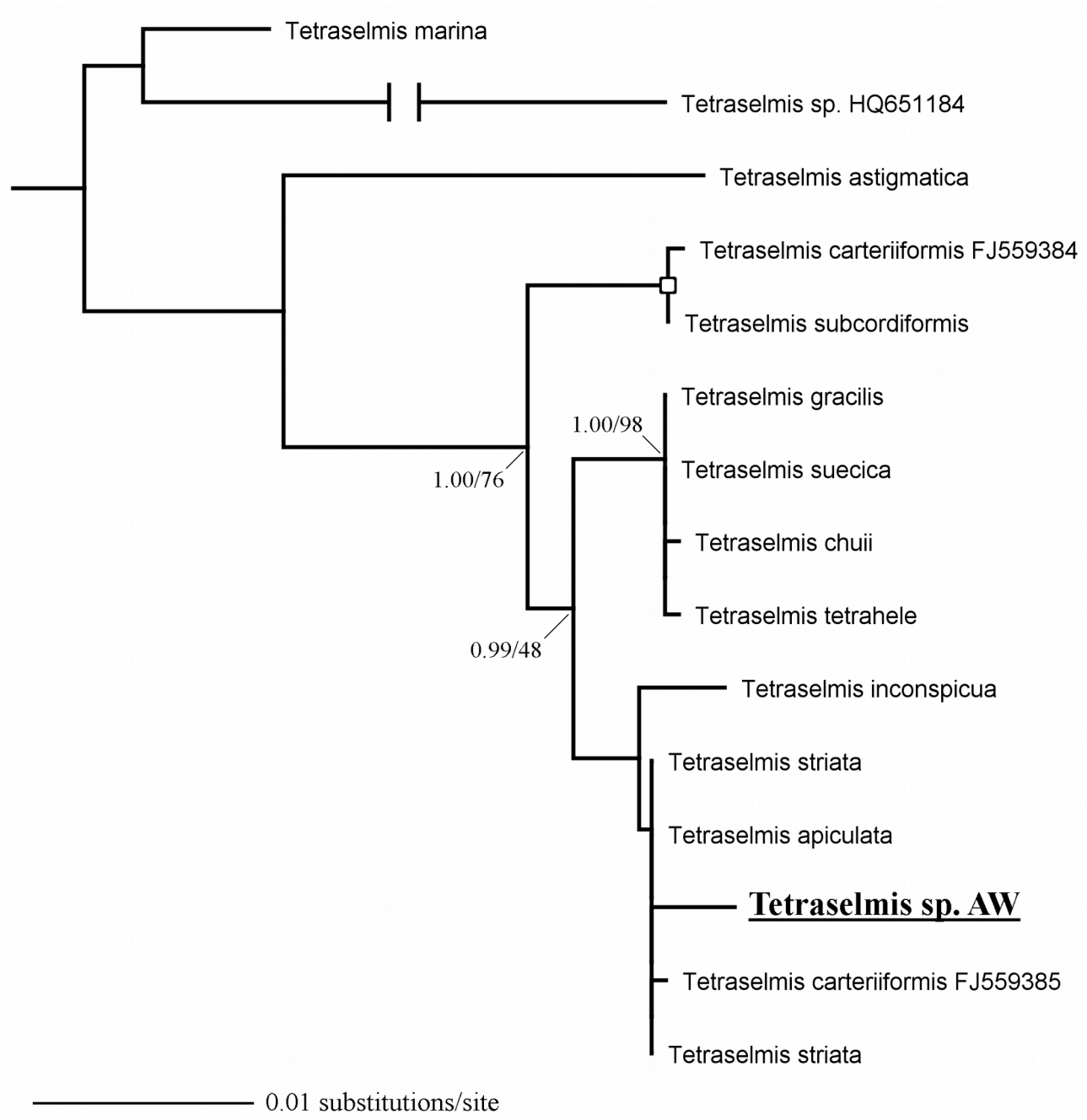

Figure 6. Maximum likelihood phylogeny of *Tetraselmis* (Chlorophyta) inferred from partial 18S rDNA sequences (1682 bp). The trebouxiophyte *Trebouxia impressa* Ahmadjian (Z21551) was used as outgroup and pruned from the tree. Values indicate Bayesian posterior probabilities (pp) and PhyML (1000 replicates) bootstrap support values (ML) (pp/ML). White squares indicate 1.00 pp and >90% ML. Support values <0.80 (pp) and <50% (ML) were excluded. Nodes marked with a hyphen (-) indicate topological incongruence between the Maximum likelihood and the Bayesian analyses. Vertical lines a breach indicate a 75% reduction in branch length. The sequence from the present study is indicated with underline.

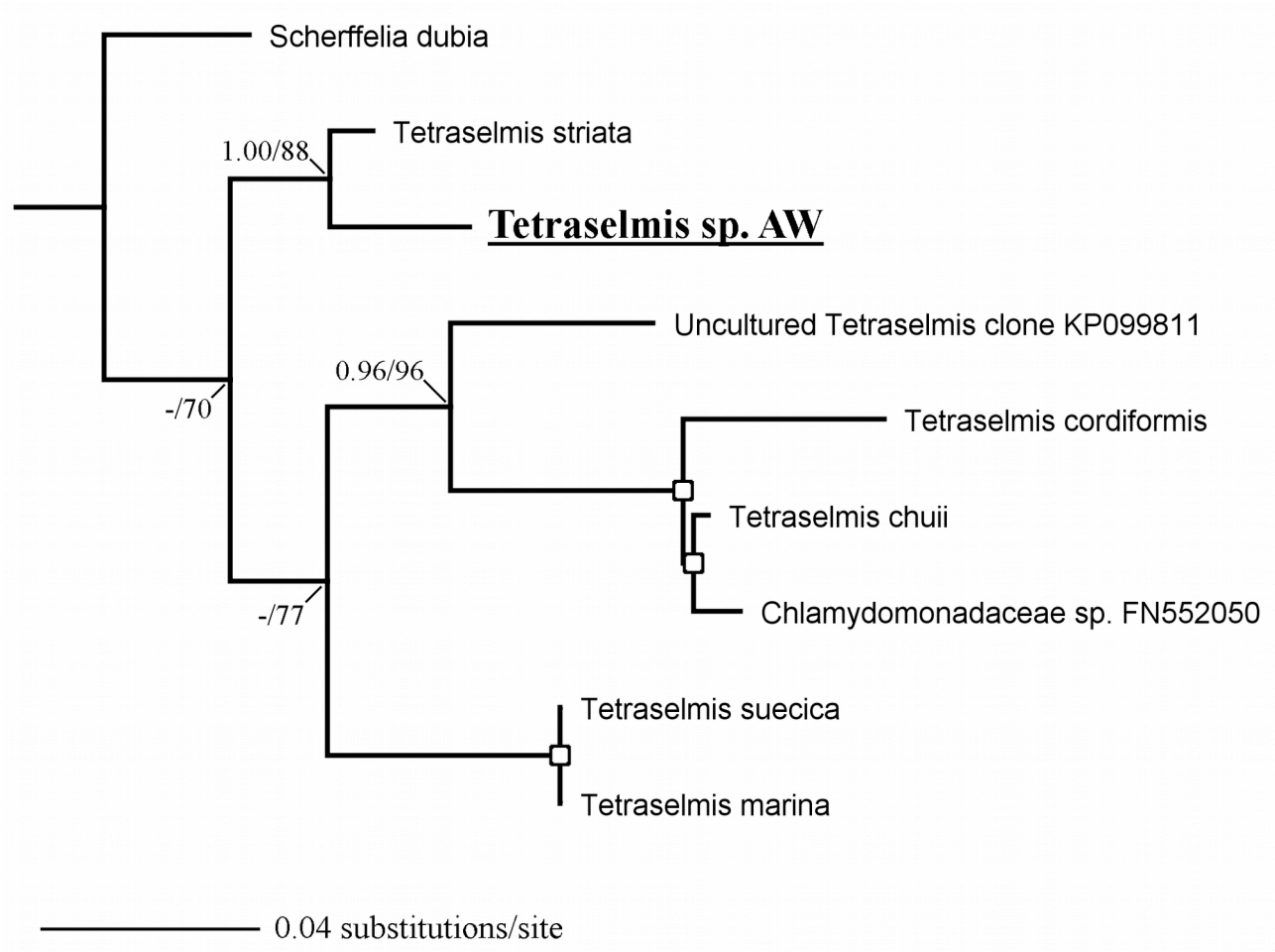

Figure 7. Maximum likelihood phylogeny of *Tetraselmis* (Chlorophyta) inferred from partial 28S rDNA sequences (1570 bp). The chlorophyte *Dunaliella salina* (Dunal) Teodoresco (EF473746) was used as outgroup and pruned from the tree. Values indicate Bayesian posterior probabilities (pp) and PhyML (1000 replicates) bootstrap support values (ML) (pp/ML). White squares indicate 1.00 pp and >90% ML. Support values <0.80 (pp) and <50% (ML) were excluded. Nodes marked with a hyphen (-) indicate topological incongruence between the Maximum likelihood and the Bayesian analyses. The sequence from the present study is indicated with underline.

Division Chlorophyta Pascher
Class Chlorophyceae Willie
Order Chlamydomonadales Fritsch
Genus *Chlamydomonas* Ehrenberg

Chlamydomonas sp.

Observations

The flagellated cells of the *Chlamydomonas* sp. strain (UIO350) were ellipsoid and approximately 6 µm long and 4 µm wide (Fig. 8a, b). The non-motile cell (Fig. 8c) was slightly larger (7 µm long and 6.1 µm wide) and spheroid with a slight bilateral compression. The two apically inserted flagella were c. 80% of the cell length (5 µm). A pronounced papilla (Fig. 8c) was located apically between the flagella. The cell division took place twice inside the mother cell wall as shown in Fig. 8d and 8e, which are micrographs of the same four cells at two different focal points. The cell wall was clearly displayed in the thin sections (Fig. 8g, h). The cells held a single green cup-shaped chloroplast with a prominent red-orange stigma and one (Fig. 8g) or two (Fig. 8h) pyrenoids. Starch grains were shielding the pyrenoids and appeared numerously elsewhere in the chloroplast. The chloroplast was also holding several lipid drops. The lamellae are shown in Fig. 8g and 8h, but the resolution is too low to show thylakoid number and grana. The Golgi body was located adjacent to the apically located nucleus. The nucleus displayed a prominent nucleolus (Fig. 8h). The cells possessed 1-2 mitochondria (Fig. 8f). Observations suggested that the UIO350 strain grew well at both 19 and 23°C. Young cultures were green in colour. The cultures turned grey as they aged. The unidentified structures (Fig. 8g-h) between the cell wall and the cell membrane are assumed to be artefacts. These were most likely caused by cell shrinking due to dehydration of the cell material during fixation. The attempt to find reports of similar structures from closely related species in the literature was unsuccessful.

In the phylogeny (Fig. 9) the sequence from the present study clustered with three reference sequences from the Marine Biotechnology Institute Culture Collection (MBIC), Japan (now NITE), named *Chlamydomonas* sp. *Chlamydomonas raudensis* Ettl and *C. parkeae* formed the sister group. The sequence in question is 100% (1748/1748 bp) identical to the most similar reference sequences (*Chlamydomonas* sp. MBIC10468, AB058349; *Chlamydomonas* sp. MBIC10471, AB058350 and *Chlamydomonas* sp. MBIC10473, AB058351).

Locality: Seagrass bay, Saudi Arabia.
Habitat: Plankton, marine.

Discussion

Genus *Chlamydomonas* is a large genus currently comprised of 577 taxonomically accepted species (Guiry & Guiry 2015), and phylogenetic analyses using 18S rDNA and chloroplast genes have shown it to be polyphyletic (Buchheim et al. 1997; Hoham et al. 2002). The polyphyly is also shown in the phylogeny from present study (Fig. 9), where genera *Chlorococcum* Meneghini, *Oogamochlamys* Pröschold, Marin, Schlösser & Melkonian and *Tetracystis* Brown & Bold among others appear within genus *Chlamydomonas*. The clustering in the present study is generally consistent with previous studies, but low support values at basal nodes render larger clades unresolved. Still, *C. parkeae*, *C. raudensis*, the MBIC strains (10468, 10471, 10473) and the strain from the present study clustered together with high support values. Attempts to retrieve morphological data for the MBIC strains have been unsuccessful, and are assumingly not available (Klochkova et al. 2008). The mentioned MBIC strains have been included in previous phylogenetic analyses (Ball 2006; Yumoto et al. 2013). *Chlamydomonas raudensis* is, in strong contrast to the UIO350 strain, a freshwater species (Ettl 1976) and can consequentially not be the same species. Also, there is striking dissimilarity in the flagella and possibly also the pyrenoid number between the UIO350 strain and the strain from the original diagnosis of *C. parkeae*, the most genetically similar species. The two flagella of UIO350 were c. 75% (Fig. 8a) and c. 90% (Fig. 8b) of the cell length. *Chlamydomonas parkeae* is described to possess flagella of three to four times the cell length (Sasa et al. 1992). Also, the UIO350 strain possessed one (Fig. 8g) or two (Fig. 8h) pyrenoids. *Chlamydomonas parkeae* is described to only possess one, although this may have occurred in the original strain without being observed.

A less striking difference between the UIO350 strain and *C. parkeae* is the colour. The cells and cultures of UIO350 are green, whereas the cells and cultures of *C. parkeae* are described to be yellow (Sasa et al. 1992; Kim et al. 1994).

Genus *Chlamydomonas* is mostly found in freshwater habitats (Guiry & Guiry 2015), but are also known to occur in the marine environment including the benthos (Throndsen et al. 2007).

A large selection of the available reference sequences most similar to the UIO350 were included in the phylogeny in the present study (Fig. 9), but many species in the genus have not been sequenced. Genus *Chlamydomonas* is characterised by its vast species diversity, and the taxonomy is in a state of confusion. This makes it impossible to conclude whether the UIO350 is an undescribed *Chlamydomonas* species or not. Ettl and Schlösser are currently re-examining, and a taxonomic revision seems inevitable (Guiry & Guiry 2015). Nevertheless, I conclude that UIO350 is the first morphological description of this genotype.

For future studies I recommend comparing the morphology of UIO350 with more known

Chlamydomonas strains.

A small selection of previous recordings of genus Chlamydomonas

English Channel, Plymouth, England (Ettl 1967).

Pacific Ocean, Hachinohe Harbor, Aomori Prefecture, Japan (Sasa et al. 1992).

Pacific Ocean, Izumi Bay, Tsushima Island, Japan (Sasa et al. 1992).

Pacific Ocean, Mitsu Bay, Hiroshima, Japan (NIES1022) (NIES 2015).

Pacific Ocean, Sanriku Coast, Iwate, Japan (NBRC102834) (NBRC 2015).

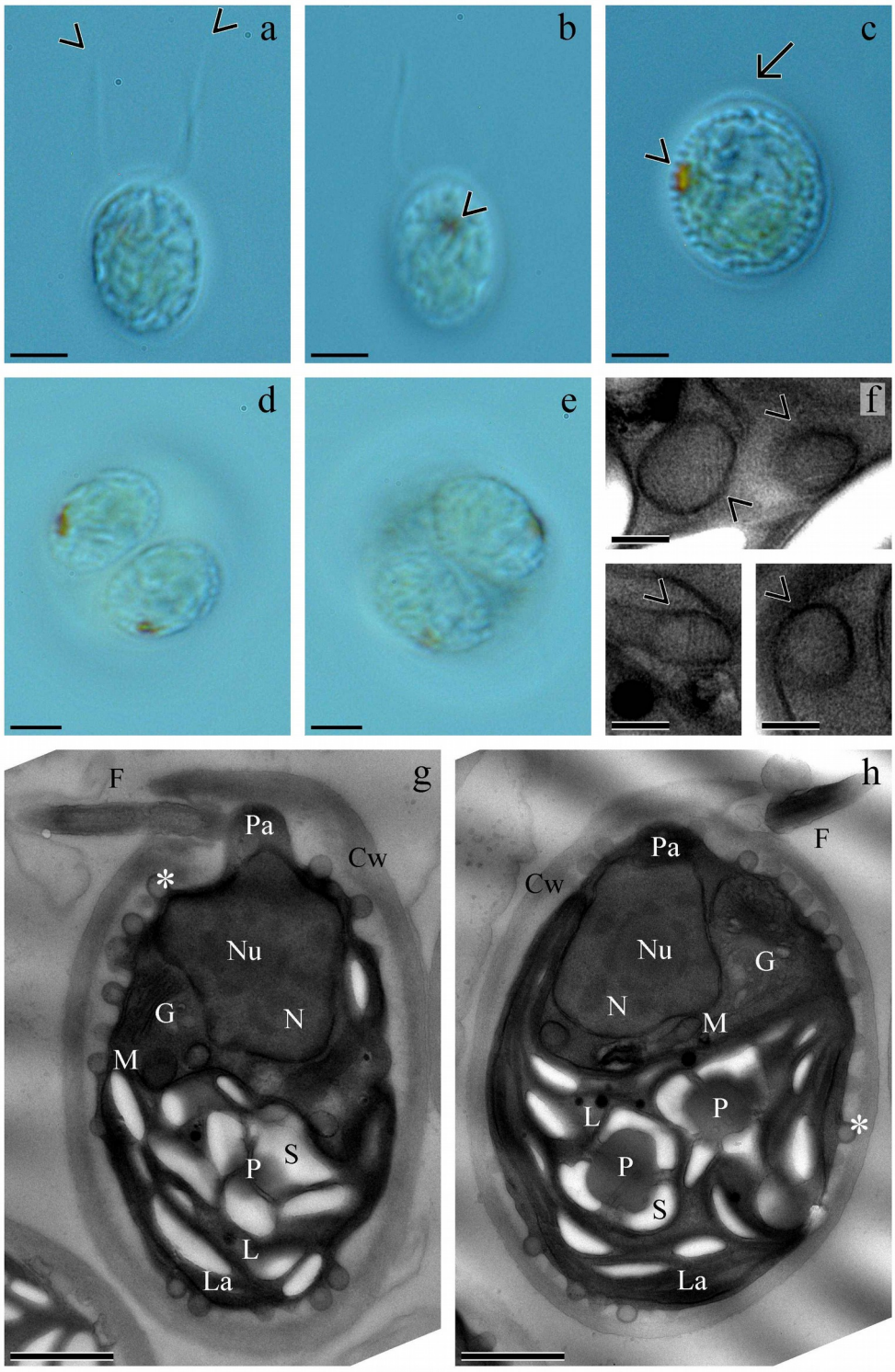

Figure 8. Diffraction interference contrast light micrographs of live cells (a-e) and transmission electron micrographs (f-h) of ultra-thin sections of *Chlamydomonas* sp. cells (UIO350) (dorsal/ventral view) showing cell shape, cell walls, chloroplasts, flagella and other structures. a: motile cell, flagellum (arrowhead); b: motile cell, stigma (arrowhead); c: non-motile cell, papilla (arrow), stigma (arrowhead); d-e: four non-motile cells at two different focal points undergoing cytokinesis inside the mother wall; f: section of motile cell, mitochondrion (arrowhead); g-h: sections of motile cells, cell wall (Cw), flagellum (F), Golgi body (G), lipid (L), lamella (La), mitochondrion (M), nucleus (N), nucleolus (Nu), pyrenoid (P), papilla (Pa), starch grains (S), unidentified structure (*); scale bars: a-e = 2 µm, f = 200 nm, g-h = 1 µm.

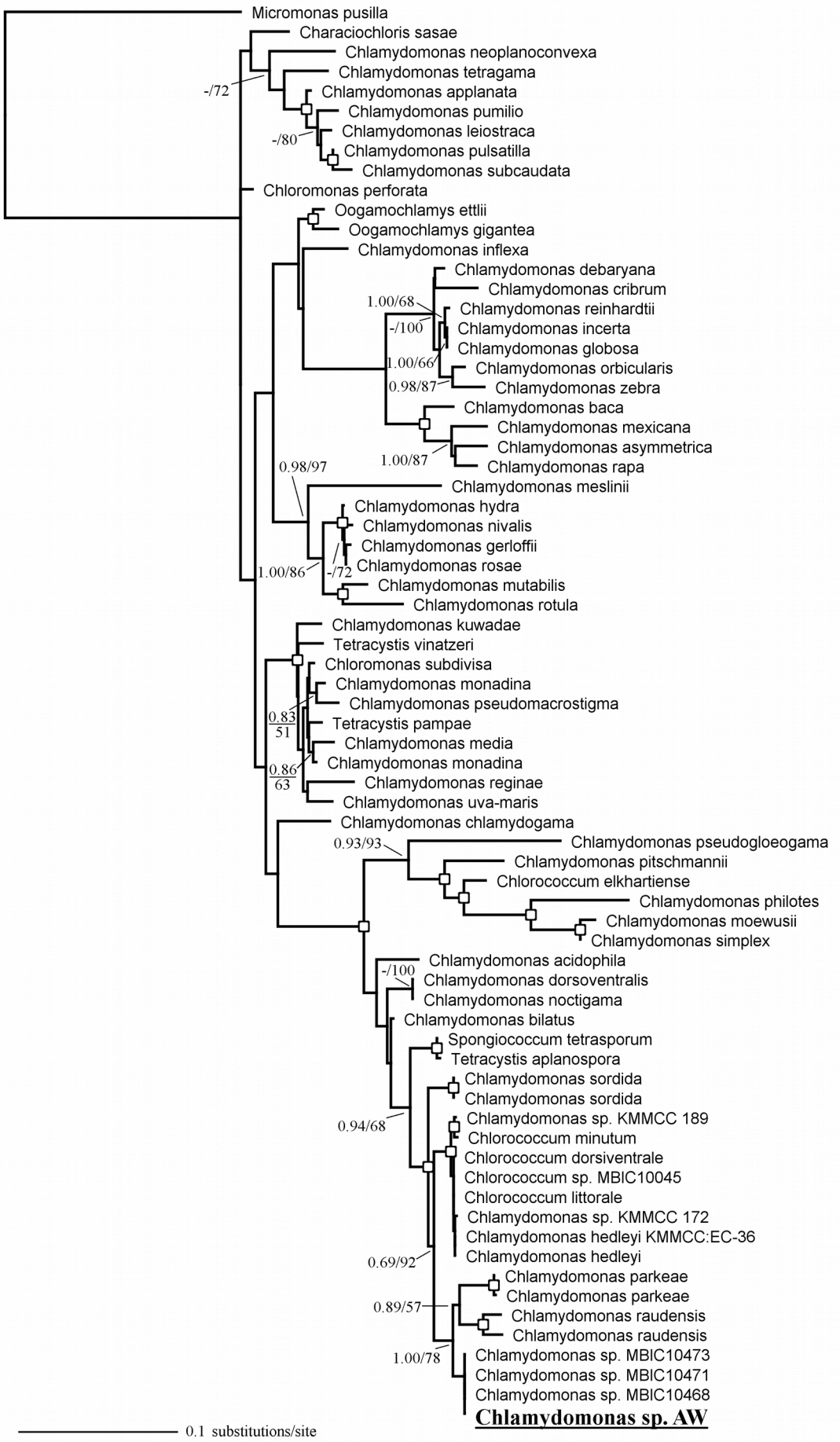
Micromonas pusilla
Characiochloris sasae
Chlamydomonas neoplanoconvexa
Chlamydomonas tetragama
-/72
Chlamydomonas applanata
Chlamydomonas pumilio
Chlamydomonas leiostraca
-/80
Chlamydomonas pulsatilla
Chlamydomonas subcaudata
Chloromonas perforata
Oogamochlamys ettlii
Oogamochlamys gigantea
Chlamydomonas inflexa
Chlamydomonas debaryana
Chlamydomonas cribrum
1.00/68
Chlamydomonas reinhardtii
-/100
Chlamydomonas incerta
Chlamydomonas globosa
1.00/66
Chlamydomonas orbicularis
0.98/87
Chlamydomonas zebra
Chlamydomonas baca
Chlamydomonas mexicana
Chlamydomonas asymmetrica
1.00/87
Chlamydomonas rapa
0.98/97
Chlamydomonas meslinii
Chlamydomonas hydra
Chlamydomonas nivalis
Chlamydomonas gerloffii
1.00/86
-/72
Chlamydomonas rosae
Chlamydomonas mutabilis
Chlamydomonas rotula
Chlamydomonas kuwadae
Tetracystis vinatzeri
Chloromonas subdivisa
Chlamydomonas monadina
Chlamydomonas pseudomacrostigma
0.83
51
Tetracystis pampae
Chlamydomonas media
Chlamydomonas monadina
0.86
63
Chlamydomonas reginae
Chlamydomonas uva-maris
Chlamydomonas chlamydogama
0.93/93
Chlamydomonas pseudogloeogama
Chlamydomonas pitschmannii
Chlorococcum elkhartiense
Chlamydomonas philotes
Chlamydomonas moewusii
Chlamydomonas simplex
Chlamydomonas acidophila
-/100
Chlamydomonas dorsoventralis
Chlamydomonas noctigama
Chlamydomonas bilatus
Spongiococcum tetrasporum
Tetracystis aplanospora
Chlamydomonas sordida
Chlamydomonas sordida
0.94/68
Chlamydomonas sp. KMMCC 189
Chlorococcum minutum
Chlorococcum dorsiventrale
Chlorococcum sp. MBIC10045
Chlorococcum littorale
Chlamydomonas sp. KMMCC 172
Chlamydomonas hedleyi KMMCC:EC-36
0.69/92
Chlamydomonas hedleyi
Chlamydomonas parkeae
0.89/57
Chlamydomonas parkeae
Chlamydomonas raudensis
Chlamydomonas raudensis
1.00/78
Chlamydomonas sp. MBIC10473
Chlamydomonas sp. MBIC10471
Chlamydomonas sp. MBIC10468
Chlamydomonas sp. AW
0.1 substitutions/site

Figure 9. Maximum likelihood phylogeny of *Chlamydomonas* (Chlorophyta) inferred from partial 18S rDNA sequences (1750 bp). The prasinophyte *Micromonas pusilla* (Butcher) Manton & Parke (KF501035) was used as outgroup and pruned from the tree. Values indicate Bayesian posterior probabilities (pp) and PhyML (1000 replicates) bootstrap support values (ML) (pp/ML). White squares indicate 1.00 pp and >90% ML. Support values <0.80 (pp) and <50% (ML) were excluded. Nodes marked with a hyphen (-) indicate topological incongruence between the Maximum likelihood and the Bayesian analyses. The sequence from the present study is indicated with underline.

Division Cryptophyta Cavalier-Smith
Class Cryptophyceae Fritsch
Order Pyrenomonadales Novarino & Lucas
Genus *Proteomonas* Hill & Wetherbee

Proteomonas aff. *sulcata* Hill & Wetherbee

Observations

The cell size of the *Proteomonas* aff. *sulcata* strain (UIO376) ranged from 6.2 µm long and 3.4 µm wide (Fig. 10a) to 7.4 µm long and 3.8 µm wide (Fig. 10b). The cells possessed two flagella (one long and one slightly shorter) inserted in the ventro-subapical depression. No furrow or gullet was observed. The longer flagellum was approximately 80% (c. 7.6 µm) of the cell length and the shorter flagellum approximately 80% (c. 6.1 µm) of the longer flagellum (Fig. 10a). The diplomorph cells (Fig. 10d) were covered with hexagonal periplast plates (c. 1.1 x 0.9 µm), and the haplomorph cells (Fig. 10e) with tetragonal plates (c. 0.5 x 0.5 µm). The cells held a single green parietal chloroplast with a prominent pyrenoid (Fig. 10b) with a starch shield (Fig. 10h) located dorsally in the cell. The chloroplast contained lamellae of two thylakoids (not shown) and a starch grain (Fig. 10f). The outer chloroplast membrane was continuous with the nuclear membrane (Fig. 10f). The Golgi body was located between the flagella and the central nucleus without a visible nucleolus. A mitochondrion was located adjacent to the flagella (Fig. 10f). No nucleomorph was observed. Observations suggested that the UIO376 strain grew slowly at 19°C and much faster at 23°C and that the colour was light green in young cultures and grey-green in older cultures.

In the phylogeny (Fig. 11) the sequence from the present study clustered with two *Proteomonas sulcata* sequences. *Falcomonas daucoides* (Conrad & Hufferath) Hill formed the sister group. The sequence in question is 99.5% (1732/1740 bp) identical to the most similar reference sequence (*P. sulcata*, HM126536).

Locality: Beach adjacent to seagrass bay, Saudi Arabia.

Habitat: Sandy beach, marine.

Discussion

The *Proteomonas* aff. *sulcata* strain (UIO376) is believed to be a novel cryptophyte species. The phylogeny from the present study is generally consistent with earlier work (Hoef-Emden 2008; Hoef-Emden et al. 2002). The topology differs at several nodes, but most clades are similar. The affinity of the *Proteomonas* clade varies greatly in earlier studies. In the nuclear 18S rDNA phylogeny from Hoef-Emden et al. (2002) *P. sulcata* formed the sister group of *Falcomonas daucoides*, the polyphyletic *Chroomonas* Hansgirg and the monophyletic *Hemiselmis* Parke clade. In the nucleomorph 18S rDNA phylogeny from the same study it showed affinity to genera *Hanusia* and *Guillardia* Hill & Wetherbee. In the nuclear 18S rDNA phylogeny from Hoef-Emden (2008) the *P. sulcata* placement was unresolved. Despite the *Proteomonas* aff. *sulcata* strain being highly similar (99.5%) to the reference sequence (*P. sulcata*, HM126536), I report a striking dissimilarity in the cell surface of the diplomorph cell and possibly also the haplomorph cell between the UIO376 and the strain from the original diagnosis. Both the original species diagnosis (Hill & Wetherbee 1986) based on the MUCC Cr8 culture and other descriptions (Cerino & Zingone 2006) described the diplomorph cells as to possess no outer or inner periplast scales, whereas the diplomorph cell of the UIO376 strain clearly possess numerous hexagonal plates. Also, Hill & Wetherbee (1986) and Cerino & Zingone (2006) reported the haplomorph cells to possess hexagonal plates, whereas the plates of the haplomorph cells of the UIO376 strain seem to be tetragonal. More work with the SEM material is needed in order to conclude on this point. Thirdly, the original diagnosis reported possession of ejectosomes which has not been observed for UIO376. The cell shape, cell size and chloroplast, pyrenoid, nucleus and Golgi body locations are consistent with the original diagnosis. Neither morphotypes of the UIO376 strain displayed furrows, but SEM photographs of different angles may uncover this cell feature. In addition to *P. sulcata*, genus *Proteomonas* consists of two taxonomically accepted species: *Proteomonas pseudobaltica* Novarino and *P. pseudobaltica* var. *leonardiana* Novarino. No 18S rDNA sequences are available for these species, and no hexagonal plates have been reported in diplomorph cells of either species (Novarino 1991). The unidentified structures (Fig. 10c, f-g) are believed to be storage products (e.g. chrysolaminarin).

The 18S rDNA sequence acquired from UIO376 is highly similar to the closest *P. sulcata* sequence (99.5% (1732/1740 bp)). By comparison, though, *Hemiselmis brunnescens* Butcher (AJ007282) and *H. rufescens* Parke (AJ007283) also share 99.5% (1753/1761 bp) of the bases in

the nuclear 18S rDNA region. The nucleomorph 18S rDNA sequences of said species, though, are only 97.4% (1649/1693) identical (EF594309 and EF594304). This high dissimilarity in nucleomorph 18S rDNA within genus *Hemiselmis* does not necessarily apply to genus *Proteomonas*, but nuclear 18S rDNA appears to be less suitable for species delimitation within Pyrenomonadales than the nucleomorph 18S rDNA.

A less striking difference between the UIO376 strain and the strains from the original diagnosis is the colour of the cultures. The diplomorph and the haplomorph strain from Hill & Wetherbee (1986) were deep red and bright red respectively in exponential phase, and both faded to yellow and green when the cultures aged. Observations suggested that UIO376, which is assumed to still possess both morphotypes, was green in exponential phase and faded to yellow as it aged. Another minor inconsistency is the nucleolus centrally located in the nucleus being present in the UIO376 strain. This structure was not reported in the original diagnosis.

Proteomonas sulcata has been recorded in too few locations to conclude where it commonly occurs, but it has been recorded in a shallow habitat on the coast of Italy (Cerino & Zingone 2006).

For future studies I recommend acquiring SEM photographs showing the furrows of both morphotypes of UIO376 if present and TEM photographs showing the nucleomorph as this will be necessary for a diagnosis. Also, light micrographs of both morphotypes and micrographs in lateral view must be obtained, as the ploidy levels of the UIO376 cells (Fig. 10a-c) are unknown, and ejectosomes must be described if present. Also, nucleomorph 18S rDNA should be sequenced from UIO376 and included in a concatenated nuclear and nucleomorph 18S rDNA phylogeny as done by Hoef-Emden et al. (2002). Additionally, a pigment analysis will be helpful as pigmentation is considered a strong criterion for cryptophyte species delimitation (Klaveness 1988; Hoef-Emden et al. 2002).

Previous recordings of Proteomonas sulcata

Mediterranean Sea, Gulf of Naples, Italy (Cerino & Zingone 2006).

Pacific Ocean, Fitzroy Island, Australia (Levy et al. 2007).

Pacific Ocean, Gulf of California, Mexico (CCMP705) (NCMA 2015).

Pacific Ocean, Victoria, Australia (Hill & Wetherbee 1986).

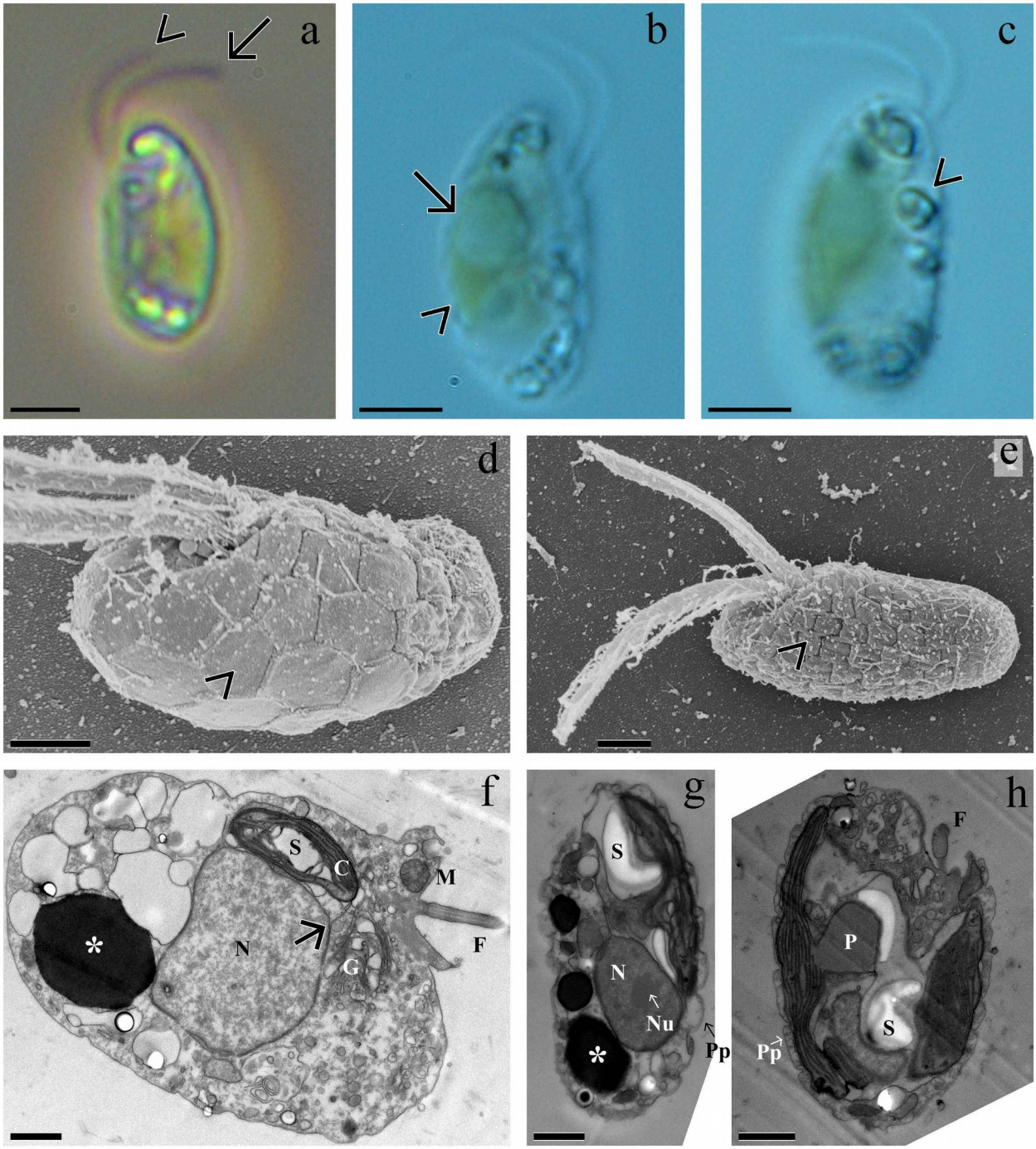

Figure 10. Phase contrast (a) and diffraction interference contrast (b-c) light micrographs of live cells, scanning electron micrographs (d-e) and transmission electron micrographs (f-h) of ultra-thin sections of *Proteomonas* aff. s*ulcata* cells (UIO376) (lateral view) showing cell shape, chloroplasts, flagella, and other cell structures. a: arrow = long flagellum, arrowhead = short flagellum; b: pyrenoid (arrow), chloroplast (arrowhead); c: unidentified structure (arrowhead); d: diplomorph cell, hexagonal periplast plate (arrowhead); e: haplomorph cell, flagellar hair (arrow), tetragonal periplast plates (arrowhead); f-h: outer chloroplast membrane continuous with nuclear membrane (arrow), flagellum (F), Golgi body (G), mitochondrion (M), nucleus (N), nucleolus (Nu), pyrenoid (P), starch grain (S), vacuole (V), unidentified structure (*); scale bars: a-c = 2 µm, d-h = 1 µm.

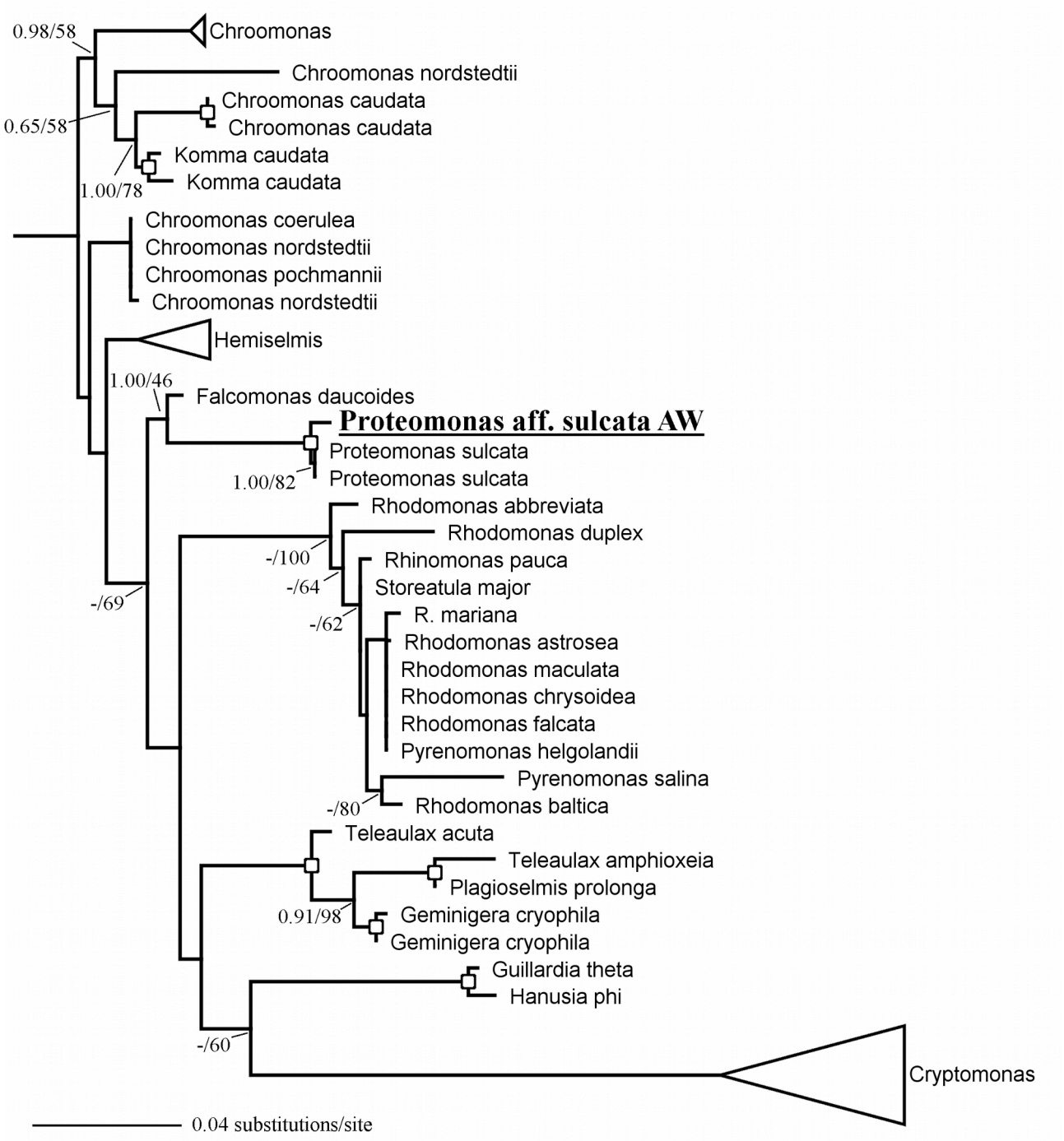

Figure 11. Maximum likelihood phylogeny of Pyrenomonadales (Cryptophyta) inferred from partial nuclear 18S rDNA sequences (1697 bp). The cryptophyte *Goniomonas amphinema* Larsen & Patterson (AY705738) was used as outgroup and pruned from the tree. Values indicate Bayesian posterior probabilities (pp) and PhyML (200 replicates) bootstrap support values (ML) (pp/ML). White squares indicate 1.00 pp and >90% ML. Support values <0.80 (pp) and <50% (ML) were excluded. Nodes marked with a hyphen (-) indicate topological incongruence between the Maximum likelihood and the Bayesian analyses. White triangles indicate collapsed clades (See Appendix IV (Fig. 23) for the complete phylogenetic tree). The sequence from the present study is indicated with underline.

Division Dinophyta Round
Class Dinophyceae Fritsch
Order Gymnodiniales Apstein
Genus *Amphidinium* Claperède & Lachmann

Amphidinium sp.

Observations

The cells of the *Amphidinium* sp. strain (UIO349) were spheroid and 11.2 µm long and 8.5 µm wide (Fig. 12a) to 13.3 µm long and 8.6 µm wide (Fig. 12d). The cells were slightly dorso-ventrally compressed (not shown). The anterior epicone was crescent- or tongue-shaped and deflected to the right in ventral view. It comprised 15% (Fig. 12g) to 20% (Fig. 12h) of the cell length. The longitudinal flagellum of 16.5 µm (Fig. 12b) was inserted in the ventro-central sulcus (not shown). No dislodged transverse flagellum was observed and consequentially not measured. Irregular green-yellow chloroplasts were visible in cells flattened by the cover slip (Fig. 12c). Most cells possessed very small but conspicuous red particles mostly appearing black in the micrographs. The particles usually clustered together in a ventro-centrally located membranous body (Fig. 12d-e). The cells were covered with hexagonal amphiesmal vesicles of approximately 1.5 µm long and 1.0 µm wide (Fig. 12f). The cells displayed a single dorso-central pyrenoid (Fig. 12a). Based on observations, the UIO349 strain grew well at both 19 and 23°C. Cells in older cultures seemed to swim much more rapidly than in younger cultures. Many cells in young cultures were virtually immotile and appeared in a common mucus. Observations also suggested the culture colour was light-brown or tan.

In the phylogeny (Fig. 13) the sequence from the present study clustered with three reference sequences named *Amphidinium* sp. *Amphidinium massartii* Biecheler formed the sister group. The sequence in question is 99.8% (1748/1752 bp) identical to the most similar reference sequence (*Amphidinium* sp. HG114, AB103389).

Locality: Seagrass bay, Saudi Arabia.
Habitat: Plankton, marine.

Discussion

The UIO349 strain shows high affinity for the *Amphidinium operculatum* Claparède & Lachmann species complex (Murray & Patterson 2002) in the phylogenetic analysis (Fig. 13). Hence, it likely belongs to genus *Amphidinium* sensu stricto: the *Amphidinium* species with a minute, triangular or left-defelected epicone (Flø Jørgensen et al. 2004; Murray et al. 2004). This complex was proposed due to uncertain delimitation of genetically similar and morphologically variable species in genus

Amphidinium. The epicone portion and shape, pyrenoid location, longitudinal flagellum insertion and cell size of UIO349 is relatively consistent with the original diagnosis for *A*. *carterae* Hulburt (Hulburt 1957) described as *A*. *carteri*, *A*. *eilatiensis* Lee (Lee et al. 2003) and *A*. *massartii* (Biecheler 1952). A way to distinguish between *A*. *carterae* and *A*. eilatiensis is the shape of the chloroplast (Lee et al. 2003). Chloroplasts were only shown in dead cells of UIO349 in the present study, and these chloroplasts are assumed to be deformed. High light intensity has been shown to decrease the size of chloroplasts in some species (Kiefer 1973). Incubation of UIO349 under lower light intensity could make it possible to get clear light micrographs of chloroplasts in live cells.

Hexagonal vesicles have been observed in *A*. *carterae* (Murray et al. 2004) and a stigma within an apical chloroplast in *A*. *cupulatisquama* Tamura & Horiguchi (Tamura et al. 2009). Most particles in UIO349 (Fig. 12d-e) do not resemble a stigma like it appears in *A*. *cupulatisquama* and most other dinophytes (Kreimer 1999; Shah et al. 2013). However, the stigma described for *A*. *elegans* Grell & Wohlfarth-Bottermann (Grell & Wohlfarth-Bottermann 1957) is highly similar in form and location. In the original diagnosis of *A*. *elegans*, the stigma is depicted (drawn) as several small particles clustered together within a membranous body located above the posteriorly located nucleus. *Amphidinium elegans*, though, is considered a taxonomic synonym of *A*. *operculatum*, a species which has not been reported to possess a stigma (Claparède & Lachmann 1859). Also, the cells of both *A*. *elegans* and *A*. *operculatum* are reported to be much larger than the cells of UIO349. Based on the small cell size and presence of chloroplasts, UIO349 is most likely *A*. *carterae*, *A*. *eilatiensis* or *A*. *massartii*.

The 18S rDNA sequence from UIO349 is 100% identical to the partial 18S rDNA sequence (1249 bp) from the other *Amphidinium* strain from the present study (UIO371) (Appendix V). No micrographs are included of the latter strain, as the strains are assumed to be identical.

Genus *Amphidinium* commonly occurs in the marine benthic habitats (Murray & Patterson 2002) and more rarely in open water (Throndsen et al. 2007).

For future studies I recommend identifying the particles, both by ultra-thin TEM sections ans proteomic analyses (Schmidt et al. 2006). Also, different growth conditions (temperature, light intensity, day length, etc.) should be used in order to get clear micrographs of the chloroplast(s) in live cells of UIO349.

Some previous recordings of Amphidinium carterae

Atlantic Ocean, Cape Cod, MA, USA (Hulburt 1957).

Baltic Sea (Hällfors 2004).

Pacific Ocean, Gulf of California (Gárate-Lizárraga 2014).

Persian Gulf, Kuwait (Al-yamani & Saburova 2010).

Previous recordings of Amphidinium eilatiensis

Red Sea, Eilat, Israel (Lee et al. 2003).

Some previous recordings of Amphidinium massartii

Atlantic Ocean, Knight Key, Florida, USA (CCMP1342) (NCMA 2015).

Atlantic Ocean, Rhode Island, USA (Lee et al. 2013).

Mediterranean Sea, Sète, France (Lee et al. 2013).

Pacific Ocean, British Columbia, Canada (Biecheler 1952).

Pacific Ocean, Jeju, Korea (Lee et al. 2013).

Pacific Ocean, Queensland, Australia (Lee et al. 2013).

Pacific Ocean, Tasmania, Australia (Murray et al. 2004).

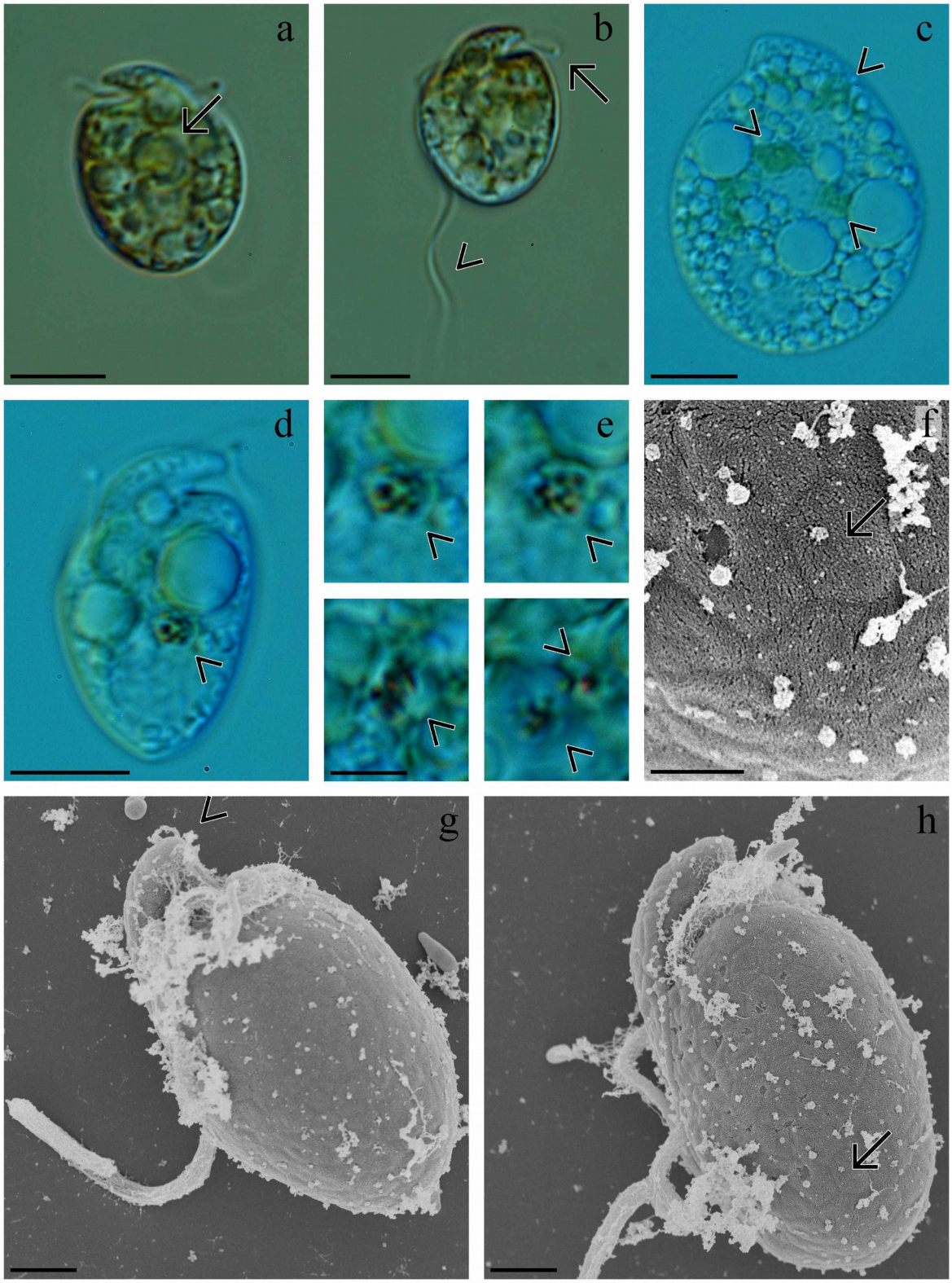

Figure 12. Diffraction interference contrast (a-e) light micrographs of live (a-b, d-e) and dead/dying (c) cells and scanning electron micrographs (f-h) of *Amphidinium* sp. cells (UIO349), showing cell shape, amphiesmal vesicles, flagella, particles and pyrenoids. a: dorsal view, pyrenoid (arrow); b: ventral view, transverse flagellum (arrow), longitudinal flagellum (arrowhead); c: dorsal view of dead cell, chloroplast (arrowhead); d-e: ventral view, red particles (arrowhead); f: amphiesmal vesicle (arrow); g: epicone (arrowhead); h: amphiesmal vesicle (arrow); scale bars: a-d = 5 µm, e = 2 µm, f =1 µm, g-h = 2 µm.

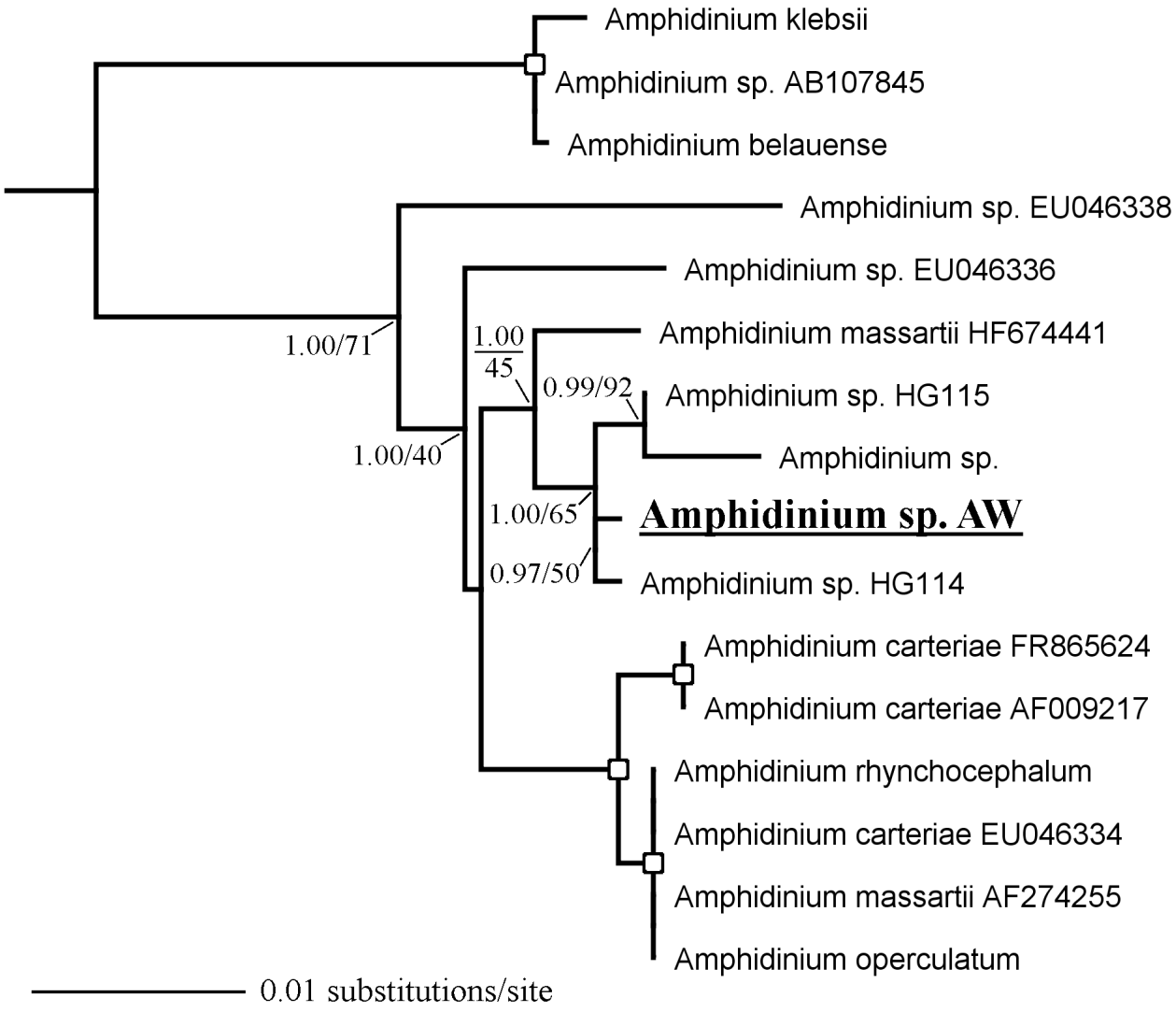

Figure 13. Maximum likelihood phylogeny of *Amphidinium* (Dinophyta) sequences closely similar to the *Amphidinium* sequence from the present study inferred from partial 18S rDNA sequences (1758 bp). The dinophyte *A. asymmetricum* Kofoid & Swezy (AF274250) was used as outgroup and pruned from the tree. Values indicate Bayesian posterior probabilities (pp) and PhyML (200 replicates) bootstrap support values (ML) (pp/ML). White squares indicate 1.00 pp and >90% ML. Support values <0.80 (pp) and <50% (ML) were excluded. The sequence from the present study is indicated with underline.

Division Dinophyta Round
Class Dinophyceae Fritsch
Order Oxyrrhinales Sournia
Genus *Oxyrrhis* Dujardin

Oxyrrhis marina Dujardin

Synonyms:
Glyphidium marinum Fresenius 1865
Oxyrrhis tentaculifera Conrad 1939
Oxyrrhis maritima Van Meel 1969

Observations

The cells of the *Oxyrrhis marina* strain (UIO381) were subovoid and had a large postero-ventral depression on the left side. The cells were colourless and the surface was smooth without plates. The cell size was 19.5 µm long and 9.7 µm wide (Fig. 14d) to 23.2 µm long and 11.4 µm wide (Fig. 14c). The cells possessed a single conspicuous antapically located vacuole (Fig. 14a, d, e) and several trichocysts (Fig. 14e). The vacuole was 2.2 µm long and 2.7 µm wide. The longitudinal flagellum was inserted left of the ventral bulge (Fig. 14b) and was approximately 35 µm (Fig. 14c). The transverse flagellum (Fig. 14a) inserted left of the ventral bulge (Fig. 14b) was not measured. Direction of swimming is shown in Fig. 14c. Observations suggested that the UIO381 strain grew slowly at 19°C and well at 23°C with a rice grain added to the medium.

No sequences were obtained from UIO381.

Locality: Beach adjacent to seagrass bay, Saudi Arabia.
Habitat: Sandy beach, marine.

Discussion

The cell size and shape, forward swimming pattern and small ventral bulge size of UIO381 is consistent with earlier descriptions of *O. marina* (Lowe et al. 2011). The swimming pattern distinguishes it from *O. phaeocysticola* Sherffel which swims with the longitudinal flagellum in front of the cell and the ventral bulge size distinguishes it from *O. tentaculifera* Conrad (not taxonomically accepted) which possesses a substantially larger bulge (Lowe et al. 2011).

Oxyrrhis marina commonly occurs in marine benthic habitats and more rarely in open waters (Watts et al. 2010).

For future studies I recommend acquiring 18S and 28S rDNA sequences from UIO381 to compare the genotype with other sequences from other strains of genus *Oxyrrhis*.

A selection of previous recordings of Oxyrrhis marina

Baltic Sea, East China Sea, Cuba, English Channel, Irish Sea, Japan, Kattegat Sea, Mediterranean Sea, Mexican Gulf, North Sea, North-American east and west coast, Persian Gulf and Red Sea (northern part) (Watts et al. 2010).

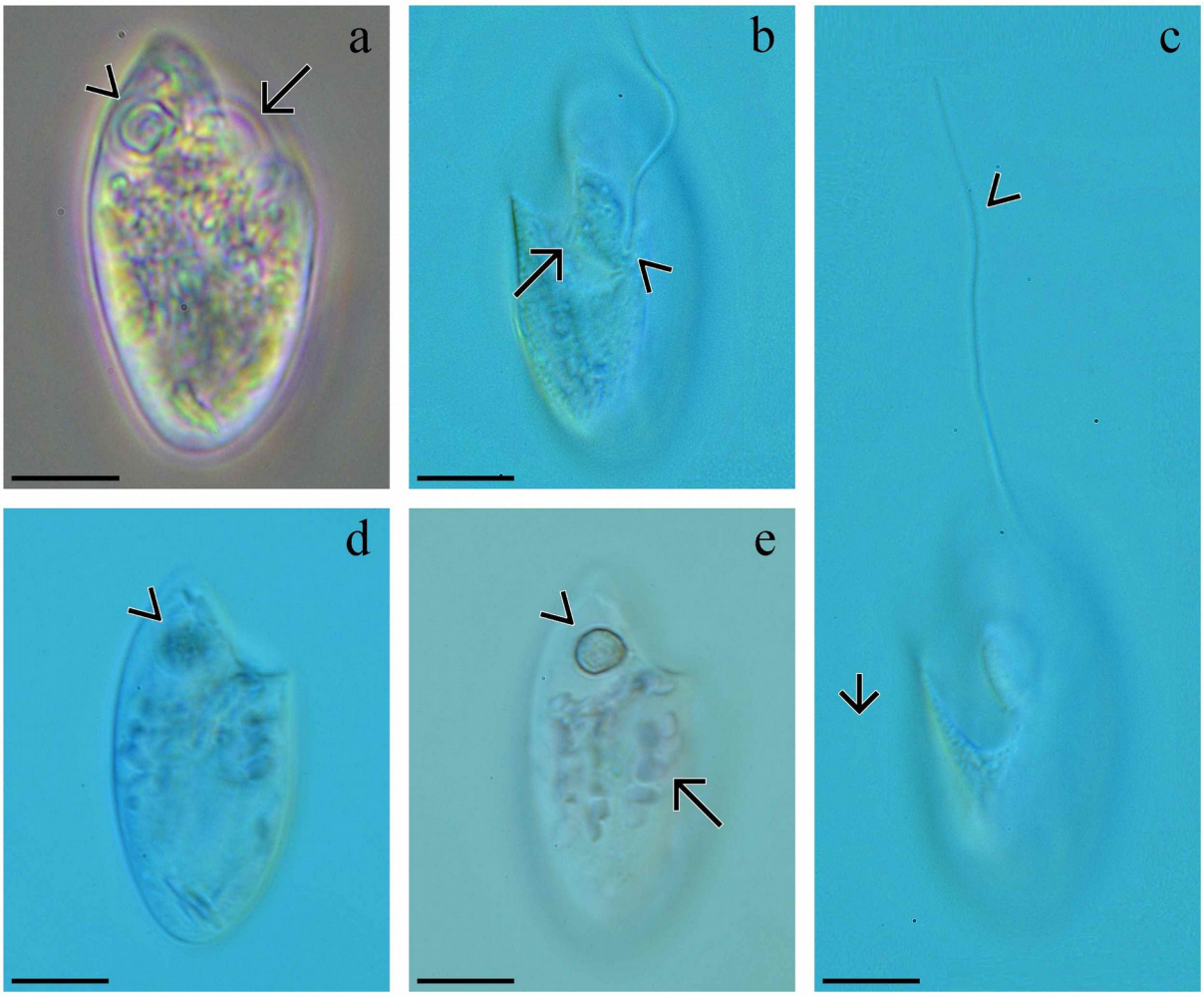

Figure 14. Phase contrast (a) and diffraction interference contrast (b-e) light micrographs of live *Oxyrrhis marina* cells (UIO381) showing cell shape, vacuole, flagella, trichocysts and ventral bulge. a: dorsal view, transverse flagellum (arrow), contractile vacuole (arrowhead); b: ventral view, transverse flagellar insertion (arrow), longitudinal flagellar insertion (arrowhead); c: ventral view, direction of swimming (arrow), longitudinal flagellum (arrowhead); d-e: dorsal view, trichocysts (arrow), vacuole (arrowhead); scale bars: a-e = 5 µm.

Division Haptophyta Cavalier-Smith
Class Pavlovophyceae Green & Medlin
Order Pavlovales Green
Genus *Pavlova* Butcher

Pavlova aff. *gyrans* Butcher

Observations

The cells of the *Pavlova* aff. g*yrans* strain (UIO375) were spheroid to ellipsoid and 3.7 µm long and 2.6 µm wide (Fig. 15a) to 5.2 µm long and 3.7 µm wide (Fig. 15e). The beating anterior flagellum was approximately 5.1 µm (Fig. 15a) to 8.2 µm (Fig. 15e). It was inserted in a subapical ventral depression (15e-f), and the posterior flagellum and the haptonema is expected to be inserted adjacently. The other appendages were 5.1 µm and 5.2 µm (Fig. 15b) to 6.7 µm and 8.4 µm (Fig. 15a). Attempts to distinguish between the posterior flagellum and the haptonema were unsuccessful. The cells seemed to possess a single green-yellow bilobed chloroplast (Fig. 15c) with a conspicuous red stigma (Fig. 15d-f). Observations suggested that the UIO375 strain grew rapidly at both 19 and 23°C. Younger cultures were light-brown or tan in colour. Older cultures were grey in colour.

In the phylogeny (Fig. 16) the sequence from the present study clustered with two reference sequences named Pavlova gyrans and one named *Pavlova pinguis* Green. Other *Pavlova* sequences formed the sister group. The sequence in question is 96.7% (1740/1799 bp) identical to the most similar reference sequence (*Pavlova gyrans*, JF714246).

Locality: Seagrass bay, Saudi Arabia.
Habitat: Sediment, marine.

Discussion

The *Pavlova* aff. *gyrans* strain (UIO375) from the present study is believed to be a novel haptophyte species. The phylogeny is consistent with earlier work (Edvardsen et al. 2000; Van Lenning et al. 2003). Genera *Pavlova*, *Diacronema* Prauser and *Exanthemachrysis* Lepailleur all form monophyletic groups, while genus *Rebecca* Green does not. *Monochrysis* Skuja sp. in the *Diacronema* clade is expected to be misidentified. The basal nodes generally display weak support values, whereas values within the genera are strong. I report a striking dissimilarity in the appendages and possibly in the cell shape between the UIO375 and the strains from the original diagnosis (Butcher 1952) and other previous works (Green & Manton 1970; Throndsen et al. 2007). *Pavlova gyrans* is reported to possess a propulsive anterior flagellum of about twice the length of the cell. The other flagellum is much shorter and very hard to observe in a light microscope, as is

the haptonema. Although the attempt to distinguish between the haptonema and the non-propulsive flagellum in UIO375 was unsuccessful, it is clear that both are longer or about equal in length to the beating flagellum and easily observed in the light microscope.

The 28S rDNA sequences from UIO375 were compared to the sequence from the *Pavlova* strain from Eikrem et al. (In prep.) which is also isolated from Saudi Arabia. The two are 100% identical, so it is believed that this is the same species.

Pavlova gyrans is most commonly found in open water close to the coast (Bendif et al. 2011).

For future studies I recommend acquiring SEM and TEM photographs of UIO375 to be able to describe the morphology for a diagnosis.

Previous recordings of Pavlova gyrans

Atlantic Ocean, Bay of Biscay, Spain (Seoane et al. 2009).

Atlantic Ocean, Canary Islands, Spain (K1308) (SCCAP 2015).

Arkansas, USA (Smith 2010).

English Channel, Helford River, Cornwall, England (Butcher 1952).

Estuary of Bilbao, Spain (UIO141) (University of Oslo, culture collection, unpublished).

Oslofjord, Norway (Tengs et al. 2000).

Pacific Ocean, Australia and New Zealand (Rhodes et al. 2012).

Red Sea, Saudi Arabia (=*Pavlova* aff. *gyrans*) (Eikrem et al. In prep.).

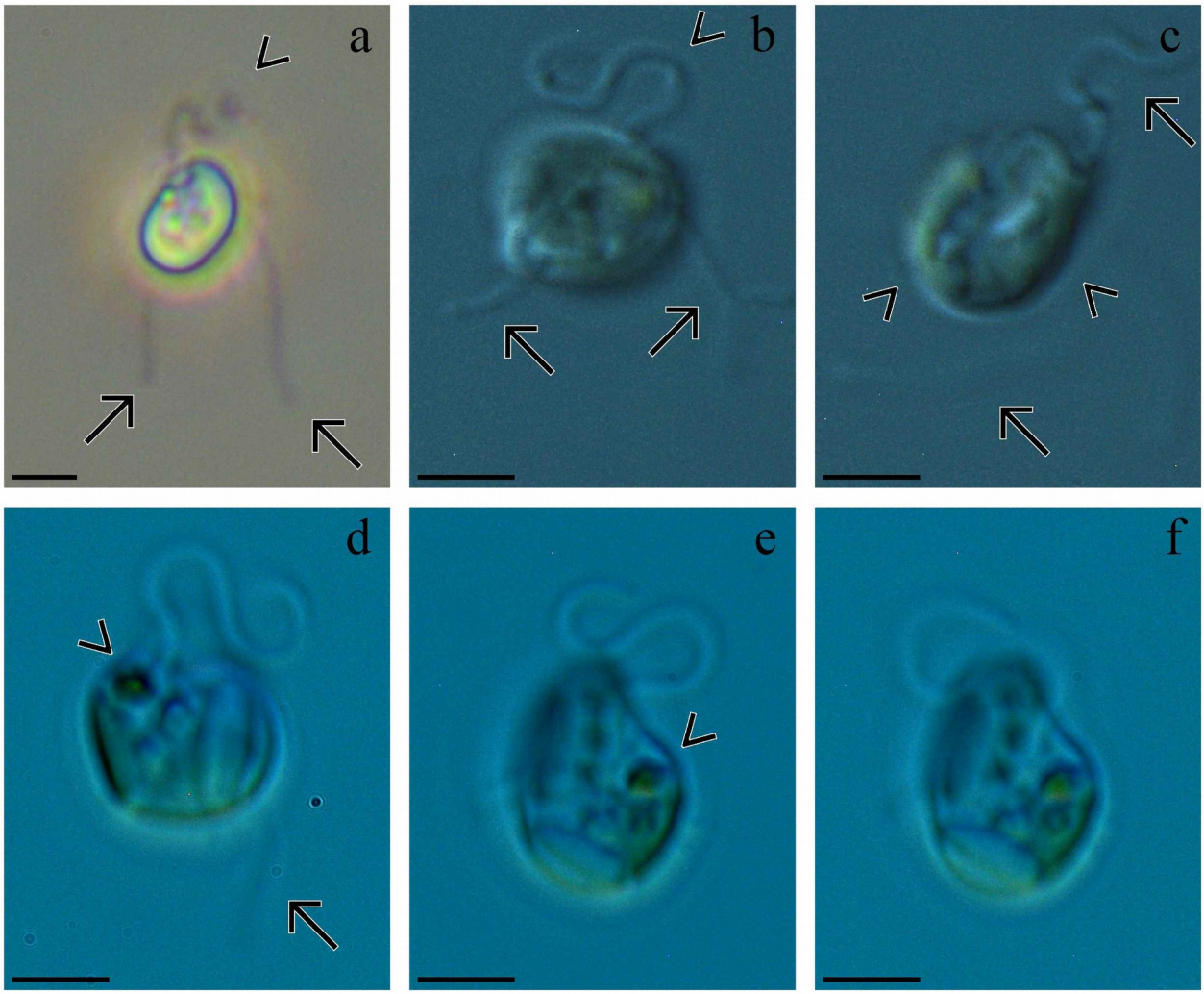

Figure 15. Phase contrast (a) and diffraction interference contrast (b-c) light micrographs of live *Pavlova* aff. g*yrans* cells (UIO375) showing cell shape, chloroplast, stigma, flagella and haptonema. a-b: haptonema and posterior flagellum (arrows), anterior flagellum (arrowhead); c: ventral view, anterior flagellum and appendage (arrows), chloroplast lobes (arrowheads); d: lateral view, appendage (arrow), stigma (arrowhead); e-f: lateral view, stigma (arrowhead); scale bars: a-f = 2 µm.

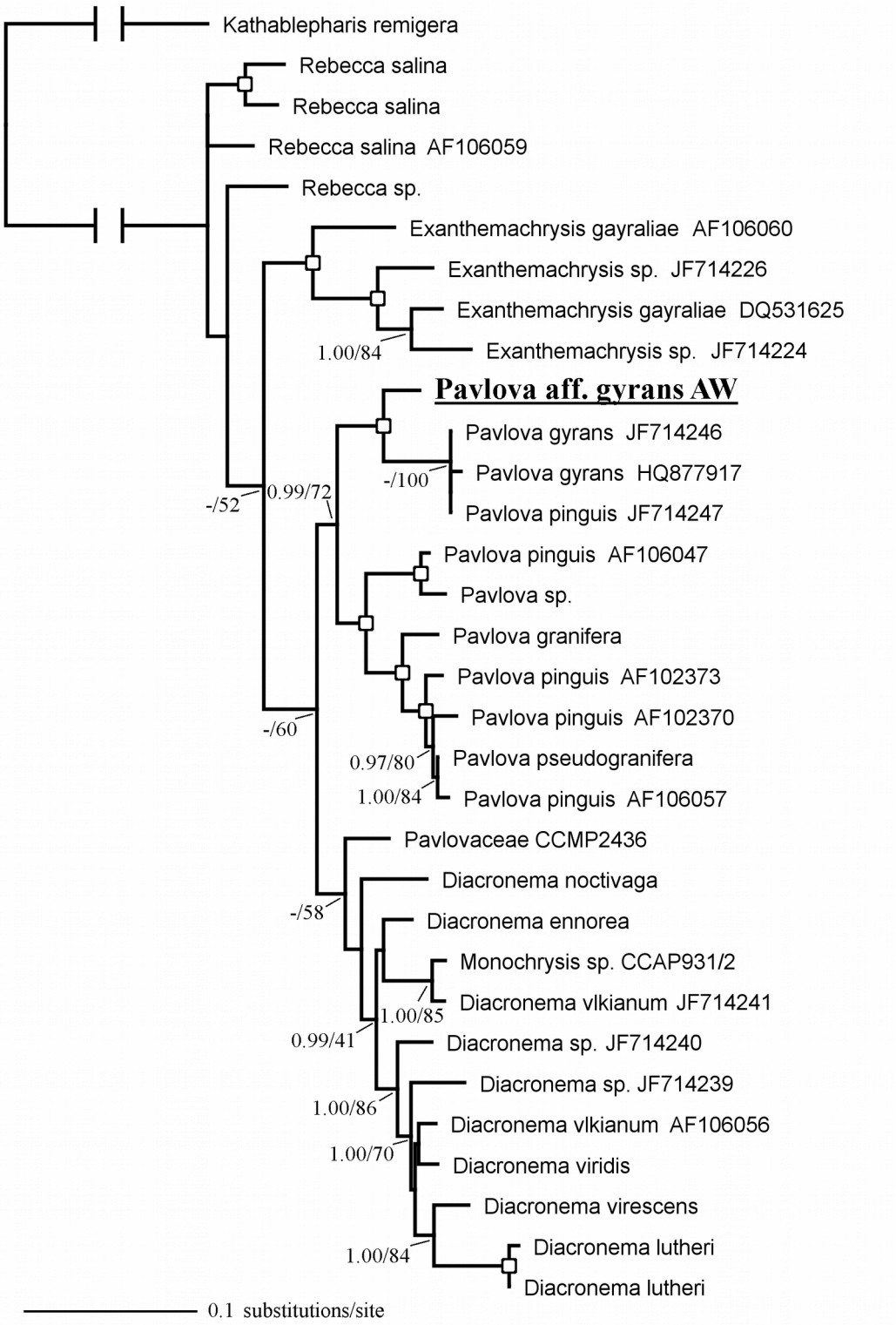

Figure 16. Maximum likelihood phylogeny of Pavlovophyceae (Haptophyta) inferred from partial 18S rDNA sequences (1755 bp). The katablepharidophyte *Katablepharis remigera* (Vørs) Clay & Kugrens (AY919672) was used as outgroup. Values indicate Bayesian posterior probabilities (pp) and PhyML (200 replicates) bootstrap support values (ML) (pp/ML). White squares indicate 1.00 pp and >90% ML. Support values <0.80 (pp) and <50% (ML) were excluded. Nodes marked with a hyphen (-) indicate topological incongruence between the Maximum likelihood and the Bayesian analyses. Vertical lines and breach indicates a 75% reduction in branch length. The sequence from the present study is indicated with underline.

Division Ochrophyta Cavalier-Smith
Class Bacillariophyceae Haeckel
Order Bacillariales Hendey
Genus *Cylindrotheca* Rabenhorst

Cylindrotheca cf. *closterium* (Ehrenberg) Reimann & Lewin

Synonyms:
Ceratoneis closterium Ehrenberg 1839 (basionym; currently accepted taxon (Guiry & Guiry 2015))
Nitzschiella closterium (Ehrenberg) Rabenhorst 1864

Observations

The cells of the *Cylindrotheca* cf. *closterium* strain (UIO353) were cylindrical with long extruded ends (rostra) (Fig. 17a-c). The frustules were seemingly spirally twisted at the rostrate ends (Fig. 17b). The cells were 18.2 µm long and 1.9 µm wide (Fig. 17a) to 19.7 µm long and 2.8 µm wide (Fig. 17b). The cells possessed two conspicuous chloroplasts taking up a substantial portion of the cell. Observations suggested that the UIO353 strain grew rapidly at both 19 and 23 °C. The strain is lost, but formalin fixed material and DNA-isolates are kept.

In the phylogeny (Fig. 19) the sequence from the present study clustered together with a reference sequence named *Cylindrotheca closterium*. All the *Nitzschia* sequences formed the sister group. The 18S rDNA sequence in question is 99.9% (1759/1760 bp) identical to the most similar reference sequence (*C. closterium*, DQ019446). The 28S rDNA sequence in question is 98.8% (479/485 bp) identical to the most similar reference sequence (*C. closterium*, JX524868).

Locality: Beach near KAUST, Saudi Arabia.
Habitat: Sandy beach, marine.

Discussion

The morphology of UIO353 is somewhat consistent with the description for *C. closterium* in Hasle & Syvertsen (1996). The frustule of UIO353 was seemingly slightly spirally twisted in the long rostrate ends and the cells contained two chloroplasts. A major inconsistency is the cell length, which is described to be 30-400µm for *C. closterium* and 125-450 µm in the morphologically similar *Nitzschia longissima* (Brébisson) Ralfs (Hasle & Syvertsen 1996). As there are no other available morphological characters described for UIO353, no conclusions can be drawn other than to assume it is a small *C. closterium*.

Cylindrotheca closterium is believed to be a cosmopolitan species (Hasle & Syvertsen 1996).

For future studies I recommend acquiring TEM photographs of acid-cleaned frustules of UIO353 to determine whether it is *C. closterium* or not.

A small selection of previous recordings of Cylindrotheca closterium

Antarctica, George V Coast (Ralph et al. 2005).

Atlantic Ocean, Britain (Hendey 1964).

Baltic Sea (Hällfors 2004).

Pacific Ocean, Do Son Beach, Vietnam (RCC1950) (RCC 2015).

As Ceratoneis closterium

Pacific Ocean, Australia and New Zealand (McCarthy 2013).

Pacific Ocean, Gulf of California, Mexico (Gárate-Lizárraga 2014).

As Nitzschia closterium (Ehrenberg) Smith

Atlantic Ocean, France (Méléder et al. 2007).

Red Sea, Egypt (Zein et al. 2014).

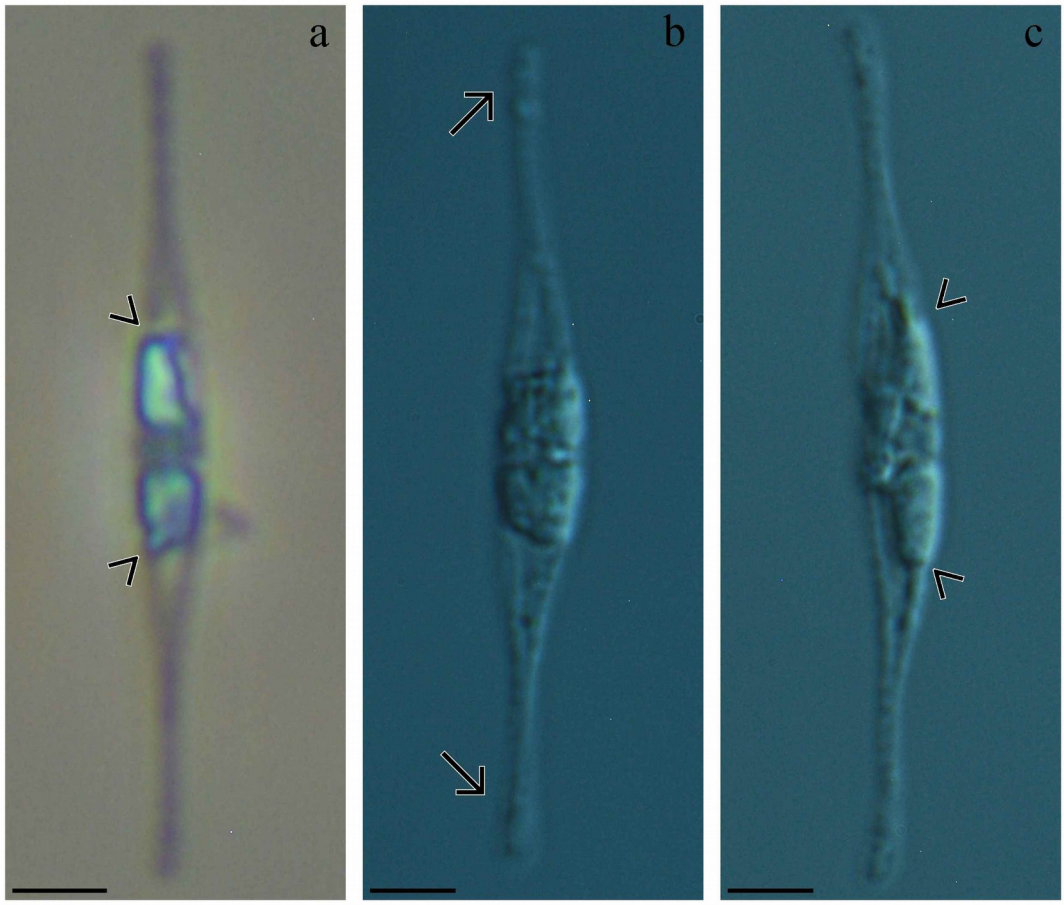

Figure 17. Phase contrast (a) and diffraction interference contrast (b-c) light micrographs of formalin fixed *Cylindrotheca* cf. *closterium* cells (UIO353) showing cell shape, chloroplasts and rostra. a-c: valve view, twisted rostrum (arrow), chloroplast (arrowhead); scale bars: a-c = 2 µm.

Division Ochrophyta Cavalier-Smith
Class Bacillariophyceae Haeckel
Order Bacillariales Hendey
Genus *Nitzschia* Hassall

Nitzschia sp.

Observations

The cells of the *Nitzschia* sp. strain (UIO383) were fusiform or naviculoid with rounded edges (Fig. 18a, b). The cells were 6.7 µm long and 3.1 µm wide (Fig. 18a) to 6.8 µm long and 2.7 µm wide (Fig. 18b) in valve view and 6.3 µm long and 2.1 µm high (left cell, Fig. 18c) to 6.8 µm long and 2.3 µm high (right cell, Fig. 18c). The cells possessed two conspicuous chloroplasts taking up a substantial portion of the cell. Observations suggested that the UIO383 strain grew rapidly at both 19 and 23°C. The strain is lost, but formalin fixed material DNA-isolates are kept.

In the phylogeny (Fig. 19) the sequence from the present study clustered with a reference sequence named *Nitzschia* cf. *agnita* Hustedt. *Nitzschia sigma* (Kützing) Smith formed the sister group. The 18S rDNA sequence in question is 98.8% (1723/1744 bp) identical to the most similar reference sequence (*N. thermalis* (Ehrenberg) Auerswald, AY485458). The 28S rDNA sequence in question is 96.5% identical to the most similar reference sequence (*Nitzschia* cf. *agnita*, AF417664).

Locality: Seagrass bay, Saudi Arabia.
Habitat: Plankton, marine.

Discussion

Genus *Nitzschia* is a very large genus currently comprised of 757 taxonomically accepted species (Guiry & Guiry 2015). Only 46 GenBank entries have available sequences assigned to species at the time of writing (NCBI 2015). It is distinguished from genus *Navicula* Bory de Saint-Vincent by the raphe which is located centrally in the apical axis of the valve of genus *Navicula* as opposed to the eccentric raphe in genus *Nitzschia* and from genus *Pseudo-nitzschia* Peragallo in that the latter forms linear colonies (Throndsen et al. 2007). In the phylogeny (Fig. 19) UIO383 shows high affinity for *Nitzschia* cf. *agnita and N. sigma. Nitzschia sigma* is, in strong contrast to UIO383, sigmoid in shape (Smith & West 1853). Species delimitation within *Nitzschia* is mostly based on frustule size and shape, and raphe, stria and fibula morphology (Hasle & Syvertsen 1996). With the very limited taxa in the phylogeny from the present study and no morphological data on the frustules of UIO383, the strain can only be identified to genus.

Genus *Nitzschia* is common in the benthos and the pelagic all over the World (Hasle &

Syvertsen 1996).

For future studies I recommend acquiring TEM photographs of acid-cleaned frustules of UIO383 to be able to describe it to species.

A small selection of previous recordings of genus Nitzschia

Baltic Sea (Hällfors 2004).

Pacific Ocean, Australia and New Zealand (McCarthy 2013).

Pacific Ocean, Gulf of California, Mexico (Gárate-Lizárraga et al. 2014).

Persian Gulf, Kuwait (Al-yamani & Saburova 2011).

Red Sea, Egypt (Zein et al. 2014).

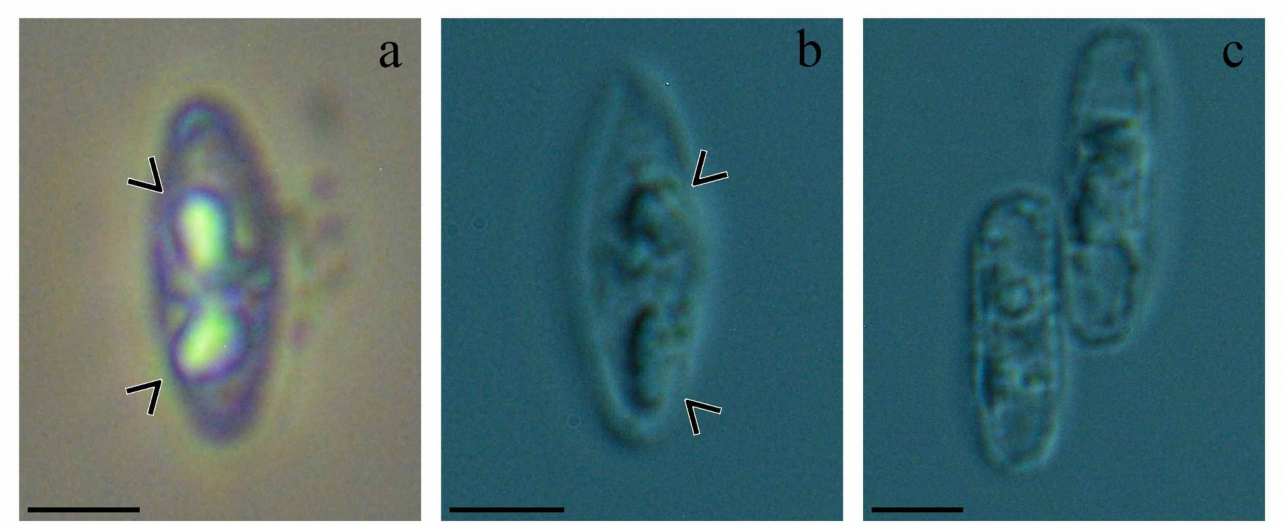

Figure 18. Phase contrast (a) and diffraction interference contrast (b-c) light micrographs of formalin fixed *Nitzschia* sp. cells (UIO383) showing cell shape and chloroplasts. a-b: valve view, chloroplast (arrowhead); c: girdle view; scale bars: a-c = 2 µm.

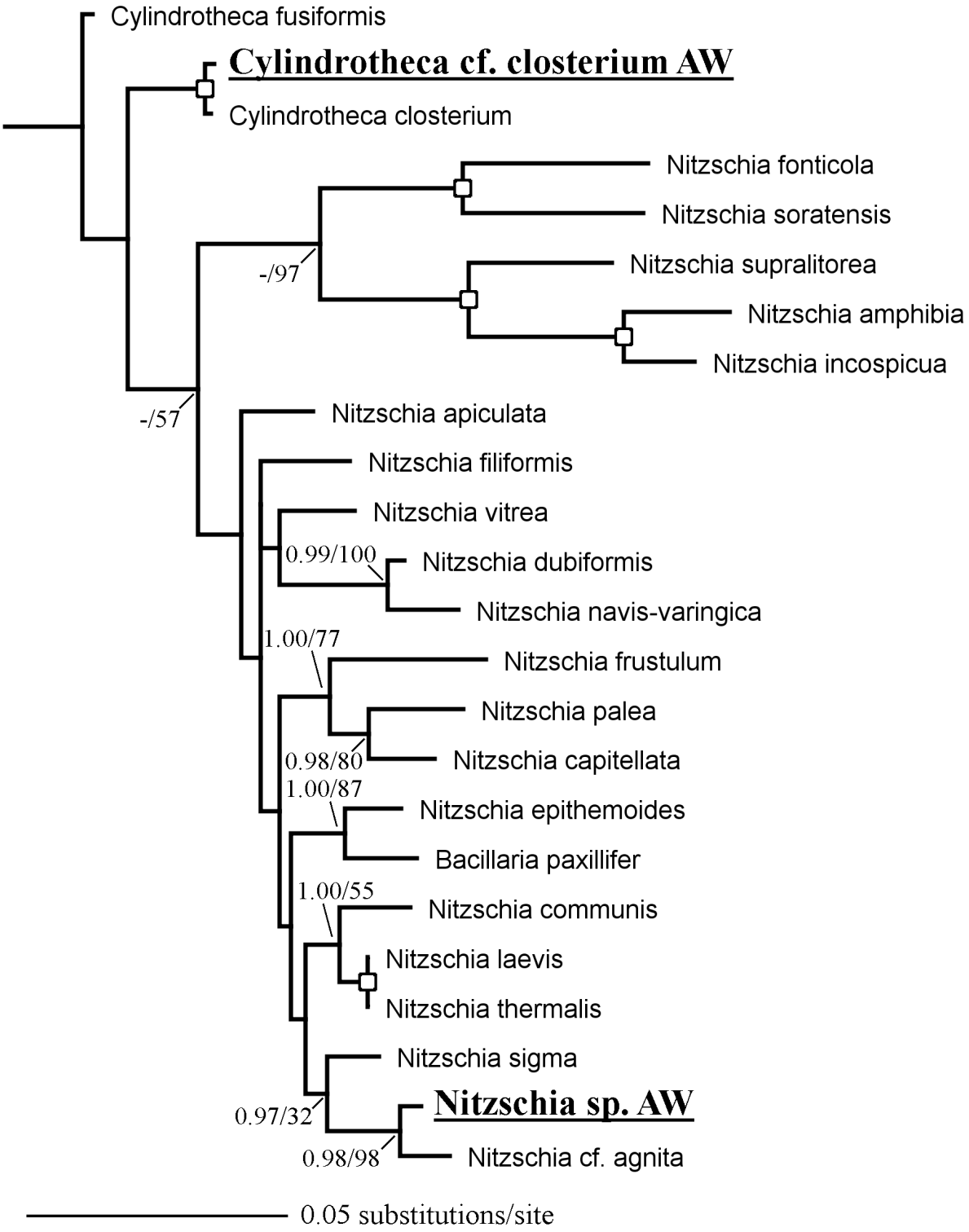

Figure 19. Concatenated maximum likelihood phylogeny of *Cylindrotheca* and *Nitzschia* (Ochrophyta) inferred from partial 18S rDNA sequences (1735 bp) and partial 28S rDNA sequences (537 bp). The Diatom *Coscinodiscus wailesii* (HQ912668/KC969894) was used as outgroup and pruned from the tree. Values indicate Bayesian posterior probabilities (pp) and PhyML (200 replicates) bootstrap support values (ML) (pp/ML). White squares indicate 1.00 pp and >90% ML. Support values <0.80 (pp) and <50% (ML) were excluded. Nodes marked with a hyphen (-) indicate topological incongruence between the Maximum likelihood and the Bayesian analyses. The sequence from the present study is indicated with underline.

Division Ochrophyta Cavalier-Smith
Class Dictyochophyceae Silva
Order Rhizochromulinales O'Kelly & Wujek
Genus *Rhizochromulina* Hibberd & Chrétiennot-Dinet

Rhizochromulina aff. *marina* Hibberd & Chrétiennot-Dinet

Observations

The cell morphology of the *Rhizochromulina* aff. *marina* strain (UIO378) was very variable (Fig. 20). Most observations in this study have been of amoeboid cells, and rarely of the flagellated zoospores. The amoeboid cells were isodiametric and the size varied from 2.4 µm long and 2.1 µm wide (Fig. 20e) to 9.3 µm long and 6.4 µm wide (Fig. 20h). The smallest observed zoospore was 5 µm long and 5 µm wide (Fig. 20c), while the largest one was 17.5 µm long and 4 µm wide at the widest and 1 µm wide at the least wide (Fig. 20b). The cells held a single flagellum of half (Fig. 20f), double (Fig. 20c) or the same length as the cell (Fig. 20d). The cell shape varied greatly and showed irregular (Fig. 20a, d), elongate hourglass-shaped (Fig. 20b), circular (Fig. 20c) and fusiform (not shown) forms. No chloroplasts were observed in the zoospores. The amoeboid cells were 2 µm long and 2 µm wide (Fig. 20e) to 9.3 µm long and 6.4 µm wide (Fig. 20h). They displayed numerous chloroplasts (Fig. 20i) and filipodia ranging from one time (Fig. 20f) to three times (Fig. 20e) the cell length. Most cells held from 3 (Fig. 20e) to >15 (Fig. 20g) filipodia. More rarely amoeboid cells without filipodia were observed (Fig. 20h). Some amoeboid cells held a single flagellum (Fig. 20d, e), whereas the flagellum was lacking in most observed amoeboid cells (Fig. 20g-i). The sectioned cells possessed several chloroplasts often containing lipid droplets (Fig. 21a-c). Lamellae consisted of three thylakoids, and a girdle lamella was present (Fig. 21c). The cells held a centrally placed nucleus without a visible central nucleolus (Fig. 21b). The Golgi body was located close to the chloroplasts (Fig. 21a). None of the sections displayed pyrenoids. Observations suggested that the UIO378 strain grew slowly at both 19 and 23°C, but the growth rate increased slightly at 19°C with an added rice grain in the medium. Growth rate seemed much higher when grown on agar. In all instances the culture colour was deep green.

In the phylogeny (Fig. 22) the sequence from the present study clustered with reference sequences named *Rhizochromulina marina*, *Rhizochromulina* cf. *marina*, *Rhizochromulina* sp., and three uncultured eukaryotic clones. Two *Ciliophrys infusionum* Cienkowski sequences formed the sister group. The sequence in question is 97.9% (1810/1848 bases) identical to the most similar reference sequence (*Rhizochromulina* cf. *marina*, U14388).

Locality: Beach near KAUST, Saudi Arabia.

Habitat: Sandy beach, marine.

Discussion

The *Rhizochromulina* aff. m*arina* strain (UIO378) from the present study is believed to be a novel ochrophyte species. The phylogeny in the present study is generally consistent with earlier work (Edvardsen et al. 2007; Hosoi-Tanabe et al. 2007). Genera *Ciliophrys* Cienkowski and *Rhizochromulina* forms a strongly supported clade, with a strongly supported split between said genera.

Based on the phylogeny in the present study (Fig. 22), genus *Rhizochromulina* is assumed to contain several cryptic species, one being the UIO378 strain. UIO378 is relatively dissimilar to the most similar *Rhizochromulina* reference sequences (97.9%), and I report a striking dissimilarity in the cell's ultrastructure compared to *R*. *marina* which is the only taxonomically accepted species in genus *Rhizochromulina*. Although the exact number of chloroplasts in the amoeboid cells of the UIO378 strain has not been determined, I report more than one chloroplasts per cell. Originally, Hibberd & Chrétiennot-Dinet (1979) described *R*. *marina* (CCAP950/1 culture) with a single chloroplast in zoospores and amoeboid cells, or two chloroplasts in larger amoeboid cells about to undergo cell division. Most transmission electron micrographs of the UIO378 strain displayed 6-8 isodiametric chloroplasts. Some of these may be lobes of a single chloroplast, only appearing to be distinct due to the plane in which the cells were sectioned. Still, the lack of observed lobed chloroplasts in the light micrographs and the observation of several relatively distinct chloroplasts for UIO378, I conclude that the cells hold more than one chloroplast.

Amoeboid cells of the CCMP237 *Rhizochromulina* sp. strain shares the trait of having several chloroplasts according to unpublished light micrographs (NCMA 2015). There are no available 18S or 28S rDNA sequences of this strain, so it has not been included in the phylogeny in the present study (Fig. 22). Also, the chloroplasts of UIO378 clearly possessed a girdle lamella, which is consistent with the general chloroplast structure of Ochrophyta (Andersen 2004), but inconsistent with the original diagnosis. The lack of reported girdle lamella in the original diagnosis may be a misinterpretation based on TEM photographs with low resolution (Appendix III).

A less striking difference between the UIO378 strain and the strain from the original diagnosis is the colour of the culture. The strain from Hibberd & Chrétiennot-Dinet (1979) was yellowish olive to a very dark orange in denser cultures. Observations suggested the UIO378 was green to deep green in denser cultures. Another minor difference is the cells of the UIO378 being significantly smaller than CCAP950/1. The amoeboid cells from Hibberd & Chrétiennot-Dinet

(1979) was reported to be 5-9 µm (mean = 7 µm) long. The smallest amoeboid cell of UIO378 was 2.4 µm (Fig. 20e). Thirdly, observations suggested the UIO378 cultures grew very slowly, but not as slowly when a grain of rice was added to the flask (more bacteria), and faster still when growing on agar (even more bacteria). No phagosomes were observed, but the growth rates implies mixotrophy.

The red particle shown in (Fig. 20h) resembles a stigma. No stigmata have been reported in Class Dictyochophyceae (Andersen 2004). Although no conclusions can be drawn at this point, the particle are assumed to be some sort of storage product or food bodies.

Finally, *Cafeteria roenbergensis* appeared as a contaminant in the original CCAP950/1 culture (O'Kelly & Patterson 1996). Based on brief light microscopy, the contaminant in another *R. marina* strain from the present study (UIO377) was also identified as *C. roenbergensis*. This is most likely incidental, but an interesting observation nonetheless.

There have been too few recordings of *R. marina* to determine which habitats it commonly occurs in, but based on sampling data on different strains in culture collections (NCMA 2015; NIES 2015; RCC 2015) it seems to be mostly pelagic.

For future studies I recommend obtaining 28S rDNA sequences and morphological data for the available *R*hizochromulina strains (*R. marina*, *Rhizochromulina* cf. *marina* and *Rhizochromulina* sp.). A concentrated 18S and 28S rDNA phylogeny will help uncover the assumingly cryptic diversity of the genus. Also, examination of the UIO378 strain in florescence light microscopy will help uncover the exact chloroplast number. Thirdly, a pigment analysis may reveal why the colour of UIO378 differs from the original CCAP950/1 strain. Finally, TEM sections of the zoospores will be needed in order to explain the UIO378 strain's morphology for a diagnosis. The attempt to produce zoospores in quantities sufficient for TEM sections as explained by Hibberd & Chrétiennot-Dinet (1979) was unsuccessful.

Previous recordings of Rhizochromulina marina

Atlantic Ocean, Florida, USA (CCMP237) (NCMA 2015).

Atlantic Ocean, open ocean (RCC4436) (RCC 2015).

Atlantic Ocean, open ocean (RCC4438) (RCC 2015).

Atlantic Ocean, Sargasso Sea, open ocean (CCMP1480) (NCMA 2015).

Mediterranean Sea, Marseille, France (Hibberd & Chrétiennot-Dinet 1979).

Pacific Ocean, Hawaii, USA (CCMP2174) (NCMA 2015).

Pacific Ocean, Isonoura Beach Wakayama, Japan (NIES1382) (NIES 2015).

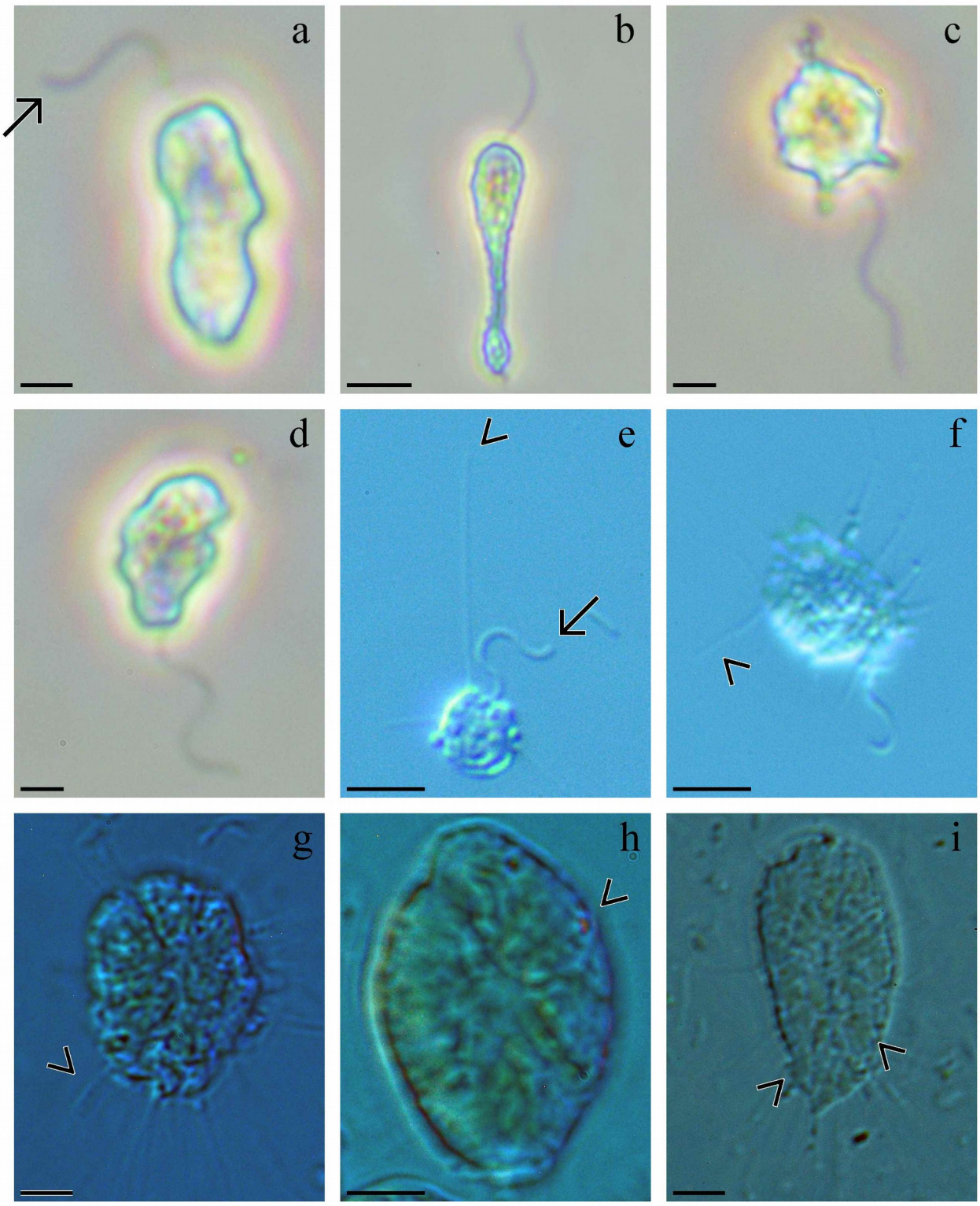

Figure 20. Phase contrast (a-d) and diffraction interference contrast (e-i) light micrographs of live *Rhizochromulina* aff. *marina* cells (UIO378) showing cell shape, chloroplasts, red particles, filipodia and flagella. a: zoospore, flagellum (arrow); b-d: zoospores; e: amoeboid cell, flagellum (arrow), filipodium (arrowhead); f-g: amoeboid cells, filipodium (arrowhead); h: amoeboid cell, red particle (arrowhead); i: amoeboid cell, chloroplast (arrowhead); scale bars: a = 2 µm, b = 5 µm, c-i = 2 µm.

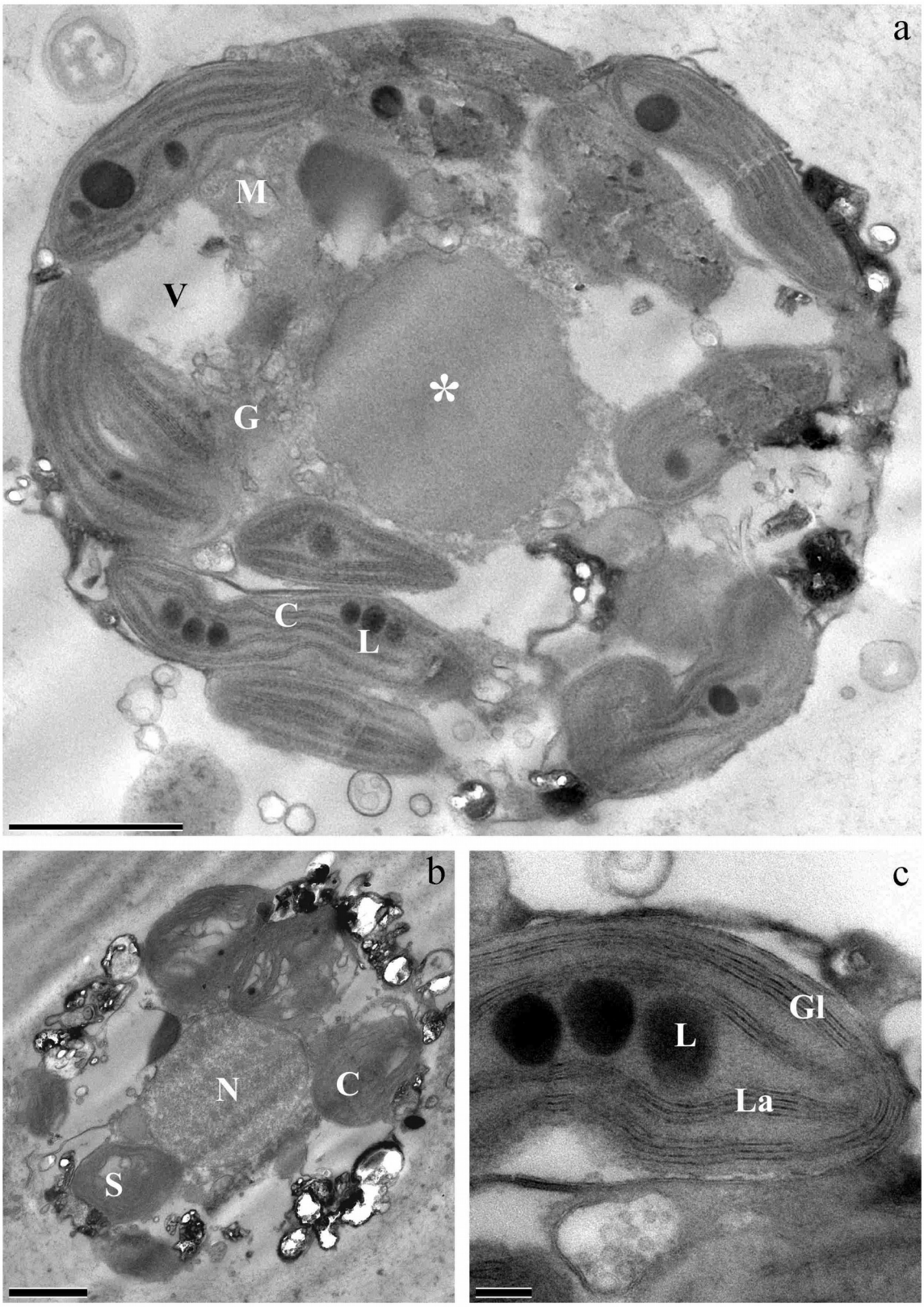

Figure 21. Transmission electron micrographs of ultra-thin sections of amoeboid *Rhizochromulina* aff. *marina* cells showing cell structures. a-b: whole cells, C = chloroplast, Golgi body (G), lipid (L), mitochondrion (M), nucleus (N), starch grain (S), vacuole (V), unidentified structure (*); c: lower left chloroplast from Fig. 21a, girdle lamella (Gl), lipid (L), lamella of three thylakoid membranes (La); scale bars: a-b = 1 μm, c = 100 nm.

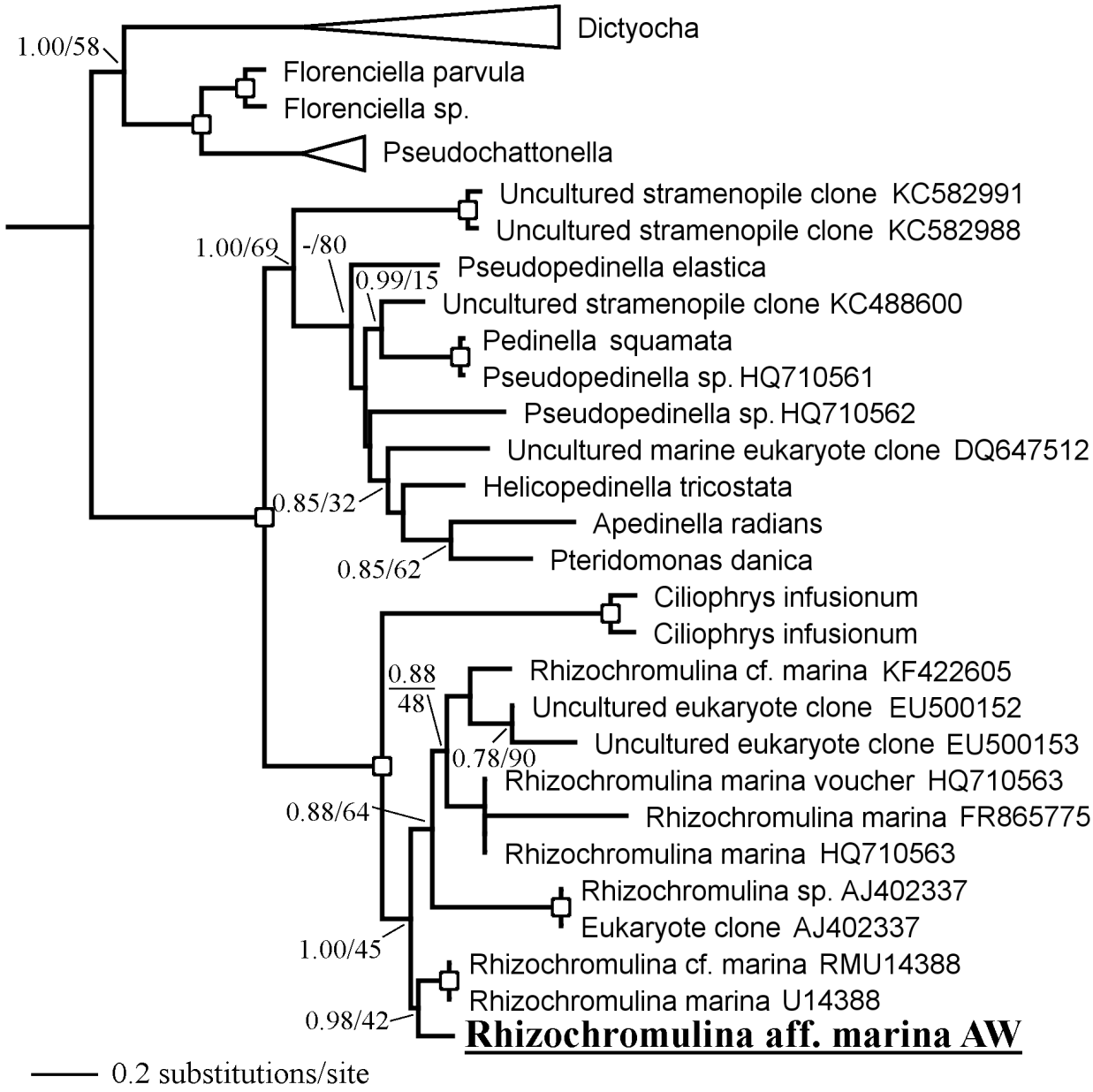

Figure 22. Maximum likelihood phylogeny of Dictyochophyceae (Ochrophyta) inferred from partial 18S rDNA sequences (1695 bp). The diatom *Thalassiosira nordenskioeldii* Cleve (DQ093365) was used as outgroup and pruned from the tree. Values indicate Bayesian posterior probabilities (pp) and PhyML (200 replicates) bootstrap support values (ML) (pp/ML). White squares indicate 1.00 pp and >90% ML. Support values <0.80 (pp) and <50% (ML) were excluded. Nodes marked with a hyphen (-) indicate topological incongruence between the Maximum likelihood and the Bayesian analyses. White triangles indicate collapsed clades (see Appendix IV (Fig. 24) for the complete phylogenetic tree). The sequence from the present study is indicated with underline.

4 Discussion of the methodology

4.1 Identification

Most species recorded in the present study were identified based on morphological traits after sequences were retrieved. As a consequence, several strains isolated from the Red Sea have not been included (see Appendix V for complete list of strains). There are many potential explanations as to why some strains were more difficult to sequence than others. Firstly, PCR products that did not give bands in the gel electrophoresis were attributed to unsuccessful DNA isolations. However, the spectrophotometry showed sufficient DNA concentrations and purities for all tested isolates. Next, it has been shown that nested PCR can improve the quality of the sequences for certain species (Edvardsen et al. 2003), but this had no effect on the isolates that did not give bands in the present study. The attempts to amplify shorter fragments of the 18S rDNA marker region in the PCR step were also unsuccessful. This was tried using 1F+1055R and 690F+1528R as PCR primers (Table 1). It is assumed that the primers used in the present study could not bind to the desired regions or that the cultures contained PCR inhibiting compounds.

The exception is *Oxyrrhis marina* (UIO381) that could be identified to species solely by microscopy, as the cells of this species are large and relatively easy to identify.

4.2 Working with cultures

Working with algal cultures gives a narrow and biased but very detailed description of the organisms present at the sampling location. The raw cultures in the present study were all examined prior to isolation to get an overview of some of the present groups, but no attempt was made to isolate specific species. Still, which species ends up as isolates will never be solely based on chance. Some species are naturally difficult to culture, e.g. species that needs to feed on prokaryotes or other eukaryotes or need higher concentrations of specific nutrients (Andersen & Kawachi 2005). Others will be more abundant in the raw cultures or may outcompete other species and thus have a higher chance to end up in mono- cultures. Also, cultures containing a single species with multiple different morphotypes may be misinterpreted as contaminated and excluded from further analysis. Finally, mono-algal cultures of smaller species are more difficult to detect.

Given the biased and time consuming nature of cultivation, only a fraction of the actual diversity was unveiled. If the species were identified directly from the raw cultures only based on morphology, a much higher number of species could be recorded with the same amount of time.

Consequentially only eleven species and genera have been identified from the 25 strains (UIO343-354, 371-383) in the present study. Thus, no conclusions about the species composition can be drawn because of the vast amount of present taxa was not recorded. On the other hand, working with cultures gives a unique insight by allowing us to connect the morphology with molecular data. This way, novel genotypes for known species and novel morphological traits for known genotypes can be described. In order to study the internal structure in greater detail than is possible with light microscopy, it is essential to have enough cell material to produce ultra-thin sections for TEM. Cultured species provide virtually unlimited access to study material. Also, with the vast retrieval of sequences from environmental samples using cloning and next-generation sequencing, reference sequences from morphologically described species must be available for the sequences to be identified.

To determine whether a culture truly is a mono-/clonal-culture or not may be a challenge. If high quality sequences are obtained from the culture using eukaryote-specific primers, it is easy to assume that the strain does not have eukaryote contaminants. This is because different genotypes present in the DNA isolate all will be amplified and sequenced, leading to ambiguous bases at variable positions. If the primers only bind to a single genotype in the isolate, the strain may falsely be considered a mono-/clonal-culture. This may in turn lead to the assignment of a morphological description to the wrong genotype for morphologically cryptic strains or strains with closely related and morphologically similar contaminants.

4.3 Morphology

There are several things that could be done differently to improve on the morphological descriptions and the micrographs in the present study. Firstly, the cells included in the micrographs were the only cells measured. More cell measurements are needed in order to determine the average dimensions (cell size, flagella, vacuoles, etc.) of the strains. Also, more sophisticated photo editing software could have been used to improve the sharpness and brightness of the micrographs. Furthermore, the cells in the SEM photographs had debris obscuring some of the morphological features. This assumingly happened because the material was gathered from old cultures. This effect could have been diminished by harvesting higher volumes of younger cultures. Some of the TEM micrographs had different artefacts (condensations/rarefactions patterns and knife marks) caused by the sectioning. Finally, some of the TEM sections were too thick, causing the smaller details to be poorly visualised.

4.4 Marker regions

18S rDNA is a marker region widely used for species delimitation in microalgae and is hence the most readily available region in most reference sequence databases (Burki 2014). This is the main reason 18S rDNA was the preferred region for phylogenetic analyses in the present study. Still, after the analyses were finished and a better overview over the literature was acquired, it became apparent that 18S do not have sufficient variability for species delimitation within certain algal groups, i.e. genus *Tetraselmis*, class Bacillariophyceae and genus *Amphidinium*.

Partial 28S rDNA (D1/D2) was retrieved for most of the strains in the present study. Originally, the idea was to do concatenated 18S and 28S rDNA phylogenies for all strains. Most species used in the phylogenies did not have both regions available as reference sequences, so it was decided to use 18S only for most trees. The reason for this is that bases appearing in less than half of the alignment is removed when filtered with Gblocks. Nevertheless, the 28S rDNA sequences were kept and will be uploaded to NCBI GenBank.

The phylogenetic tree inferred from 18S rDNA for genus *Tetraselmis* (Fig. 6) generally had very low support values and unresolved clades. Twelve of the 16 sequences have a variation of 1% between them, and the sequence from the present study is relatively short and had low quality (1150 bp, 18.3% HQ). Partial 28S rDNA (D1/D2) was also retrieved from *Tetraselmis* sp. (UIO346), but very few 28S rDNA reference sequences for this genus are available (5/36, NCBI GenBank).

The concatenated phylogenetic tree inferred from 18S and 28S rDNA for genera *Cylindrotheca* and *Nitzschia* (Fig. 19) showed relatively high support values for genus *Cylindrotheca* and the smaller major *Nitzschia* clade (*N. amphibia*, *N. fonticola*, *N. incospicua*, *N. soratensis* and *N. supralitorea*). The other major clade containing the *Nitzschia* sp. (UIO383) from the present study, though, was mostly unresolved. This is likely because reference sequences for both 18S and 28S rDNA are available for too few taxa in the latter clade (6/15, NCBI GenBank). Also, the variability of 18S rDNA among diatom species is relatively low (Theriot et al. 2009).

4.5 Phylogenetic analyses

For the phylogenetic analyses, all available reference sequences from the most convenient taxonomic groups based on Guiry & Guiry (2015) were included. For smaller groups, such as classes Dictyochophyceae and Chlorarachniophyceae and order Pyrenomonadales, all available reference sequences were included. For larger groups, such as classes Chlorodendrophyceae and Chlorophyceae, only species from genera *Tetraselmis* and *Chlamydomonas* respectively were

included. A selection of the reference sequences most similar to the sequences from the present study were also added. This also includes sequence only identified to suggested species (cf.), genus or higher taxonomic groups, such as environmental sequences. The outgroups were chosen based on previous work. An exception is the phylogeny for class Pavlovophyceae (Fig. 16) where *Katablepharis remigera* was used instead of genera *Chrysochromulina* Lackey or *Phaeocystis* Lagerheim (Edvardsen et al. 2000).

All the alignments were filtered with Gblocks v0.91b (Castresana 2000) to remove hyper-variable and ambiguously aligned regions. This was done to decrease the risk of getting phylogenetic artefacts such as long-branch attraction (LBA) (Brinkmann et al. 2005). LBA is the phenomenon where one taxon shows higher affinity for another taxon than it should. This may be caused by rapidly evolving sites known as saturated bases. If several point mutations have happened in a single base, e.g. from A (adenine) to T (thymine) and the back to A, species who shares the A may in-fact be more distantly related than with species with a T. Because the phylogenetic algorithms cannot distinguish between an evolved and non-evolved A, these regions must be removed from the alignments.

The Generalised time-reversible substitution model (GTR) was used for all the phylogenetic analyses. A few 18S rDNA alignments were tested with JModelTest v.2.1.7 (Darriba et al. 2012), and the analyses recommended the GTR model. This has also been shown for other algal groups, e.g. order Prymnesiales (Edvardsen et al. 2011). Also, a few phylogenetic analyses were run with different substitution models without showing any significant differences in tree topology and support values. This observation may not apply to all the alignments, but it was decided that GTR was the proper model to use for PhyML and MrBayes for both 18S and 28S rDNA.

Several algorithms in addition to Maximum likelihood (PhyML) and Bayesian analysis were considered for the phylogenetic analyses. A few alignments where analysed with Neighbor-Joining using the Jukes-Cantor, HKY and Tamura-Nei genetic distance models. No significant incongruence with the PhyML and Bayesian analyses was shown, except for some poorly resolved clades. It was hence considered that PhyML and Bayesian analysis were the proper algorithms to use.

4.6 Taxonomy

The taxonomic nomenclature used in the present study was chosen to present the species in the clearest possible way based on selected literature. To minimize potential confusion this was done by using the traditional algal taxon-suffixes (division: -phyta; class: -phyceae; order: -ales) as recommended by the International Code of Botanical Nomenclature (Vienna Code) (McNeill et al.

2006) where possible. This is done in contrast to the recent Melbourne Code (McNeill et al. 2012), where the recommended taxon-suffixes were redefined (division: -phycota; class: -phyceae; order: -ales). It is also done in contrast to the recently published Catalogue of Life (CoL) (Ruggiero et al. 2015) where division Chlorarachniophyta is named class Chlorarachnea (phylum Cercozoa, subphylum Reticulofilosa), division Cryptophyta is named phylum Cryptista and division Dinophyta is named superclass Dinoflagellata (phylum Miozoa, infraphylum Dinozoa) to mention a few. Finally, genus *Cylindrotheca* is used for *C. closterium* (Reimann & Lewin 1964) as proposed by Medlin & Mann (2007) instead of *Ceratoneis* as proposed by Jahn & Kusber (2005).

5 Conclusion

Eleven strains isolated from the Red Sea have been identified morphologically and phylogenetically in the present study. Four have been identified to species: *Cafeteria roenbergensis*, *Lotharella reticulosa*, *Cylindrotheca* cf. *closterium* and *Oxyrrhis marina*. The latter two have previously been recorded in the Red Sea, whereas the first two have been recorded in similar habitats, e.g. the Mediterranean Sea with warm water and high salinity. Four strains have been identified to genus: genera *Amphidinium*, *Chlamydomonas*, *Nitzschia* and *Tetraselmis*, all of which are previously recorded in the Red Sea and similar habitats, e.g. the Persian Gulf, Kuwait. Only two of the 18 sequences from the present study (*Cafeteria roenbergensis* UIO345 and *Chlamydomonas* sp. UIO350) are 100% genetically identical to available reference sequences. They will all be uploaded to NCBI GenBank.

The three potentially novel species were partially described. The first belongs to genus *Proteomonas* with *P. sulcata* as the closest relative. More work (morphology, pigment analysis and further barcoding) is needed for a species diagnosis. The second belongs to genus *Pavlova* with *P. gyrans* as the closest relative. It is believed that this is the species Eikrem et al. (In prep.) is currently describing. The third belongs to genus *Rhizochromulina* with *R. marina* as the closest relative and the only taxonomically accepted species of this genus. Transmission electron micrographs of the zoospores of this strain is needed for a species diagnosis.

Bibliography

Aberle-Malzahn N (2004) *The Microphytobenthos and Its Role in Aquatic Food Webs*. Doctor thesis, University of Kiel, Germany. 150 pp.

Al-Qassab S, Lee WJ, Murray S, Simpson AGB & Patterson DJ (2002) Flagellates from stromatolites and surrounding sediments in Shark Bay, Western Australia. *Acta Protozoologica* **41**:91–144.

Al-yamani FY & Saburova MA (2011) *Illustrated Guide on the Benthic Diatoms of Kuwait's Marine Environment*, 1st ed., Kuwait Instritute for Scientific Research, Safat, Kuwait, 352 pp.

Al-yamani FY & Saburova MA (2010) *Illustrated Guide on the Flagellates of Kuwait's Intertidal Soft Sediments*, 1st ed., Kuwait Institute for Scientific Research, Safat, Kuwait, 197 pp.

Andersen RA (2004) Biology and systematics of heterokont and haptophyte algae. *American Journal of Botany* **91**:1508–1522.

Andersen RA & Kawachi M (2005) *Traditional Microalgae Isolation Techniques. In: Andersen CD (ed.): Algal Culturing Techniques*, 1st ed., Elsevier Academic Press, Waltham, MA, USA, pp. 83-100.

Armitage AR, Frankovich TA, Heck KL & Fourqurean JW (2005) Experimental nutrient enrichment causes complex changes in seagrass, microalgae, and macroalgae community structure in Florida Bay. *Estuaries* **28**:422–434.

Arora M, Anil AC, Leliaert F, Delany J & Mesbahi E (2013) *Tetraselmis indica* (Chlorodendrophyceae, Chlorophyta), a new species isolated from salt pans in Goa, India. *European Journal of Phycology* **48**:61–78.

Ball H (2006) *A Morphological and Molecular Approach to the Study of Planktonic Protist Phylogenetics with a Focus on Taxa from Old Woman Creek National Estuarine Research Reserve*. Master thesis, University of Akron, OH, USA. 81 pp.

Banguera-Hinestroza E, Eikrem W, Mansour H, Solberg I, Curdia J, Holtermann K, Edvardsen B & Kaartvedt S Seasonality and toxin production of *Pyrodinium bahamense* in a Red Sea lagoon. *In prep.*

Bendif EM, Probert I, Hervé A, Billard C, Goux D, Lelong C, Cadoret JP & Véron B (2011) Integrative taxonomy of the Pavlovophyceae (Haptophyta): a reassessment. *Protist* **162**:738–761.

Biecheler B (1952) Recherches sur les Péridiniens. *Bulletin Biologique du France et de Belgique* **24**:1–149.

Björk M, Short F, Mcleod E & Beer S (2008) *Managing Seagrasses for Resilience to Climate Change*, IUCN, Gland, Switzerland, 55 pp.

Bower AS, Hunt HD & Price JF (2000) Character and dynamics of the Red Sea and Persian Gulf outflows. *Journal of Geophysical Research* **105**:6387–6414.

Brewster R (2014) Paint.NET - Free Software for Digital Photo Editing. *http://www.getpaint.net/index.html (accessed June 2015)*.

Brinkmann H, van der Giezen M, Zhou Y, Poncelin de Raucourt G & Philippe H (2005) An empirical assessment of long-branch attraction artefacts in deep eukaryotic phylogenomics. *Systematic Biology* **54**:743–757.

Broady PA (1981) Ecological and taxonomic observations on subaerial epilithic algae from Princess Elizabeth Land and Mac.Robertson Land, Antarctica. *British Phycological Journal* **16**:257–266.

Buchheim MA, Buchheim JA & Chapman RL (1997) Phylogeny of *Chloromonas* (Chlorophyceae): a study of 18S ribosomal RNA gene sequences. *Journal of Phycology* **33**:286–293.

Burki F (2014) The eukaryotic tree of life from a global phylogenomic perspective. *Cold Spring Harbor Perspectives in Biology* **6**:1–17.

Butcher RW (1952) Contributions to our knowledge of the smaller marine algæ. *Journal of the Marine Biological Association of the United Kingdom* **31**:175–191.

Caron DA, Countway PD, Jones AC, Kim DY & Schnetzer A (2012) Marine Protistan Diversity. *Annual Review of Marine Science* **4**:467–493.

Castresana J (2000) Selection of conserved blocks from multiple alignments for their use in phylogenetic analysis. *Molecular Biology and Evolution* **17**:540–552.

Cavalier-Smith T & Chao EEY (2006) Phylogeny and megasystematics of phagotrophic heterokonts (kingdom Chromista). *Journal of Molecular Evolution* **62**:388–420.

Cerino F & Zingone A (2006) A survey of cryptomonad diversity and seasonality at a coastal Mediterranean site. *European Journal of Phycology* **41**:363–378.

Claparède É & Lachmann J (1859) *Amphidinium operuculatum*. *Mémoires de l'Institut National Genevois* **6**:261–482.

Darriba D, Taboada GL, Doallo R & Posada D (2012) jModelTest 2: more models, new heuristics and parallel computing. *Nature Methods* **9**:772–772.

Das S, Lyla PS & Khan SA (2006) Marine microbial diversity and ecology: importance and future perspectives. *Current Science* **90**:1325–1335.

Duarte CM (2002) The future of seagrass meadows. *Environmental Conservation* **29**:192–206.

Edvardsen B, Eikrem W, Green JC, Andersen RA, Van Der Staay SYM & Medlin LK (2000) Phylogenetic reconstructions of the Haptophyta inferred from 18S ribosomal DNA sequences and available morphological data. *Phycologia* **39**:19–35.

Edvardsen B, Eikrem W, Shalchian-Tabrizi K, Riisberg I, Johnsen G, Naustvoll L & Throndsen J (2007) *Verrucophora farcimen* gen. et sp. nov. (Dictyochophyceae, Heterokonta) - A bloom-forming ichthyotoxic flagellate from the Skagerrak, Norway. *Journal of Phycology* **43**:1054–1070.

Edvardsen B, Eikrem W, Throndsen J, Sáez AG, Probert I & Medlin LK (2011) Ribosomal DNA phylogenies and a morphological revision provide the basis for a revised taxonomy of the Prymnesiales (Haptophyta). *European Journal of Phycology* **46**:202–228.

Edvardsen B & Paasche E (1992) Two motile stages of *Chrysochromulina polylepis* (Prymnesiophyceae): morphology, growth and toxicity. *Journal of Phycology* **28**:104–114.

Edvardsen B, Shalchian-tabrizi K, Jakobsen KS & Medlin LK (2003) Genetic variability and molecular phylogeny of *Dinophysis* species (Dinophyceae) from Norwegian waters inferred from single cell analyses of rDNA. *Journal of Phycology* **39**:395–408.

Eikrem W, Dittami S & Wold A A new psammobian pavlovales from Saudi Arabia. *In prep.*

Ekebom J, Patterson DJ & Vørs N (1996) Heterotrophic flagellates from coral reef sediments (Great Barrier Reef, Australia). *Archiv für Protistenkunde* **146**:251–272.

Elwood HJ, Olsen GJ & Sogin ML (1985) The small-subunit ribosomal RNA gene sequences from the hypotrichous ciliates *Oxytricha nova* and *Stylonychia pustulata*. *Molecular Biology and Evolution* **2**:399–410.

Emery KO (1956) Sediments and water of Persian Gulf. *Bulletin of the American Association of Petroleum Geologists* **40**:2354–2383.

Eppley RW, Holmes RW & Strickland JDH (1967) Sinking rates of marine phytoplankton measured with a fluorometer. *Journal of Experimental Marine Biology and Ecology* **1**:191–208.

Ettl H (1967) *Chlamydomonas parkeae*, eine neue marine Chlamydomonade. *Revue der gesamten Hydrobiologie und Hydrographie* **52**:437–440.

Ettl H (1976) Die Gattung *Chlamydomonas* Ehrenberg. *Beihefte zur Nova Hedwigia* **49**:1–1122.

Farnsworth EJ & Ellison AM (1996) Scale-dependent spatial and temporal variability in biogeography of mangrove root epibiont communites. *Ecological Society of America* **66**:45–66.

Fenchel T (1967) The ecology of marine microbenthos I. The quantitative importance of ciliates as compared with metazoans in various types of sediments. *Ophelia* **4**:121–137.

Fenchel T (1969) The ecology of marine microbenthos IV. Structure and function of the benthic ecosystem, its chemical and physical factors and the microfauna comuunities with special reference to the ciliated Protozoa. *Ophelia* **6**:1–182.

Fenchel T & Patterson DJ (1988) *Cafeteria roenbergensis* nov. gen., nov. sp., a heterotrophic microflagellate from marine plankton. *Marine Microbial Food Webs* **3**:9–19.

Field CB, Behrenfeld MJ, Randerson JT & Falkowski P (1998) Primary production of the biosphere: integrating terrestrial and oceanic components. *Science* **281**:237–240.

Flø Jørgensen M, Murray S & Daugbjerg N (2004) *Amphidinium* revisited. I. Redefinition of *Amphidinium* (Dinophyceae) based on cladistic and molecular phylogenetic analyses. *Journal of Phycology* **40**:351–365.

Fumanti B, Cavacini P & Alfinito S (1996) Benthic algal mats of some lakes of Inexpressible Island (northern Victoria Land, Antarctica). *Polar Biology* **17**:25–30.

Garai EZ (2005) *Diversity of Sandflagellates in the Oslofjord*. Master thesis, University of Oslo, Norway. 92 pp.

Gárate-Lizárraga I (2014) Proliferation of *Levanderina fissa* and *Polykrikos hartmannii* (Dinophyceae: Gymnodiniales) in Bahía de la Paz, Gulf of Californiam México. *CICIMAR Oceánides* **29**:25–35.

Gárate-Lizárraga I, Muñetón-Gómez MDS, Pérez-Cruz B & Díaz-Ortíz JA (2014) Bloom of *Gonyaulax spinifera* (Dinophyceae: Gonyaulacales) in Ensenada de la Paz lagoon, Gulf of California. *CICIMAR Oceánides* **29**:11–18.

Gile GH, Stern RF, James ER & Keeling PJ (2010) DNA barcoding of chlorarachniophytes using nucleomorph ITS sequences. *Journal of Phycology* **46**:1–8.

Graham LE, Graham JM & Wilcox LW (2009) *Algae*, 2nd ed., Pearson Education Inc., San Fransisco, CA, USA, 616 pp.

Green JC & Manton FRS (1970) Studies in the fine structure and taxonomy of flagellates in the genus *Pavlova*. A revision of the *Pavlova gyrans*, the type species. *Journal of the Marine Biological Association of the United Kingdom* **50**:1113–1130.

Grell KG & Wohlfarth-Bottermann KE (1957) Licht- und elektronenmikroskopische Untersuchungen an dem Dinoflagellaten *Amphidinium elegans* n. sp. *Zeitschrift für Zellforschung und Mikroskopische Anatomie* **47**:7–17.

Guindon S & Gascuel O (2003) A simple, fast, and accurate algorithm to estimate large phylogenies by maximum likelihood. *Systematic Biology* **52**:696–704.

Guiry MD (2012) How many species of algae are there? *Journal of Phycology* **48**:1057–1063.

Guiry MD & Guiry GM (2015) AlgaeBase. World-wide electronic publication, National University of Ireland, Galway. *http://www.algaebase.org (accessed May 2015)*.

Hällfors G (2004) *Checklist of Baltic Sea Phytoplankton Species*, Baltic Sea Environmental Proceedings, Helsinki, Finland, 208 pp.

Hardison AK, Canuel EA, Anderson IC, Tobias CR, Veuger B & Waters MN (2013) Microphytobenthos and benthic macroalgae determine sediment organic matter composition in shallow photic sediments. *Biogeosciences* **10**:5571–5588.

Hasle GR & Syvertsen EE (1996) *Marine Diatoms. In: Tomas, CR (ed.): Identifying Marine Diatoms and Dinoflagellates*, Academic Press, Inc., San Diego, CA, USA, pp. 5-386.

Hendey NI (1964) A revised check-list of British marine diatoms. *Journal of the Marine Biological Association of the United Kingdom* **54**:277–300.

Hibberd DJ & Chrétiennot-Dinet MJ (1979) The ultrastructure and taxonomy of *Rhizochromulina marina* gen. et sp. nov., an amoeboid marine chrysophyte. *Journal of the Marine Biological Association of the United Kingdom* **59**:179–193.

Hibberd DJ & Norris RE (1984) Cytology and ultrastructure of *Chlorarachnion reptans* (Chlorarachniophyta divisio nova, Chlorarachniophyceae classis nova). *Journal of Phycology* **20**:310–330.

Hill DRA & Wetherbee R (1986) *Proteomonas sulcata* gen. et sp. nov. (Cryptophyceae), a cryptomonad with two morphologically distinct and alternating forms. *Phycologia* **25**:521–543.

Hoef-Emden K (2008) Molecular phylogeny of phycocyanin-containing cryptophytes: evolution of biliproteins and geographical distribution. *Journal of Phycology* **44**:985–993.

Hoef-Emden K, Marin B & Melkonian M (2002) Nuclear and nucleomorph SSU rDNA phylogeny in the Cryptophyta and the evolution of cryptophyte diversity. *Journal of Molecular Evolution* **55**:161–179.

Hoham RW, Bonome TA, Martin CW & Leebens-Mack JH (2002) A combined 18S rDNA and rbcL phylogenetic analysis of *Chloromonas* and *Chlamydomonas* (Chlorophyceae, Volvocales) emphasizing snow and other cold-temperature habitats. *Journal of Phycology* **38**:1051–1064.

Hoppenrath M, Murray SA, Chomérat N & Horiguchi T (2014) *Marine Benthic Dinoflagellates - Unveiling their Worldwide Biodiversity*, Schweizerbart'sche Verlagsbuchhandlung, Stuttgart, Germany, 276 pp.

Hori T, Norris RE & Chihara M (1982) Studies on the ultrastructure and taxonomy of the genus *Tetraselmis* (Prasinophyceae) I. Subgenus *Tetraselmis*. *The Botanical Magazine Tokyo* **95**:49–61.

Hori T, Norris RE & Chihara M (1986) Studies on the ultrastructure and taxonomy of the genus *Tetraselmis* (Prasinophyceae) III. Subgenus *Parviselmis*. *The Botanical Magazine Tokyo* **99**:123–135.

Hosoi-Tanabe S, Honda D, Fukaya S, Otake I, Inagaki Y & Sako Y (2007) Proposal of *Pseudochattonella verruculosa* gen. nov., comb. nov. (Dictyochophyceae) for a formar raphidophycean alga *Chattonella verruculosa*, based on 18S rDNA phylogeny and ultrastructural characteristics. *Phycological Research* **55**:185–192.

Huelsenbeck JP & Ronquist F (2001) MRBAYES: Bayesian inference of phylogenetic trees. *Bioinformatics* **17**:754–755.

Hulburt EM (1957) The taxonomy of unarmored Dinophyceae of shallow embayments on Cape Cod, Massachusetts. *Biological Bulletin* **112**:196–219.

Ishida K, Green BR & Cavalier-Smith T (1999) Diversification of a chimaeric algal group, the chlorarachniophytes: phylogeny of nuclear and nucleomorph small-subunit rRNA genes. *Molecular Biology and Evolution* **16**:321–331.

Jahn R & Kusber W-H (2005) Reinstatement of the genus *Ceratoneis* Ehrenberg and lectotypification of its type specimen: *C. closterium* Ehrenberg. *Diatom Research* **20**:295–304.

Jaschinski S, Aberle N, Gohse-Reimann S, Brendelberger H, Wiltshire KH & Sommer U (2009) Grazer diversity effects in an eelgrass-epiphyte-microphytobenthos system. *Oecologia* **159**:607–615.

Jin-Eong O (1995) The ecology of mangrove conservation & management. *Hydrobiologia* **295**:343–351.

Kaas H (1987) Algal studies of the Danish Wadden Sea. V. Blue-green algae in higher salt march areas - their seasonal and spatial distribution. *Nordic Journal of Botany* **7**:735–749.

Katoh K, Misawa K, Kuma K & Miyata T (2002) MAFFT: a novel method for rapid multiple sequence alignment based on fast Fourier transform. *Nucleic acids research* **30**:3059–3066.

Khalil ASM (2004) *Status of Mangroves in the Red Sea and Gulf of Aden. PERSGA Technical Series No. 11.*, PERSGA, Jeddah, Saudi Arabia. 60 pp.

Kiefer DA (1973) Chlorophyll a fluorescence in marine centric diatoms: responses of chloroplasts to light and nutrient stress. *Marine Biology* **23**:39–46.

Kim Y-S, Oyaizu H, Matsumoto S, Watanabe MM & Nozaki H (1994) Chloroplast small-subunit ribosomal RNA gene sequence from *Chlamydomonas parkeae* (Chlorophyta): molecular phylogeny of a green alga with a peculiar pigment composition. *European Journal of Phycology* **29**:213–217.

Klaveness D (1988) *Ecology of the Cryptomonadida: A First Review. In: Sandgren, CD (ed.): Growth and Reproductive Strategies of Freshwater Phytoplankton*, Cambridge University Press, New York, NY, USA, pp. 105-133.

Klochkova TA, Cho GY, Boo SM, Chung KW, Kim SJ & Kim GH (2008) Interactions between marine facultative epiphyte *Chlamydomonas* sp. (Chlamydomonadales, Chlorophyta) and ceramiaceaen algae (Rhodophyta). *Journal of Environmental Biology* **29**:427–435.

Kreimer G (1999) Reflective properties of different eyespot types in dinoflagellates. *Protist* **150**:311–323.

Larsen J & Patterson DJ (1990) Some flagellates (Protista) from tropical marine sediments. *Journal of Natural History* **24**:801–937.

Lee JJ, Olea R, Cevasco M, Pochon X, Correia M, Shpigel M & Pawlowski J (2003) A marine dinoflagellate, *Amphidinium eilatiensis* n. sp., from the benthos of a mariculture sedimentation pond in Eilat, Israel. *Journal of Eukaryot Microbiology* **50**:439–448.

Lee KH, Jeong HJ, Park K, Kang NS, Yoo YD, Lee MJ, Lee J-W, Lee S, Kim T, Kim HS & Noh JH (2013) Morphology and molecular characterization of the epiphytic dinoflagellate *Amphidinium massartii*, isolated from the temperate waters off Jeju Island, Korea. *Algae* **28**:213–231.

Lee WJ & Patterson DJ (2002) Abundance and biomass of heterotrophic flagellates, and factors controlling their abundance and distribution in sediments of Botany Bay. *Microbial Ecology* **43**:467–481.

Van Lenning K, Latasa M, Estrada M, Sáez AG, Medlin L, Probert I, Véron B & Young J (2003) Pigment signatures and phylogenetic relationship of the Pavlovophyceae (Haptophyta). *Journal of Phycology* **39**:379–389.

Levy JL, Stauber JL & Jolley DF (2007) Sensitivity of marine microalgae to copper: the effect of biotic factors on copper adsorption and toxicity. *Science of the Total Environment* **387**:141–154.

Lewin J (1996) Silicon metabolism in diatoms. V. Germanium dioxide, a specific inhibitor of diatom growth. *Phycologia* **6**:1–12.

Lowe CD, Keeling PJ, Martin LE, Slamovits CH, Watts PC & Montagnes DJS (2011) Who is *Oxyrrhis marina*? Morphological and phylogenetic studies on an unusual dinoflagellate. *Journal of Plankton Research* **33**:555–567.

LuZhen C, WenQing W, YiHui Z, Li H, ChunLei, Zhao, ShengChang Y, ZhiWei Y, YueChao C, HuaLin X, CaiRong Z, Bo S, BaiZhou F, NaiMing C, ChuanZhi Z & GuangHui L (2010) Damage to mangroves from extreme cold in early 2008 in southern China. *Journal of Plant Ecology* **34**:186–194.

MacIntyre HL, Geider RJ & Miller DC (1996) Microphytobenthos: the ecological role of the "secret garden" of unvegetated, shallow-water marine habitats. I. Distribution, abundance and primary production. *Estuaries* **19**:186–201.

Maillard C & Soliman G (1986) Hydrography of the Red Sea and exchanges with the Indian Ocean in summer. *Oceanologica Acta* **9**:249–269.

Marshall N (1994) Mangrove conservation in relation to overall environmental considerations. *Hydrobiologia* **285**:303–309.

McCarthy PM (2013) Census of Australian Marine Diatoms. Australian Biological Resources Study, Canberra. *http://www.anbg.gov.au/abrs/Marine_Diatoms/index.html (accessed June 2015)*.

McLachlan A & Brown AC (2006) *The Ecology of Sandy Shores*, 2nd ed., Elsevier Academic Press, Waltham, MA, USA, 373 pp.

McNeill J, Barrie FR, Buck WR, Demoulin V, Greuter W, Hawksworth DL, Herendeen PS, Knapp S, Marhold K, Prado J, Prud'Homme van Reine WF, Smith GF, Wiersema JH & Turland NJ (2012) *International Code of Nomenclature for algae, fungi and plants (Melbourne Code)*, Koeltz Scientific Books, Königstein, Germany, Art. 16, 17.

McNeill J, Barrie FR, Burdet HM, Demoulin V, Hawksworth DL, Marhold K, Nicolson DH, Prado J, Silva PC, Skog JE, Wiersema JH & Turland NJ (2006) *International Code of Botanical Nomenclature (Vienna Code)*, Gantner Verlag, KG, Ruggell, Liechtenstein, Art. 16, 17.

Medlin L, Elwood HJ, Stickel S & Sogin ML (1988) The characterization of enzymatically amplified eukaryotic 16S-like rRNA-coding regions. *Gene* **71**:491–499.

Medlin LK & Mann DG (2007) Proposal to conserve the name *Cylindrotheca* against *Ceratoneis* (Bacillariophyceae). *Taxon* **56**:953–955.

Méléder V, Rincé Y, Barillé L, Gaudin P & Rosa P (2007) Spatiotemporal changes in microphytobenthos assemblages in a macrotidal flat (Bourgneuf Bay, France). *Journal of Phycology* **43**:1177–1190.

Moncreiff C & Sullivan M (2001) Trophic importance of epiphytic algae in subtropical seagrass beds: evidence from multiple stable isotope analyses. *Marine Ecology Progress Series* **215**:93–106.

Murray S, Flø Jørgensen M, Daugbjerg N & Rhodes L (2004) *Amphidinium* revisited. II. Resolving species boundaries in the *Amphidinium operculatum* species complex (Dinophyceae), including the descriptions of *Amphidinium trulla* sp. nov. and *Amphidinium gibbosum*. comb. nov. *Journal of Phycology* **40**:366–382.

Murray S & Patterson DJ (2002) The benthic dinoflagellate genus *Amphidinium* in south-eastern Australian waters, including three new species. *European Journal of Phycology* **37**:279–298.

Nandkeolyar N, Raman M & Kiran GS (2013) Comparative analysis of sea surface temperature pattern in the eastern and western gulfs of Arabian Sea and the Red Sea in recent past using satellite data. *International Journal of Oceanography* **2013**:1–16.

NBRC (2015) NBRC Strains (NBRC Strains). *http://www.nite.go.jp/en/nbrc/cultures/nbrc/index.html (accessed June 2015)*.

NCBI (2015) National Center for Biotechnology Information (National Center for Biotechnology Information). *http://www.ncbi.nlm.nih.gov/ (accessed May 2015)*.

NCMA (2015) NCMA at Bigelow Laboratory - Culturing Diversity (NCMA (Formerly the CCMP)). *https://ncma.bigelow.org/ (accessed June 2015)*.

Neustupa J & Škaloud P (2008) Diversity of subaerial algae and cyanobacteria on tree bark in tropical mountain habitats. *Biologia* **63**:806–812.

NIES (2015) NIES Collection - Microbial Culture Collection (NIES Collection - Microbial Culture Collection). *http://mcc.nies.go.jp/ (accessed June 2015)*.

Novarino G (1991) Observations on some new and interesting Cryptophyceae. *Nordic Journal of Botany* **11**:599–611.

Nurkin B (1994) Degradation of mangrove forests in South Sulawesi, Indonesia. *Hydrobiologia* **285**:271–276.

O'Kelly CJ & Patterson DJ (1996) The flagellar apparatus of *Cafeteria roenbergensis* Fenchel & Patterson, 1988 (Bicosoecales = Bicosoecida). *European Journal of Protistology* **32**:216–226.

Orth RJ, Carruthers TJB, Dennison WC, Duarte CM, Fourqurean JW, Heck Jr. KL, Hughes AR, Kendrick GA, Kenworthy WJ, Olyarnik S, Short FT, Waycott M & Williams SL (2006) A global crisis for seagrass ecosystems. *BioScience* **56**:987–966.

Orth RJ, Heck KL & van Montfrans J (1984) Faunal communities in seagrass beds: a review of the influence of plant structure and prey characteristics on predator-prey relationships. *Estuarine Research Federation* **7**:339–350.

Ota S & Vaulot D (2012) *Lotharella reticulosa* sp. nov.: a highly reticulated network forming chlorarachniophyte from the Mediterranean Sea. *Protist* **163**:91–104.

Ota S, Vaulot D, Le Gall F, Yabuki A & Ishida K (2009) *Partenskyella glossopodia* gen. et sp. nov., the first report of a chlorarachniophyte that lacks a pyrenoid. *Protist* **160**:137–150.

Pawlowski J, Audic S, Adl S, Bass D, Belbahri L, Berney C, Bowser SS, Cepicka I, Decelle J, Dunthorn M, Fiore-Donno AM, Gile GH, Holzmann M, Jahn R, Jirků M, Keeling PJ, Kostka M, Kudryavtsev A, Lara E, Lukeš J, Mann DG, Mitchell EAD, Nitsche F, Romeralo M, Saunders GW, Simpson AGB, Smirnov A V, Spouge JL, Stern RF, Stoeck T, Zimmermann J, Schindel D & de Vargas C (2012) CBOL Protist Working Group: barcoding eukaryotic richness beyond the animal, plant, and fungal kingdoms. *PLoS Biology* **10**:e1001419.

Preen A (1995) Impacts of dugong foraging on seagrass habitats: observational and experimental evidence for cultivation grazing. *Marine Ecology Progress Series* **124**:201–213.

Price ARG, Medley PAH, McDowall RJ, Dawson-Shepherd AR, Hogarth PJ & Ormond RFG (1987) Aspects of mangal ecology along the Red Sea coast of Saudi Arabia. *Journal of Natural History* **21**:449–464.

Ralph PJ, McMinn A, Ryan KG & Ashworth C (2005) Short-term effect of temperature on the photokinetics of microalgae from the surface layers of Antarctic pack ice. *Journal of Phycology* **41**:763–769.

RCC (2015) Roscoff Culture Collection (Roscoff Culture Collection). *http://roscoff-culture-collection.org/ (accessed June 2015)*.

Reimann BEF & Lewin JC (1964) The diatom genus *Cylindrotheca* Rabenhorst. *Journal of the Royal Microscopical Society* **83**:283–296.

Rhodes LL, Edwards AR, Bojo O & Chang FH (2012) *Phylum Haptophyta: Haptophytes. In: Gordon DP (ed.): New Zealand Inventory of Biodiversity*, Canterbury University Press, Christchurch, New Zealand, pp. 313-321.

Ricklefs RE & Latham RE (1993) *Global patterns of diversity in mangrove floras. In: Ricklefs RE & Schluter D (eds.): Species Diversity in Ecological Communities: Historical and Geographical Perspectives*, University of Chicago Press, Chicago, IL, USA, pp. 215-229.

Riisberg I, Orr RJS, Kluge R, Shalchian-Tabrizi K, Bowers HA, Patil V, Edvardsen B & Jakobsen KS (2009) Seven gene phylogeny of heterokonts. *Protist* **160**:191–204.

Rodelli MR, Gearing JN, Gearing PJ, Marshall N & Sasekumar A (1984) Stable isotope ratio as a tracer of mangrove carbon in Malaysian ecosystems. *Oecologia* **61**:326–333.

Ruggiero MA, Gordon DP, Orrell TM, Bailly N, Bourgoin T, Brusca RC, Cavalier-Smith T, Guiry MD & Kirk PM (2015) A higher level classification of all living organisms. *Plos One* **10**:1–60.

Sahoo K & Dhal NK (2009) Potential microbial diversity in mangrove ecosystems : a review. *Indian Journal of Marine Sciences* **38**:249–256.

Sanger F, Nicklen S & Coulson AR (1977) DNA sequencing with chain-terminating inhibitors. *Proceedings of the National Academy of Sciences of the United States of America* **74**:5463–5467.

Sasa T, Suda S, Watanabe MM & Takaichi S (1992) A yellow marine *Chlamydomonas*: morphology and pigment composition. *Plant and Cell Physiology* **33**:527–534.

Sasekumar A, Chong VC, Leh MU & D'Cruz R (1992) Mangroves as a habitat for fish and prawns. *Hydrobiologia* **247**:195–207.

SCCAP (2015) The Collection (Scandinavian Culture Collection for Algae & Protozoa). *http://www.sccap.dk/collection/ (accessed June 2015)*.

Schmidt M, Gessner G, Luff M, Heiland I, Wagner V, Kaminski M, Geimer S, Eitzinger N, Reissenweber T, Voytsekh O, Fiedler M, Mittag M & Kreimer G (2006) Proteomic analysis of the eyespot of *Chlamydomonas reinhardtii* provides novel insights into its components and tactic movements. *The Plant Cell* **18**:1908–1930.

Scholin CA, Herzog M, Sogin M & Anderson DM (1994) Identification of group- and strain-specific genetic markers for globally distributed *Alexandrium* (Dinophyceae). II. Sequence analysis of a fragment of the LSU rRNA gene. *Journal of Phycology* **30**:999–1011.

Seoane S, Eikrem W, Arluzea J & Orive E (2009) Haptophytes of the Nervión River estuary, northern Spain. *Botanica Marina* **52**:47–59.

Shah MMR, An SJ & Lee JB (2013) Presence of benthic dinoflagellates around coastal waters of Jeju Island including newly recorded species. *Journal of Ecology and Environment* **36**:347–370.

Short F, Carruthers T, Dennison W & Waycott M (2007) Global seagrass distribution and diversity: a bioregional model. *Journal of Experimental Marine Biology and Ecology* **350**:3–20.

Smith TE (2010) Revisited list of algae from Arkansas (USA) and new additions. *International Journal of Algae* **12**:230–256.

Smith W & West T (1853) *A synopsis of the British Diatomaceæ: with remarks on their structure, functions and distribution; and instructions for collecting and preserving specimens*, Vol. 1. John van Voorst, London, England. 89 pp.

Snowdon P, Eamus D, Gibbons P, Keith H, Raison J & Kirschbaum M (2000) *Synthesis of Allometrics, Review of Root Biomass, and Design of Future Woody Biomass Sampling Strategies*, Australian Greenhouse Office, Canberra, Australia, 114 pp.

Tamura M, Takano Y & Horiguchi T (2009) Discovery of a novel type of body scale in the marine dinoflagellate, *Amphidinium cupulatisquama* sp. nov. (Dinophyceae). *Phycological Research* **57**:304–312.

Taylor FJR, Hoppenrath M & Saldarriaga JF (2007) Dinoflagellate diversity and distribution. *Biodiversity and Conservation* **17**:407–418.

Tengs T, Dahlberg OJ, Shalchian-Tabrizi K, Klaveness D, Rudi K, Delwiche CF & Jakobsen KS (2000) Phylogenetic analyses indicate that the 19'Hexanoyloxy-fucoxanthin-containing dinoflagellates have tertiary plastids of haptophyte origin. *Molecular Biology and Evolution* **17**:718–729.

Theriot EC, Cannone JJ, Gutell RR & Alverson AJ (2009) The limits of nuclear-encoded SSU rDNA for resolving the diatom phylogeny. *European Journal of Phycology* **44**:277–290.

Throndsen J, Hasle GR & Tangen K (2007) *Phytoplankton of Norwegian coastal waters*, Almater forlag AS, Oslo, Norway, 343 pp.

Turrill WB (1942) Taxonomy and phylogeny. *The Botanical Review* **8**:655–707.

Valentine JF & Heck Jr. KL (1999) Seagrass herbivory: evidence for the continued grazing of marine grasses. *Marine Ecology Progress Series* **176**:291–302.

Valiela I, Bowen JL & York JK (2001) Mangrove forests: one of the World's threatened major tropical environments. *BioScience* **51**:807–815.

Vørs N (1993a) Heterotrophic amoebae, flagellates and heliozoa from Arctic marine waters (North West Territories, Canada and West Greenland). *Polar Biology* **13**:113–126.

Vørs N (1993b) Marine heterotrophic amoebae, flagellates and heliozoa from Belize (Central America) and Tenerife (Canary Islands), with descriptions of new species, *Luffisphaera bulbochaete* N. SP., *L. Longihastis* N. Sp., *L. turriformis* N. Sp. and *Paulinella intermedia* N. *Journal of Eukaryotic Microbiology* **40**:272–287.

Waisel Y, Eshel A & Agami M (1986) Salt balance of leaves of the mangrove *Avicennia marina*. *Physiologia Plantarum* **67**:67–72.

Watts PC, Martin LE, Kimmance SA, Montagnes DJS & Lowe CD (2010) The distribution of *Oxyrrhis marina*: a global disperser or poorly characterized endemic? *Journal of Plankton Research* **33**:579–589.

Waycott M, Duarte CM, Carruthers TJB, Orth RJ, Dennison WC, Olyarnik S, Calladine A, Fourqurean JW, Heck KL, Hughes AR, Kendrick GA, Kenworthy WJ, Short FT & Williams SL (2009) Accelerating loss of seagrasses across the globe threatens coastal ecosystems. *PNAS* **106**:12377–12381.

Whatley JM (1993) *Chloroplast Ultrastructure. In: Berner, T (ed.): Ultrastructure of Microalgae*, CRC Press, Inc., Boca Raton, FL, USA, pp. 135-204.

WoRMS (2015) WoRMS - World Register of Marine Species (WoRMS - World Register of Marine Species). *http://www.marinespecies.org/index.php (accessed June 2015)*.

Yumoto K, Kasai F & Kawachi M (2013) Taxonomic re-examination of *Chlamydomonas* strains maintained in the NIES-Collection. *Microbiology and Culture Collections* **29**:1–12.

Zein M, Nassar A & Khairy HM (2014) Checklist of phytoplankton species in the Egyptian waters of the Red Sea and some surrounding habitats (1990-2010). *Annual Research & Review in Biology* **4**:3566–3585.

Appendix I

Table 7. Recipe for IMR 1/2 modified after (Eppley et al. 1967). Seawater is prefiltered at 1.2 µm mesh, added the solutions, postfiltered at 0.22 µm and pasteurised at 80 ^{0}C for 20 minutes. Silicate and hydrochloric acid (0.1 M) is added in media used for diatoms.

Compound	Amount
Seawater (34 PSU)	1000 mL
Nitrate	0.5 mL
Phosphate	0.5 mL
Trace metal solution	0.5 mL
Vitamin solution	0.5 mL
Selenite solution	1 mL
Silicate	5 mL
Hydrochloric acid (0.1 M)	5 mL

Table 8. Stock solutions for IMR 1/2.

Compound	Formula	Total of 1000 mL (added to MilliQ)
Nitrate	KNO_3	50 g
Phosphate	KH_2PO_4	6.8 g
Trace metal solution	Na_2EDTA	6 g
	NaFeEDTA	1360 mg
	$MnSO_4$ x 1 H_2O	620 mg
	$ZnSO_4$ x 7 H_2O	250 mg
	Na_2MoO_4 x 2 H_2O	130 mg
	$CoCl_2$ + $CuSO_4$ [4 mg/L]	1 mL
Vitamin solution	Tiamin B_1	100 mg
	Cyanokobalamin B_{12}	1 mg
	Biotin	1 mg
Selenite (dilute 1:100)	Na_2O_3Se x 5 H_2O	263 mg
Silicate	Na_2SiO_3 x 9 H_2O	14 g
Hydrochloric acid (0.1 M)	Titrisol, 0.1 M (Merck)	1 unit

Appendix II

Table 9. Bicosoeacales. Reference sequences (18S rDNA).

Genus	Species	Accession number
Bicosoeca	kenaiensis	KM816648
Bicosoeca	petiolata	AY520444
Bicosoeca	vacillans	AY520445
Cafeteria	minima	AY520448
Cafeteria	roenbergensis	AF174364
Coscinodiscus	wailesii	HQ912668
Mallomonas	akrokomos	MAU73229
Pseudobodo	tremulans	DQ220718
Siluania	monomastiga	AF072883

Table 10. Chlorarachniophyceae. Reference sequences (nuclear 18S rDNA).

Genus	Species	Accession number
Amorphochlora	amoebiformis	AF076170
Bigelowiella	natans	AF054832
Chlorarachnion	reptans	CRU03477
Chlorarachnion	sp.	AB453001
Chlorarachniophyceae	sp.	CSU03479
Chlorarachniophyceae	sp.	EF622547
Gymnochlora	stellata	AF076171
Lotharella	globosa	AF076169
Lotharella	globosa	JF826445
Lotharella	oceanica	EF622538
Lotharella	reticulosa	EF622539
Lotharella	sp.	AF076168
Lotharella	vacuolata	AF054890
Minorisa	minuta	JX272635
Norrisiella	sphaerica	AF076172
Partenskyella	glossopodia	AB452995
Partenskyella	glossopodia	KF422630
Spongomonas	minima	AF411280

Table 11. *Tetraselmis*. Reference sequences (18S rDNA).

Genus	Species	Accession number
Tetraselmis	apiculata	KJ756817
Tetraselmis	astigmatica	JN376804
Tetraselmis	carteriiformis	FJ559384
Tetraselmis	carteriiformis	FJ559385
Tetraselmis	chuii	DQ207405
Tetraselmis	gracilis	KJ756816
Tetraselmis	impressa	Z21551
Tetraselmis	inconspicua	KJ756818
Tetraselmis	marina	HE610131
Tetraselmis	sp.	HQ651184
Tetraselmis	striata	FJ559398
Tetraselmis	striata	X70802
Tetraselmis	subcordiformis	FJ559380
Tetraselmis	suecica	FJ559381
Trebouxia	tetrahele	FJ517749

Table 12. *Tetraselmis*. Reference sequences (28S rDNA).

Genus	Species	Accession number
Chlamydomonadaceae	sp.	FN552050
Dunaliella	salina	EF473746
Scherffelia	dubia	HE610128
Tetraselmis	chuii	AB491617
Tetraselmis	cordiformis	HE610130
Tetraselmis	marina	HE610131
Tetraselmis	striata	HE610129
Tetraselmis	suecica	KC415759
Tetraselmis	Uncultured clone	KP099811

Table 13. *Chlamydomonas*. Reference sequences (18S rDNA).

Genus	Species	Accession number
Characiochloris	sasae	AB360741
Chlamydomonas	acidophila	AJ783844
Chlamydomonas	applanata	FR865570
Chlamydomonas	asymmetrica	FR865583
Chlamydomonas	baca	FR865613
Chlamydomonas	bilatus	AF517098
Chlamydomonas	chlamydogama	AY220560
Chlamydomonas	cribrum	AF517099
Chlamydomonas	debaryana	AB542922
Chlamydomonas	dorsoventralis	FR865582
Chlamydomonas	gerloffii	FR865610
Chlamydomonas	globosa	AB511838
Chlamydomonas	hedleyi	GQ122368
Chlamydomonas	hedleyi	JQ315503
Chlamydomonas	hydra	FR865605
Chlamydomonas	incerta	AY781664
Chlamydomonas	inflexa	FR865584
Chlamydomonas	kuwadae	AB451190
Chlamydomonas	leiostraca	FR865590
Chlamydomonas	media	AB694003
Chlamydomonas	meslinii	FR865617
Chlamydomonas	mexicana	AF395434.
Chlamydomonas	moewusii	EU925395
Chlamydomonas	monadina	FR854382
Chlamydomonas	monadina	FR854384
Chlamydomonas	mutabilis	U57695
Chlamydomonas	neoplanoconvexa	AB602849
Chlamydomonas	nivalis	U57696
Chlamydomonas	noctigama	AJ781311
Chlamydomonas	orbicularis	AB511839
Chlamydomonas	parkeae	AB058373
Chlamydomonas	parkeae	AB701507
Chlamydomonas	philotes	FR865529

Table 13. (continued)

Chlamydomonas	pitschmannii	AJ628980
Chlamydomonas	pseudogloeogama	AF517097
Chlamydomonas	pseudomacrostigma	AB694004
Chlamydomonas	pulsatilla	AB001037
Chlamydomonas	pumilio	AB290340
Chlamydomonas	rapa	FR865611
Chlamydomonas	raudensis	AJ781313
Chlamydomonas	raudensis	JF343798
Chlamydomonas	reginae	DQ009749
Chlamydomonas	reinhardtii	AB511834
Chlamydomonas	rosae	FR865603
Chlamydomonas	rotula	FR865577
Chlamydomonas	simplex	FR865572
Chlamydomonas	sordida	AB290341
Chlamydomonas	sordida	AB290341
Chlamydomonas	sp.	JQ315515
Chlamydomonas	sp.	JQ315516
Chlamydomonas	sp. MBIC10468	AB058349
Chlamydomonas	sp. MBIC10471	AB058350
Chlamydomonas	sp. MBIC10473	AB058351
Chlamydomonas	subcaudata	AJ781310
Chlamydomonas	tetragama	AB007370
Chlamydomonas	uva-maris	FR854390
Chlamydomonas	zebra	U70792
Chlorococcum	dorsiventrale	AB058302
Chlorococcum	elkhartiense	AJ628976
Chlorococcum	littorale	AB058336
Chlorococcum	minutum	GQ122365
Chlorococcum	perforata	FR865585
Chloromonas	sp. MBIC10045	AB183580
Chloromonas	subdivisa	FR854374
Micromonas	pusilla	KF501035
Oogamochlamys	ettlii	AJ410469
Oogamochlamys	gigantea	AJ410465
Spongiococcum	tetrasporum	KM020135

Table 13. (continued)

Tetracystis	aplanospora	KM020026
Tetracystis	pampae	KM020018
Tetracystis	vinatzeri	KM020017

Table 14. Pyrenomonadales. Reference sequences (nuclear 18S rDNA).

Genus	Species	Accession number
Chroomonas	africana	HG328376
Chroomonas	caudata	AB240963
Chroomonas	caudata	HG328379
Chroomonas	coerulea	AM901370
Chroomonas	coerulea	HG328375
Chroomonas	coerulea	HG328380
Chroomonas	coerulea	HG328381
Chroomonas	coerulea	HG328382
Chroomonas	dispersa	AB240961
Chroomonas	mesostigmatica	AF508268
Chroomonas	mesostigmatica	AM901347
Chroomonas	nordstedtii	AB240962
Chroomonas	nordstedtii	AF508269
Chroomonas	nordstedtii	HG328378
Chroomonas	pauciplastida	AM901346
Chroomonas	placoidea	AM901345
Chroomonas	pochmannii	AM901369
Cryptomonas	borealis	AM051188
Cryptomonas	commutata	AM901364
Cryptomonas	gyropyrenoidosa	AJ421149
Cryptomonas	lundii	AM051190
Cryptomonas	marssonii	AM051191
Cryptomonas	marssonii	AM051192
Cryptomonas	ovata	AJ420695
Cryptomonas	ovata	AM051193
Cryptomonas	paramaecium	AM051194
Cryptomonas	paramaecium	AM051196
Cryptomonas	platyuris	AF508271

Table 14. (continued)

Cryptomonas	pyrenoidifera	AJ421147
Cryptomonas	tetrapyrenoidosa	AM051198
Cryptomonas	tetrapyrenoidosa	AM051199
Falcomonas	daucoides	AF143943
Geminigera	cryophila	GCU53124
Geminigera	cryophila	AB058365
Goniomonas	amphinema	AY705738
Guillardia	theta	X57162
Hanusia	phi	CCU53126
Hemiselmis	andersenii	AM901350
Hemiselmis	andersenii	AM901353
Hemiselmis	andersenii	AM901351
Hemiselmis	brunnescens	AJ007282
Hemiselmis	cf. virscens	AM901362
Hemiselmis	cf. virscens	AM901368
Hemiselmis	cryptochromatica	AM901354
Hemiselmis	pacifica	AM901352
Hemiselmis	rufescens	AJ007283
Hemiselmis	rufescens	AM901349
Hemiselmis	virescens	AJ007284
Komma	caudata	AM901358
Komma	caudata	KCU53122
Plagiomonas	amylosa	AF143944
Plagioselmis	prolonga	AF508272
Proteomonas	sulcata	AJ007285
Proteomonas	sulcata	HM126536
Pyrenomonas	salina	X54276
Pyrenomonas	helgolandii	AB240964
R. (=Rhodomonas)	mariana (=marina)	X81373
Rhinomonas	pauca	RPU53132
Rhodomonas	abbreviata	RAU53128
Rhodomonas	astrosea	AB240957
Rhodomonas	baltica	AB241128
Rhodomonas	chrysoidea	AB240958
Rhodomonas	duplex	AB240960

Table 14. (continued)

Rhodomonas	falcata	AB240959
Rhodomonas	maculata	AF508274
Storeatula	major	SMU53130
Teleaulax	acuta	AF508275
Teleaulax	amphioxeia	AJ007287

Table 15. Pavlovophyceae. Reference sequences (18S rDNA).

Genus	Species	Accession number
Diacronema	ennorea	JF714242
Diacronema	lutheri	AF102369
Diacronema	lutheri	JF714236
Diacronema	noctivaga	JF714222
Diacronema	sp.	JF714239
Diacronema	sp.	JF714240
Diacronema	virescens	JF714235
Diacronema	viridis	DQ075201
Diacronema	vlkianum	AF106056
Diacronema	vlkianum	JF714241
Exanthemachrysis	gayraliae	AF106060
Exanthemachrysis	gayraliae	DQ531625
Exanthemachrysis	sp.	JF714224
Exanthemachrysis	sp.	JF714226
Kathablepharis	remigera	AY919672
Monochrysis	sp.	FR865766
Pavlova	granifera	JF714231
Pavlova	gyrans	HQ877917
Pavlova	gyrans	JF714246
Pavlova	pinguis	AF102370
Pavlova	pinguis	AF102373
Pavlova	pinguis	AF106047
Pavlova	pinguis	AF106057
Pavlova	pinguis	JF714247
Pavlova	pseudogranifera	AJ515249
Pavlova	sp.	JF714234

Table 15. (continued)

Pavlovaceae	sp.	EU247835
Rebecca	salina	AF106059
Rebecca	salina	JF714244
Rebecca	salina	L34669
Rebecca	sp.	JF714245

Table 16. Dictyochophyceae. Reference sequences (18S rDNA).

Genus	**Species**	**Accession number**
Apedinella	radians	HQ710559
Ciliophrys	infusionum	AB081641
Ciliophrys	infusionum	L37205
Dictyocha	fibula	AB096710
Dictyocha	globosa	HQ646558
Dictyocha	octonaria	HQ646562
Dictyocha	speculum	U14385
Eukaryote	clone	AJ402337
Florenciella	parvula	AY254857
Florenciella	sp.	EU106830
Helicopedinella	tricostata	AB097408.
Pedinella	sp.	AB081517
Pseudochattonella	farcimen	AM850217
Pseudochattonella	farcimen	AM850220
Pseudochattonella	sp.	JN832758
Pseudochattonella	verruculosa	AM075625
Pseudochattonella	verruculosa	AM850221
Pseudopedinella	sp.	HQ710561
Pseudopedinella	sp.	HQ710562
Pseudopedinella	elastica	U14387
Pteridomonas	danica	L37204
Rhizochromulina	cf. marina	KF422605
Rhizochromulina	cf. marina	RMU14388
Rhizochromulina	marina	FR865775
Rhizochromulina	marina	HQ710563

Table 16. (continued)

Rhizochromulina	marina	HQ710563
Rhizochromulina	marina	U14388
Rhizochromulina	sp.	AJ402337
Thalassiosira	nordenskioeldii	DQ093365
Uncultured	eukaryote clone	EU500152
Uncultured	eukaryote clone	EU500153
Uncultured	marine eukaryote clone	DQ647512
Uncultured	stramenopile clone	KC488600
Uncultured	stramenopile clone	KC582988
Uncultured	stramenopile clone	KC582991

Table 17. Bacillariophyceae. Reference sequences (18S and 28S rDNA).

Genus	Species	Accession number (18S)	Accession number (28S)
Bacillaria	navis-varingica	-	AB218886
Coscinodiscus	wailesii	HQ912668	KC969894
Cylindrotheca	closterium	DQ019446	JX524868
Cylindrotheca	fusiformis	AY485457	AF417665
Nitzschia	amphibia	AJ867277	AM182194
Nitzschia	apiculata	M87334	-
Nitzschia	capitellata	-	HF679149
Nitzschia	cf. agnita	-	AF417664
Nitzschia	communis	AJ867278	AF417661
Nitzschia	dubiformis	AB430616	AB430656
Nitzschia	epithemoides	FR865501	-
Nitzschia	filiformis	HQ912589	-
Nitzschia	fonticola	KF417686	AM182191
Nitzschia	frustulum	AJ535164	HQ396834
Nitzschia	incospicua	KC736636	HF679152
Nitzschia	laevis	KF177775	HQ396835
Nitzschia	palea	DQ288289	AM183226
Nitzschia	paxillifer	FR865483	-
Nitzschia	sigma	AJ867279	-
Nitzschia	soratensis	-	HF679198
Nitzschia	supralitorea	AJ867019	AM182196

Table 17. (Continued)

Nitzschia	thermalis	AY485458	-
Nitzschia	vitrea	AJ867280	-

Appendix III

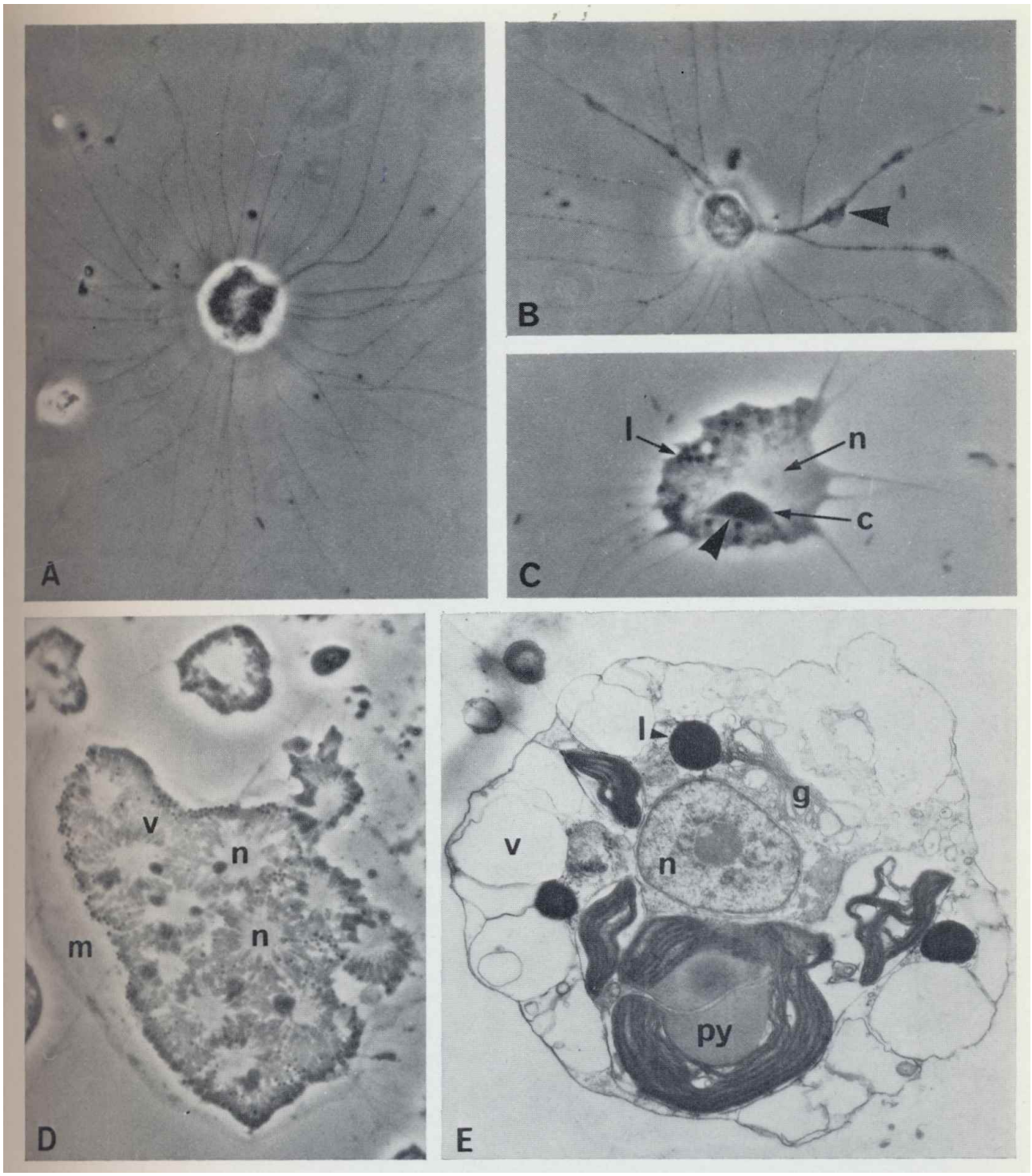

Plate 1. Light micrographs (A-D) and TEM section (E) of *Rhizochromulina marina* from Hibberd & Chrétiennot-Dinet (1979). Beaded appearance of the filopodia (arrowhead), chloroplast (c), Golgi body (g), lipodial droplets (l), mucilage (m), nucleus (n), pyrenoid (py) and leucosin vesicle (v).

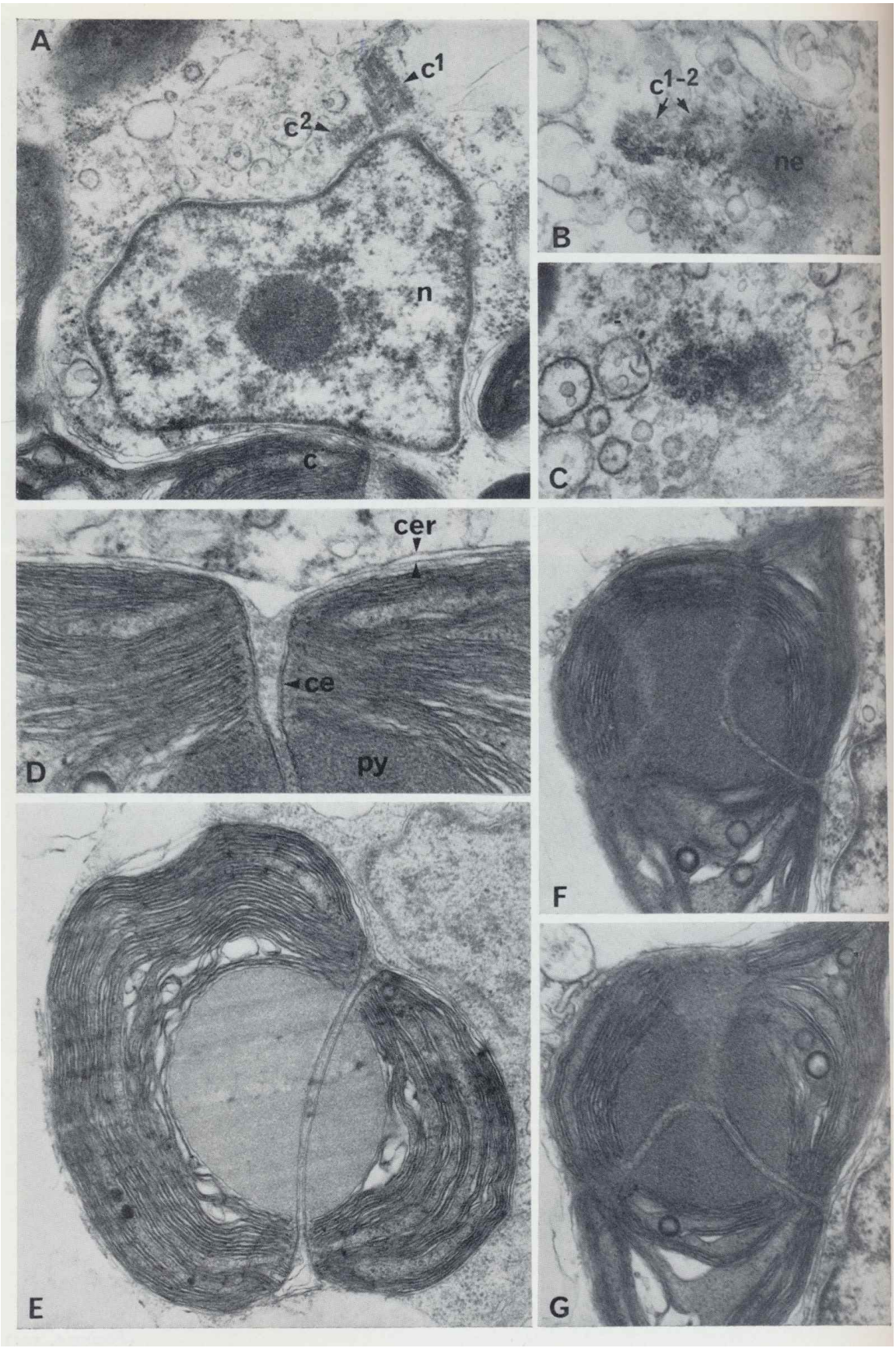

Plate 2. TEM sections of *Rhizochromulina marina* from Hibberd & Chrétiennot-Dinet (1979). Centriole (c^1), second centriole (c^2), chloroplast endoplasmatic reticulum (cer), nuclear envelope (ne), nucleus (n) and pyrenoid (py).

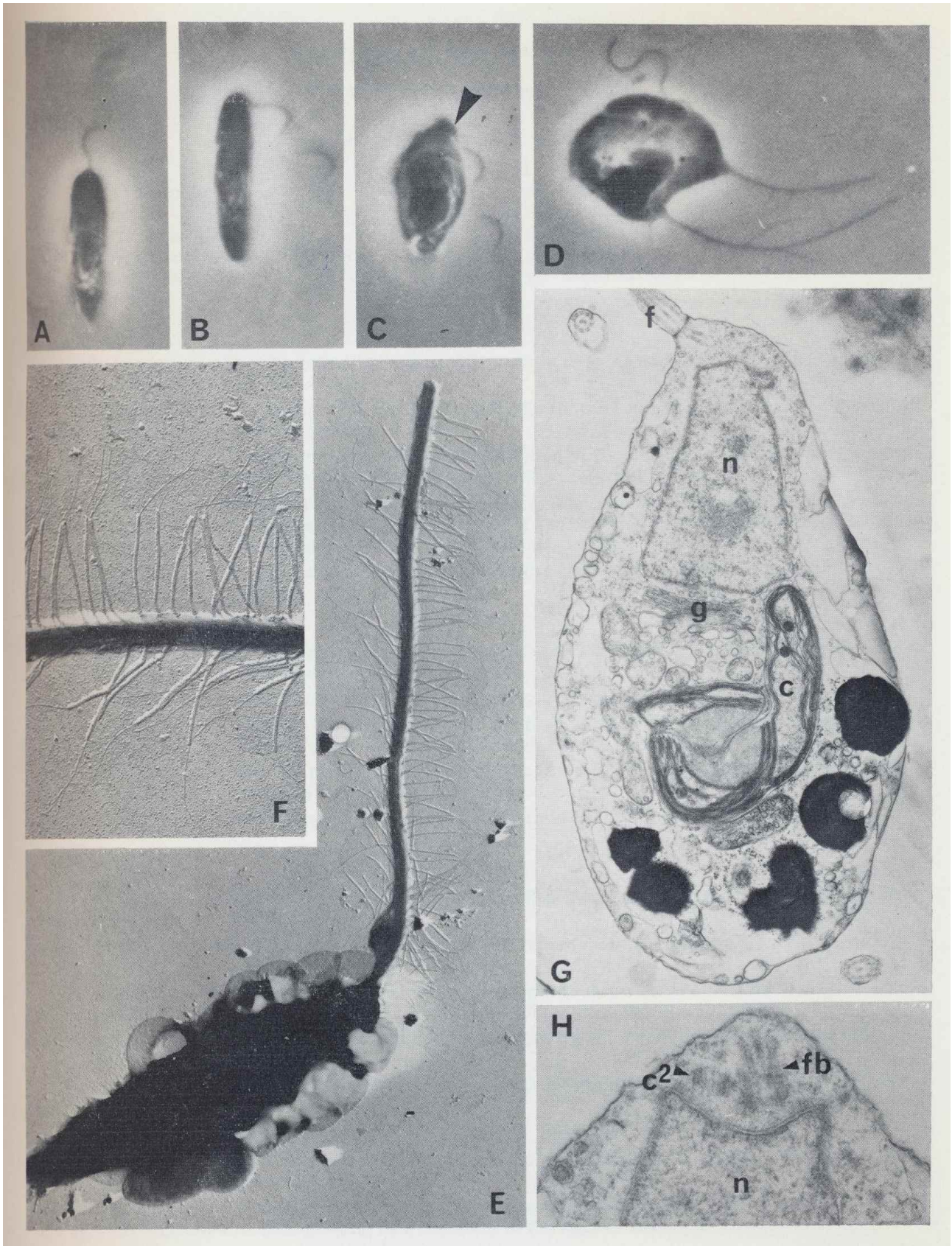

Plate 3. Micrographs (A-D), TEM whole-mounts (E-F) and TEM sections (G-H) of *Rhizochromulina marina* from Hibberd & Chrétiennot-Dinet (1979). Flagellum (arrowhead), chloroplast (c), second centriole (c^2), flagellar basal body (fb), Golgi body (g) and nucleus (n).

Appendix IV

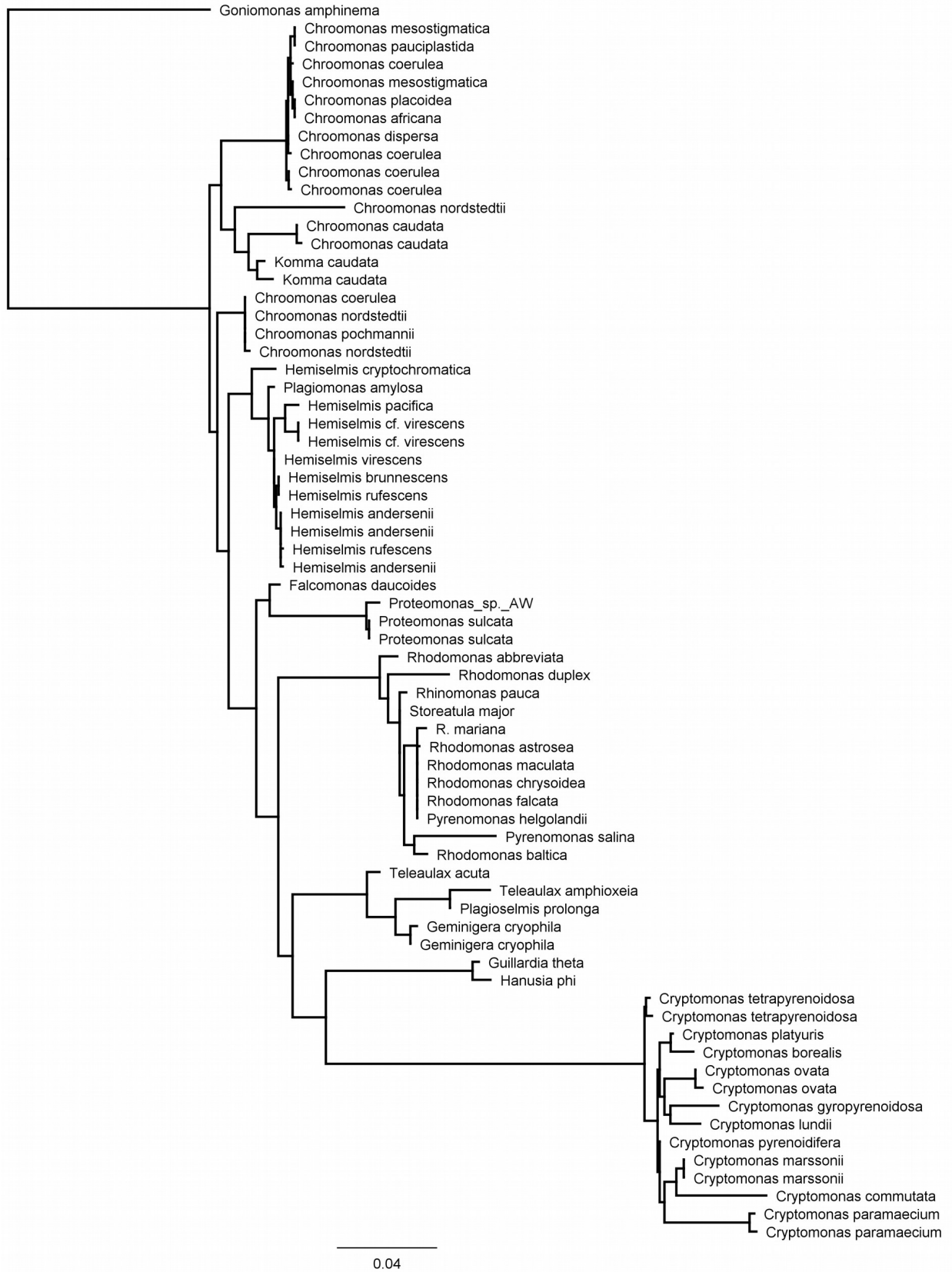

Figure 23. Maximum likelihood phylogeny of Pyrenomonadales (Cryptophyta) inferred from partial nuclear 18S rDNA sequences (1697 bp).

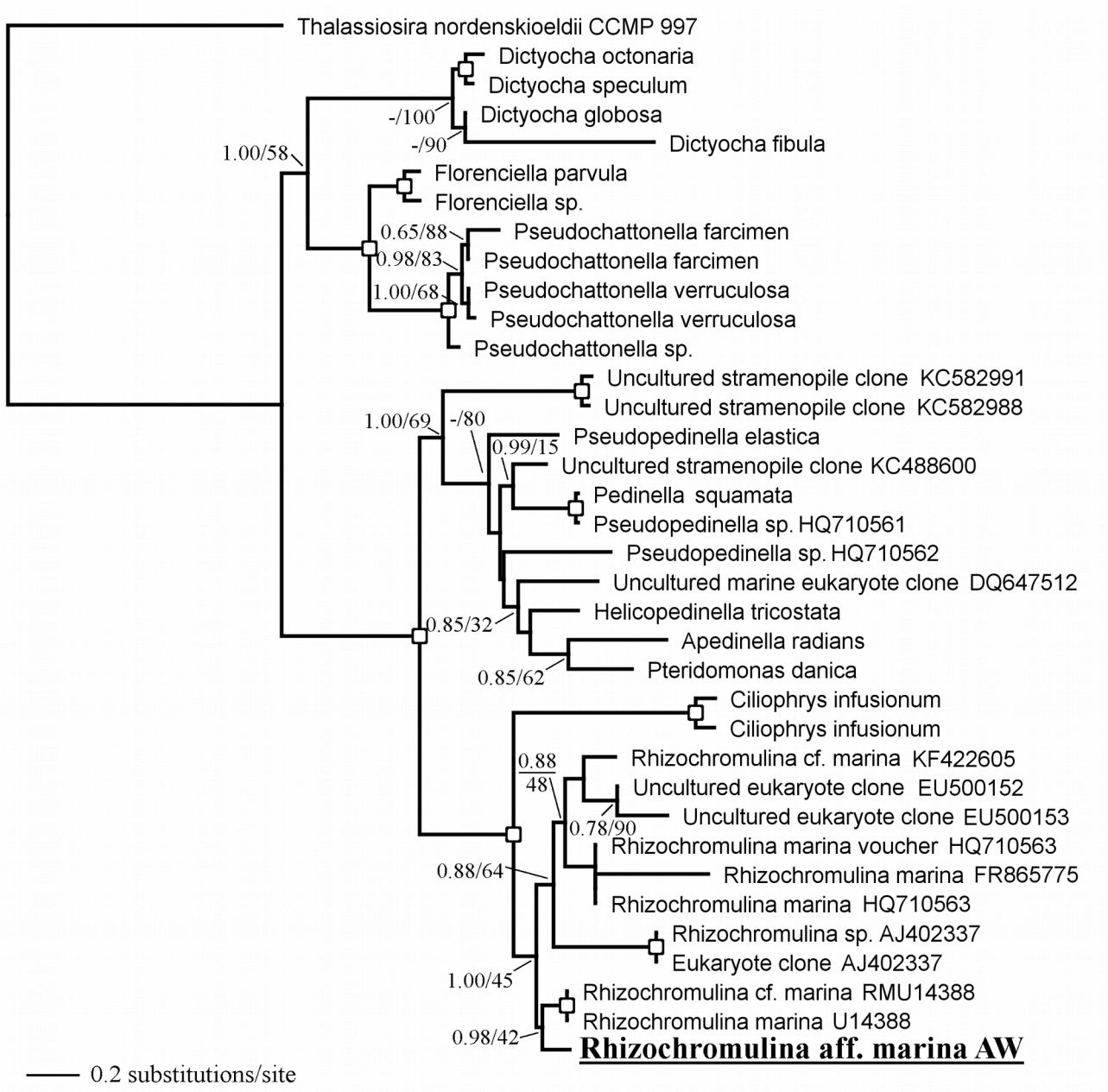

Figure 24. Maximum likelihood phylogeny of Dictyochophyceae (Ochrophyta) inferred from partial nuclear 18S rDNA sequences (1695 bp).

Appendix V

Table 18. Complete list of strains form isolated in the present study. Culture code, genus, species, date of sampling and isolator are included.

UIO code	Genus	Species	Date	Isolator
343	Nitzschia	sp.	13.11.2012	Anders Wold
344	Nitzschia	sp.	13.11.2012	Anders Wold
345	Cafeteria	roenbergensis	13.11.2012	Anders Wold
346	Tetraselmis	sp.	13.11.2012	Anders Wold
347	Chlamydomonas	sp.	13.11.2012	Anders Wold
348	Chlamydomonas	sp.	13.11.2012	Anders Wold
349	Amphidinium	sp.	13.11.2012	Anders Wold
350	Chlamydomonas	aff. parkeae	13.11.2012	Anders Wold
351	Amphidinium	sp.	13.11.2012	Anders Wold
352	Lotharella	reticulosa	13.11.2012	Anders Wold
353	Cylindrotheca	cf. closterium	13.11.2012	Anders Wold
354	Nitzschia	sp.	07.11.2014	Anders Wold
371	Amphidinium	sp.	07.11.2014	Anders Wold
372	cf. Pseudoanabaena	sp.	07.11.2014	Anders Wold
373	Cylindrotheca	sp.	07.11.2014	Anders Wold
374	cf. Ochrophyta	sp.	13.11.2012	Anders Wold
375	Pavlova	sp.	13.11.2012	Anders Wold
376	Proteomonas	aff. sulcata	07.11.2014	Anders Wold
377	Rhizochromulina	aff. marina	13.11.2012	Anders Wold
378	Rhizochromulina	aff. marina	13.11.2012	Anders Wold
379	cf. Amastigomonas	sp.	13.11.2012	Anders K. Krabberød
380	cf. Amastigomonas	sp.	07.11.2014	Anders Wold
381	Oxyrrhis	marina	07.11.2014	Anders Wold
382	cf. Chlorophyta	sp.	13.11.2012	Anders Wold
383	Nitzschia	sp.	13.11.2013	Anders Wold